

TALLINN UNIVERSITY OF TECHNOLOGY
DOCTORAL THESIS
49/2018

Synthesis of $\text{Cu}_2\text{ZnSnS}_4$ Nano-powders and Nano-structured Thin Films

SURESH KUMAR



TALLINN UNIVERSITY OF TECHNOLOGY

School of Engineering

Department of Materials and Environmental Technology

This dissertation was accepted for the defence of the degree 10/07/2018

Supervisor: Dr. Maarja Grossberg, Professor
Department of Materials and Environmental Technology
Tallinn University of Technology
Tallinn, Estonia

Co-supervisor: Dr. Mare Altosaar, Senior Research Scientist
Department of Materials and Environmental Technology
Tallinn University of Technology
Tallinn, Estonia

Opponents: Dr. Stela Canulescu, Associate Professor
DTU Fotonik – Department of Photonics Engineering
Technical University of Denmark
Lyngby, Denmark

Dr. Vambola Kisand, Senior Research Scientist
Faculty of Science and Technology, Institute of Physics
University of Tartu
Tartu, Estonia

Defence of the thesis: August 29, 2018 at 13:00
Lecture Hall : U05 – 103
Tallinn University of Technology, Ehitajate Tee 5, Tallinn

Declaration:

Hereby I declare that this doctoral thesis, my original investigation and achievement, submitted for the doctoral degree at Tallinn University of Technology, has not been previously submitted for doctoral or equivalent academic degree.

Suresh Kumar

signature



Copyright: Suresh Kumar, 2018
ISSN 2585-6898 (publication)
ISBN 978-9949-83-314-6 (publication)
ISSN 2585-6901 (PDF)
ISBN 978-9949-83-315-3 (PDF)

TALLINNA TEHNIKAÜLIKOO
DOKTORITÖÖ
49/2018

$\text{Cu}_2\text{ZnSnS}_4$ nano-pulbrite ja nano- struktuursete kilede süntees

SURESH KUMAR

Contents

List of Publications	7
Author's Contribution to the Publications	8
List of Abbreviations	9
Introduction	10
1. Literature Overview and Aim of the Study.....	12
1.1 Cu ₂ ZnSnS ₄ (CZTS).....	12
1.2 Nano-powders	13
1.3 Thin Films by Nano-powder Ink Technology	14
1.4 Solution-based Nano-powder Synthesis.....	14
1.4.1 Solvents Used in Nano-powder Synthesis.....	14
1.4.2 Oleylamine as a Solvent in Nano-powder Synthesis.....	15
1.4.3 Complex Formation and Nucleation.....	15
1.4.4 Nano-powder Growth	16
1.5 CZTS Nano-powder Synthesis in Oleylamine by the Hot-injection Method	16
1.5.1 The Influence of Synthesis Temperature on CZTS Nano-powder Synthesis.....	17
1.5.2 The Effect of Initial Concentration of Precursors	17
1.5.3 The Influence of Additional Alkali Compound on CZTS Nano-powder Synthesis .	18
1.6 Sol-gel Method	18
1.6.1 Methanol as Solvent in the Sol-gel Method	18
1.6.2 CZTS Thin Films by the Sol-gel Method	18
1.7 Summary of the Literature Overview and Aim of the Study	19
2. Experimental	21
2.1 Synthesis of CZTS Nano-powders by the Hot-injection Method	21
2.2 Preparation of Precursor Solutions with Alkali Metal Compounds.....	22
2.3 CZTS Thin Films by the Sol-gel Method	22
2.4 Characterization Methods.....	23
3. Results and Discussion	25
3.1 Tailoring the CZTS Nano-particle Formation and Growth by Varying Cu and Zn Concentrations at Different Temperatures [I].....	25
3.2 Effect of Alkali Ions (Na ⁺ , K ⁺ , Cs ⁺) on the Reaction Mechanism of CZTS Nano-particle Synthesis [II]	29
3.2.1 Analysis of FTIR Spectra of Oleylamine and Oleylamine-Cation Precursors	29
3.2.2 Analysis of FTIR Spectra of Oleylamine, Oleylamine-Cation Precursors and Oleylamine-Alkali Compounds.....	32
3.2.3 Analysis of CZTS Nano-powders Synthesized in the Presence of Alkali Compounds	35
3.2.4 Effect of Concentration of CsOH	36
3.3 CZTS Thin Films by the Sol-gel Method [III]	38

3.3.1 Morphology and Elemental Composition of Films Pre-annealed in Nitrogen.....	38
3.3.2 Raman Studies of CZTS Thin Films Pre-annealed in Nitrogen.....	39
3.3.3 Vacuum Annealed CZTS Thin Films.....	40
Conclusions	42
References	43
Acknowledgements.....	48
Abstract.....	49
Kokkuvõte	50
Appendix	51
Curriculum Vitae	83
Elulookirjeldus.....	85

List of Publications

The dissertation is based on the following publications that are referred to in the text by Roman numerals I-III:

- I. **Suresh Kumar**, Vikash Kumar, Valdek Mikli, Tiit Varema, Mare Altosaar, Maarja Grossberg, Study of CZTS nano-powder synthesis by hot injection method by variation of Cu and Zn concentrations, *Energy Procedia* 102 (2016) 136-143.
- II. **Suresh Kumar**, Mare Altosaar, Maarja Grossberg, Valdek Mikli, Effect of Alkali ions (Na⁺, K⁺, Cs⁺) on Reaction Mechanism of CZTS Nano-particles Synthesis, *Superlattices and Microstructures* 116 (2018) 54-63.
- III. **Suresh Kumar**, Bharath Kasubosula, Mihkel Loorits, Jaan Raudoja, Valdek Mikli, Mare Altosaar, Maarja Grossberg, Synthesis of Cu₂ZnSnS₄ Solar Cell Absorber Material by Sol-Gel Method, *Energy Procedia* 102 (2016) 102-109.

Copies of these articles are included in Appendix.

Author's Contribution to the Publications

The contribution by the author to the papers included in the thesis is as follows:

- I. Synthesis of CZTS nano-powders, Raman and SEM analysis, characterization and analysis of the results, major role in writing.
- II. Preparation and FTIR studies of solutions of oleylamine-cation precursors and solutions of oleylamine-alkali compounds, synthesis of CZTS nano-powders with alkali compounds, Raman and SEM analysis, analysis of the results, major role in writing.
- III. CZTS thin film preparation, characterization and analysis of the results, major role in writing.

List of Abbreviations

CZTS	$\text{Cu}_2\text{ZnSnS}_4$
CZTSe	$\text{Cu}_2\text{ZnSnSe}_4$
CIGS	$\text{Cu}(\text{In,Ga})\text{Se}_2$
DEG	Di-Ethylene Glycol
EDS	Energy Dispersive X-ray Spectroscopy
FTIR	Fourier Transform Infrared Spectroscopy
FWHM	Full Width at Half Maxima
ITO	Indium Tin Oxide
OAm	Oleylamine
PCE	Power Conversion Efficiency
PEG	Poly-Ethylene Glycol
PMCA	Pre-Mixed Cu-Au
SEM	Scanning Electron Microscopy
XRD	X-Ray Diffraction

Introduction

The whole world is concerned about the global warming and its future impact on the society and nature. All countries are looking forward to use clean energy and new technologies to reduce carbon emissions. The direct conversion of solar energy to electricity using a photovoltaic (PV) cell is a clean energy production method. The first prerequisite for solar energy conversion is a good absorber material composed of earth abundant elements with least toxicity, and having high absorption coefficient and direct band gap. Most of the commercially available PV solar cells are made from silicon that has indirect band gap and low absorption coefficient, which makes the production of Si based photovoltaic modules very material consuming. As a material saving alternative, direct band gap inorganic compound absorber materials are used in solar cell mass production, namely CdTe and Cu(InGa)Se₂ (CIGS), showing record power conversion efficiencies (PCE) 22.1% [1] and 22.9% [2], respectively. However, there are concerns with toxicity (Cd) and/or scarcity (In and Te) of the constituent elements. Therefore, Cu₂ZnSnS₄ (CZTS) semiconductor compound with excellent environmental profile and required high absorption coefficient ($\geq 10^4$ cm⁻¹) and direct band gap (1.5 eV) [3] has drawn significant attention as an alternative for CdTe and CIGS [4]. Intensive research of CZTS as absorber material in photovoltaic cells started in the early 2000s. CZTS is used not only as an absorber material in photovoltaic cells, but also for thermoelectric applications, photo-catalysis and as a battery electrode material.

Nanotechnology can be incorporated into solar panels to convert sunlight to electricity more efficiently, promising inexpensive solar power in the future, resulting from cheaper manufacturing using print-like roll-to-roll deposition processes and reduced material consumption. In addition, material in the form of nano-powders provides additional degrees of freedom for tuning the physical and chemical properties of the material. Nano-powders are highly crystalline with variable size, shape and composition. The properties of nano-scale materials are different from the bulk materials due to the large surface to volume ratio of nano-powders, e.g. the catalytic activity of nano-particle Au for CO oxidation even at -30 °C [5, 6].

There are several ways for the synthesis of nano-powders. In the present thesis, the solution-based method was selected for the synthesis of CZTS [I, II]. Nano-powder inks can be used in cost-effective roll-to-roll printing processes. The solution based method provides a wide selection of solvents for the synthesis, e.g. oleylamine (OAm), diethylene glycol (DEG), polyethylene glycol (PEG), hydrazine, octadecene, methanol. There are several cheap and non-toxic organic solvents with long chain hydrocarbons and different functional groups available. The highest PCE of CZTS-type solar cell 12.6% is achieved by using hydrazine as a solvent in the synthesis of absorber material [7]. Hydrazine is very toxic. Therefore, it is highly recommended to replace it by a cheap and non-toxic solvent like oleylamine. The PCE of 8.4% is achieved using oleylamine instead of hydrazine in the CZTS nano-powder synthesis [8]. In the first part of the present thesis, oleylamine is primarily used as a solvent for nano-powder synthesis [I, II]. One of the most successful routes for the synthesis of CZTS nano-powders is the so called "hot-injection" synthesis method that utilizes surfactant-controlled growth of nano-powders in a hot organic solvent [9]. Nano-powder synthesis process can be tailored by varying different technological parameters. In this thesis research, the influence of the synthesis temperature and the composition of initial precursor mixtures on the size and shape and phase composition of produced nano-powders was

studied [I]. Furthermore, the solvent oleylamine was modified by addition of compounds containing different alkali metal ions and their effect on the CZTS nano-particle formation and growth was analyzed [II]. That kind of solvent modification has not been used before in the CZTS nano-powder synthesis. The modification allows us to control the active functional group part of the oleylamine solvent. As a result of the study of the properties of the modified solvent solutions, a possible structure of the formed oleylamine complex with metal ions was proposed. In addition, the influence of the solvent modification on the nano-particle growth was investigated.

As an alternative approach in this study, methanol as a solvent was used in the sol-gel method for CZTS thin film preparation by dip coating, as it is a simple and low-temperature deposition method [III]. Methanol is a low cost solvent and a good polar liquid for preparation of individual precursor solutions as sources of cations and sulphur. Thiourea is a popular source of sulphur that can easily form complexes with Cu, Zn and Sn, which yield in sulphides on thermal decomposition [10]. The CZTS thin film formation on bare soda-lime glass, Mo and ITO substrates was studied. The second part of the thesis focuses on the influence of annealing procedure in controlled gas atmosphere at different temperatures on the quality of CZTS thin films.

The dissertation is divided into three chapters. Chapter 1 covers the literature overview that contains different subsections where properties of CZTS and different aspects of the formation of CZTS in the nano-powder synthesis are described. The objectives of the thesis research are formulated on the basis of the summary of the literature overview. The experimental details of CZTS nano-powder synthesis by the hot injection method and used characterization methods are described in Chapter 2. The preparation of CZTS thin films by the sol-gel method with details of thin films annealing in air, nitrogen and vacuum is described. The results of the studies and discussions are presented in the last chapter. The thesis is based on three published papers and the results have been presented at different conferences.

1. Literature Overview and Aim of the Study

1.1 $\text{Cu}_2\text{ZnSnS}_4$ (CZTS)

$\text{Cu}_2\text{ZnSnS}_4$ (CZTS) belongs to the $\text{A}_2\text{B}^{\text{II}}\text{C}^{\text{IV}}\text{X}^{\text{VI}}_4$ compound family with $\text{A} = \text{Cu}$, $\text{B} = \text{Zn}$, Fe (in the case of natural kesterite), $\text{C} = \text{Sn}$ and $\text{X} = \text{S}$, Se [11]. CZTS as a compound semiconductor has been studied intensively for the replacement of expensive and scarce indium (In) (or Ga) by zinc and tin in CuInSe_2 (or CuGaSe_2) semiconductor by cation substitution in which the overall valence state is maintained and the compound remains charge neutral [4]. The compositional elements of CZTS are earth abundant, cheap and non-toxic. CZTS is a p -type semiconductor that has high absorption coefficient ($\geq 10^4 \text{ cm}^{-1}$) and a direct band gap (1.5 eV) [3]. Due to its properties, CZTS has been found suitable for various applications, not only as an absorber material in PV solar cells [7, 12] but also as a photo-catalyst [13, 14], as a thermoelectric material [15, 16] and as a battery electrode material [17].

According to the theoretical calculations, CZTS exists in two tetragonal crystal structures – in kesterite (space group $I4$) and in stannite (space group $I-42m$) structure [18]. These are two structurally similar but distinct crystal structures that differ in the ordering of the Cu-Zn sub lattice: kesterite is derived from the chalcopyrite (201) ordering and stannite is derived from the Cu-Au (001) ordering [18]. The lowest energy structure of CZTS is kesterite. Stannite is the disordered phase of kesterite having the same symmetry. Stannite symmetry occurs randomly because of a relatively low energy of Cu-Zn cation exchange in the kesterite structure [18]. Only 2.86 meV/atom higher crystal energy was determined for stannite compared to the kesterite structure [18]. Due to the presence of three cations in the quaternary system, many possible defect complexes exist, from which the bound anti-site pair between Cu and Zn has particularly low formation energy [18]. In addition, low formation energies have been calculated for $[\text{V}_{\text{Cu}} + \text{Zn}_{\text{Cu}}]$ and $[2\text{Cu}_{\text{Zn}} + \text{Sn}_{\text{Zn}}]$ defect pairs and Cu_{Zn} and V_{Cu} individual defects [18]. Cu_{Zn} and Cu_{Sn} deep acceptor defects have been experimentally detected in CZTS by admittance and photoluminescence spectroscopy [19, 20]. Also, the existence of $[2\text{Cu}_{\text{Zn}} + \text{Sn}_{\text{Zn}}]$ defect pair in CZTS has been detected by photoluminescence spectroscopy [21].

The experimental lattice parameters of kesterite CZTS are $a=5.443 \text{ \AA}$ and $c=10.840 \text{ \AA}$ [22], being very close to the calculated lattice constants $a=5.432 \text{ \AA}$ and $c=10.786 \text{ \AA}$ [23]. Calculations show that the band gaps of the kesterite, stannite and partially disordered kesterite (PMCA) structures can differ by as much as 0.15 eV [24] and it is suggested that the estimated band gap for kesterite CZTS is 1.45 eV at room temperature [24, 25]. Various room temperature band gap energy values have been determined from experiments, i.e. 1.5 eV [3], 1.4-1.45 eV [26], 1.49 [27], 1.45 eV [28]. It is also possible to have partially disordered form of kesterite (PMCA, space group $P42m$), where the Cu and Zn atoms can be randomly arranged on their shared lattice plane [23]. The values of calculated lattice constants of the kesterite CZTS are slightly larger than those of PMCA structures [29].

CZTS compound consists of four elements and the single phase compositional region of the compound changes with temperature as can be seen from the phase diagram in Figure 1. Therefore, the synthesis temperature is one of the factors influencing the formation of by-products (other than CZTS compound). Olekseyuk *et al.* [30] investigated the phase equilibrium in the system of $\text{Cu}_2\text{S}-\text{ZnS}-\text{SnS}_2$ using differential

thermal, X-ray diffraction phase and microstructure analysis methods. For the studies, CZTS was synthesized through solid state chemical reaction between ZnS, Cu₂S and SnS₂. Figure 1 shows the T-X section Cu₂S-CZTS-(ZnS+SnS₂). In the phase diagram, the composition marked as ZnS+SnS₂ consists of 50 mol% of ZnS and 50 mol% of SnS₂. ZnS crystallizes in two structural types: sphalerite (low-temperature-ZnS) and wurtzite, the temperature of polymorphic transformation is 1020 K. In the system Cu₂S-SnS₂, several ternary compounds exist: Cu₂SnS₃, Cu₄SnS₄ and Cu₂Sn₄S₉. A ternary compound Cu₂Sn₄S₉ forms in the quasi-binary section Cu₂S-SnS₂ by the peritectoid reaction Cu₂SnS₃ + SnS₂ ⇌ Cu₂Sn₄S₉ at 943 K [30]. Therefore, in low-temperature synthesis (as in the nano-powder synthesis), the formation probability of this compound would be low.

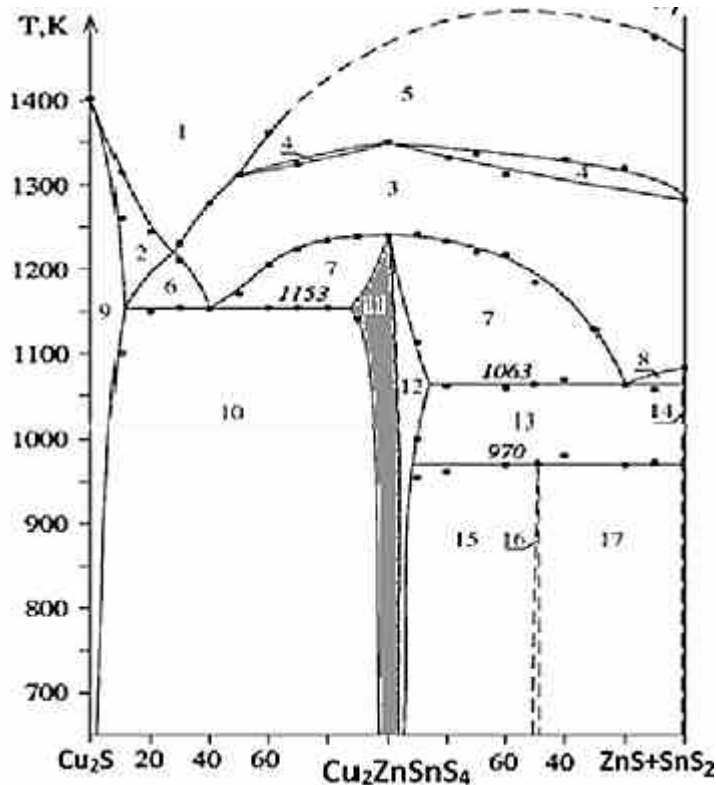


Figure 1 Phase diagram of the Cu₂S-(Cu₂ZnSnS₄)-(ZnS+SnS₂) section, where α - Cu₂S, β - ZnS, δ - Cu₂ZnSnS₄, γ - SnS₂ (1) L, (2) L+α, (3) L+β', (4) L+β+β', (5) L+β, (6) L+α+β', (7) L+β'+δ, (8) L+β'+γ, (9) α, (10) α+δ, (11) δ, (12) β'+δ, (13) β'+γ+δ, (14) β'+γ, (15) β'+δ+Cu₂ZnSn₃S₈, (16) β'+Cu₂ZnSn₃S₈, (17) β'+γ+Cu₂ZnSn₃S₈, adapted from [30, 31].

1.2 Nano-powders

Nano-powders are single crystals in the size range of some nano-meters. Nano-material means an intentionally manufactured material with one or more external dimensions, or an internal structure, on the scale from 1 to 100 nm [32]. The properties of nano-powders are different from the bulk materials due to the large surface to volume ratio of nano-powders. For example, melting point is lower, mechanical strength is higher

due to the reduction of defects; electrical and optical properties exhibited by nano-materials are quite different from their bulk counterpart. Chemical properties of the materials are also changed when converted to nano-scale. Due to the increase of the exposed surface area of the nano-powders as compared with conventional bulk materials, the reactivity of those nano-powders is enormously increased. Nano-powders can be prepared generally by two possible approaches - top down and bottom up [33]. Top down approach involves the breakdown of large size particles to nano size powders, for example in the high-speed ball milling process. Milling is a mechanical process accompanied with the formation of several defects. Bottom up approach involves the crystal nuclei formation and growth of nano-powders from atomic level like in wet chemical processes (sol-gel process, solution-based method) or in chemical vapour condensation. The bottom up approach provides several possibilities for tailoring the synthesis process starting from nuclei formation up to crystal growth.

Nano-powders have large active surface area that makes their handling and storage complicated. Large active surface makes them sensitive to interact with the components of surrounding atmosphere or with impurities. Nano-powders have to be encapsulated or covered by surfactant or by capping ligands. The recycling and reuse studies of nano-powders are in their early stages. The toxicity of some of the solvents used in the solution-based and sol-gel based synthesis is one of the disadvantages of these methods and use of non-toxic solvents is preferred. The processing of by-products of the nano-powder synthesis is also a challenging task.

1.3 Thin Films by Nano-powder Ink Technology

The synthesized nano-powders are ordinarily dispersed in a solvent to form stable inks that are used for making thin films for solar cells. Nano-powder ink technology offers advantages over conventional thin film deposition methods. From the manufacturing cost point of view, it is important that nano-powder inks can be used in cost-effective roll-to-roll printing processes. The flexible or non-flexible substrates can be used for printing, providing an additional value in terms of the applications of the thin films. The fabrication of CZTSSe solar cells based on nano-powder inks starts from the synthesis of nano-powders, followed by sintering of the thin films in sulphur or selenium vapours [12, 34]. Solution-based methods adapted for nano-powder synthesis of CZTS, $\text{Cu}_2\text{ZnSnSe}_4$ (CZTSe) and their solid solutions with tuneable band gap (CZTSSe) have led to the highest PCE of 12.6% of the kesterite solar cells [7] compared to 11.4% for solar cells based on vacuum processed kesterite materials [35].

1.4 Solution-based Nano-powder Synthesis

Solutions are homogeneous mixtures of two or more than two components [36]. Homogeneous mixtures mean that their properties are uniform throughout the mixture [36]. The solvents used in this thesis research are in the liquid state, i.e. oleylamine (OAm) [I, II] and methanol [III]. The solutes, on the other hand, are in solid form, i.e. zinc acetate, copper 2,4-pentanedionate, tin (II) chloride, elemental sulphur, copper (II) chloride, and zinc (II) chloride.

1.4.1 Solvents Used in Nano-powder Synthesis

A wide range of non-toxic and cheap solvents is available for the synthesis of nano-powders. Nano-powders have been synthesized in different organic solvents, e.g. hydrazine, octadecene, di-ethylene glycol, oleylamine, methanol, and ethanol. Some of

these solvents act as a solvent, a surfactant and a capping ligand during the synthesis. The solvent and solute precursors are selected based on their roles in the solution and in the nano-powder synthesis. A 12.6% efficient CZTS solar cell was prepared using CZTS nano-powders synthesized in hydrazine solvent [7]. As hydrazine is a very toxic solvent, an alternative nontoxic solvent for CZTS nano-powder synthesis is required. CZTS based thin film solar cell with 8.4% efficiency was prepared by using CZTS nano-powders synthesized in oleylamine (OAm) [37].

1.4.2 Oleylamine as a Solvent in Nano-powder Synthesis

The solvent is the most crucial part in the solution-based synthesis of nano-powders. There are three ways to tailor the nano-powder synthesis through the solvent: a) by using different amount of solvent, b) by using alternative solvents, and c) by influencing the properties of the solvent for example by adding a salt. Oleylamine that is used in this study is a fatty amine; it has one amine group attached to the hydrocarbon chain with 18 carbon atoms in length (see Figure 2).

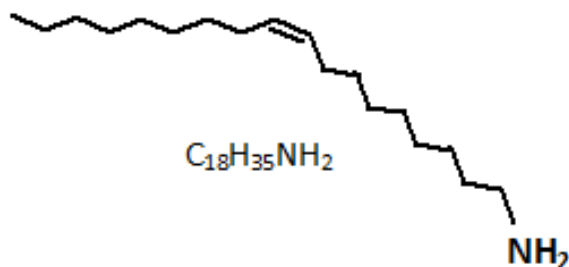


Figure 2 Structure of oleylamine

The molecular formula of oleylamine is C₁₈H₃₅NH₂. The molecule of OAm has two functional groups - a double bond and an amine group. The double bond in the molecular structure distinguishes OAm from other fatty amines. Because of double bond in its molecule, OAm has an angled structure instead of a linear structure. OAm as a long-chain primary alkyl-amine can act as an electron donor at elevated temperatures [38]. OAm has been used as a coordinating alkyl solvent, surfactant and reducing agent at the same time for controlled preparation of a wide range of nano-materials - metals, metal- chalcogenides, metal oxide and inter-metallic compounds and alloys [39]. OAm was used as a solvent, a surfactant and a capping ligand in the solution-based synthesis of CZTS and other nano-powders [39]. For example, magnetic nano-powders of Co [40], CoO [40], Ni [41, 42] and NiO [41, 42] were synthesized in the presence of oleylamine solvent. Oleylamine is successfully used to synthesize noble metal nano-powders i.e. Pt [43, 44], Pt-Au [45, 46, 47], Pt-Ag [48] and nano-structures, i.e. Pd [49]. Nano-scale semiconductors such as CdS [50], CdSe [50], PbS [51], Cu₂S [52], Ni₃S₄ [52] and ZnS [53] have also been prepared by using oleylamine.

1.4.3 Complex Formation and Nucleation

Most of the solution-based methods for preparing metal nano-powders involve the use of a salt precursor dissolved in a solvent [54]. It is generally assumed that metal ions exist as monomeric units through complexation with anions, ligands, or solvent molecules [54]. Oleylamine forms complexes with the cation elements available in the solution of the cation precursors and solvents. The cation precursors are selected in

such a way that they can readily release the cation elements into the solutions (metal acetyl-acetonates, metal-oxides, metal carbonyls, metal chlorides, etc.).

Nucleation is the first step in the formation of either a new thermodynamic phase or a new structure. There are two probable routes of nucleation in the solution-based synthesis of nano-powders: a) decomposition route and b) reduction route. In the decomposition route, the concentration of the metal atoms steadily increases with time as the precursor is decomposed [55]. La Mer and co-workers studied the solution-based synthesis of mono-disperse sulphur colloids and proposed the nucleation mechanism by decomposition route [55]. In the reduction route, the precursor compound is in higher oxidation state than the atomic species and precursor compound is reduced into zero valent atoms, which aggregate into nuclei and then grow into nano-particles [56, 57, 58].

1.4.4 Nano-powder Growth

A solution-based method for nano-powder growth can be surface limited or/and diffusion limited, i.e. the reaction rate is controlled by the rate of transport of the reactants through the reaction medium [55]. There are two mechanisms for the surface processes: mononuclear growth and poly-nuclear growth. The mononuclear growth proceeds layer by layer, i.e. the species are incorporated into one layer and the incorporation proceeds to another layer only after the growth of the previous layer is complete [59]. During the poly-nuclear growth, the surface process is so fast that the growth of the second layer proceeds before the first layer growth is complete. Nano-powders synthesized by the solution-based method follow homogeneous nucleation.

Homogeneous nucleation could be defined as solute molecules within a liquid combine to produce nuclei in the absence of solid interface [55]. Homogeneous nucleation occurs randomly and spontaneously [59]. The control of size distribution by changing the super saturation and evolution of precursor concentration during nucleation and growth were explained by Lamer and Dinegar [55, 59]. Riha *et al.* synthesized 12.8 ± 1.8 nm mono-disperse CZTS nano-powders using stoichiometric initial precursor concentration at the synthesis temperature of 300 °C [9]. Karimi *et al.* synthesized spherical platelet CZTS nano-powders with a particle size in the range of 20-25 nm using choline chloride and urea acting as a solvent and a template [60].

1.5 CZTS Nano-powder Synthesis in Oleylamine by the Hot-injection Method

The solution-based hot-injection method is a bottom up process of nano-powder synthesis. One of the most successful routes for the synthesis of CZTS nano-powders is the hot-injection synthesis method that utilizes surfactant-controlled growth of agglomerated nano-powders in a hot organic solvent [9]. Several research groups have synthesized CZTS nano-powders using oleylamine [9, 12, 34, 37, 60, 61, 62]. The solution-based CZTS nano-powder synthesis enables tailoring the nano-powder synthesis process by varying the synthesis process parameters. Some of the possibilities are discussed in the following paragraphs. The factors affecting the process are a) the synthesis temperature and time; b) amount of oleylamine solvent on the CZTS nano-powder synthesis; c) addition of salt to the oleylamine solvent; d) initial concentration of precursors.

1.5.1 The Influence of Synthesis Temperature on CZTS Nano-powder Synthesis

The solution-based synthesis of nano-powders can be performed at temperatures higher than room temperature. In normal conditions (without overpressure), one of the limiting factors is the boiling temperature of the solvent at which the process is difficult to tailor. In the studies performed on CZTS nano-powder synthesis in oleylamine at different temperatures from 225 °C to 330 °C in open air atmosphere [61], the most favourable synthesis temperature of 250 °C was proposed. The work of Ahmad and co-workers [61] was mainly focused on the crystal structure analysis of the CZTS nano-particles formed at different synthesis temperatures - cubic, tetragonal or hexagonal structures. It was also found in [61] that the size of the formed nano-particles decreased with the increasing synthesis temperature, but at the highest temperature (330 °C), the particle size suddenly increased up to micrometer scale.

In the hot-injection method, cation precursors in the solvent are usually mixed at room temperature in a three-neck flask by stirring. The mixture is heated up to the synthesis temperature. It requires some time to raise the solution temperature to the synthesis temperature. During this period of time, cation precursor salts dissolve in oleylamine and form oleylamine-cation complexes. To control the particle growth in the nano-powder synthesis, capping agents are often used to decrease the surface energy of particles. Organic capping provides chemical passivation of the surface dangling bonds prevents uncontrolled growth and agglomeration of the nano-particles. Also chemical manipulations of the nano-materials similar to large molecules having their solubility and reactivity determined by the nature of the surface ligands are permitted by the organic capping [63, 64]. In [62], the shape of the formed CZTS nano-particles (nano-rods and ellipsoids, as well as atypical tadpole-shaped and p-shaped nano-particles) was tailored by tuning amine concentration in two-solvent systems of octadecene and oleylamine.

1.5.2 The Effect of Initial Concentration of Precursors

CZTS compound contains three cations; it is possible to modify the synthesis by changing the concentrations of cation precursors and by selection of different cation precursors for the same element. Coughlan and Ryan showed how the shape of formed nano-particles changed from acorn shaped nano-powders to pencil shaped nano-particles of CZTS by changing the Cu precursor (Copper acetylacetonate to copper (I) chloride) and Zn precursor (zinc acetate to zinc chloride) [64]. The formation of the final composition of the nano-powders is, however, determined by the initial concentrations of the metal precursors in the nano-powder synthesis [65]. The molar ratios of the metal ion precursors in the synthesis solution may have an important effect on the chemical potential of each element and eventually on the phase composition of the obtained nano-materials [65]. It has been shown that the properties of CZTS like the band gap and electrical conductivity can be controlled by varying the precursor concentration ratios [66]. It was reported that the CZTS thin film with a $[\text{Cu}]/([\text{Zn}] + [\text{Sn}])$ ratio of 0.86 and $[\text{Zn}]/[\text{Sn}]$ ratio of 1.37 showed the highest photocurrent response [67]. Ping and co-workers [65] have shown that higher initial Zn concentration promotes the formation of quaternary CZTS; the results of these studies were based on the variation of $[\text{Cu}]/([\text{Zn}] + [\text{Sn}])$ ratio from 1.0 to 0.90. In order to tailor the properties of CZTS in a wider range, it would be useful to vary the initial $[\text{Cu}]/([\text{Zn}] + [\text{Sn}])$ concentration ratio in the extended range. The effect of the initial precursors' concentration in present thesis was studied at three different synthesis temperatures (215 °C, 225 °C and 235 °C) by varying the $[\text{Cu}]/([\text{Zn}] + [\text{Sn}])$ ratio from 0.33 to 0.82 [1].

The chosen synthesis temperatures are suitable for the synthesis of CZTS nano-powders in oleylamine because oleylamine shows very high stabilizing effect in this temperature range [9, 12, 34, 62].

1.5.3 The Influence of Additional Alkali Compound on CZTS Nano-powder Synthesis

The cation precursors are ordinarily added into oleylamine at room temperature and as the temperature of the mixture is increased to the synthesis temperature at a steady rate, the cation precursors start to dissolve in the solvent. As the temperature of the mixture increases, the cations of copper, zinc and tin are released into the solution, where they form complexes with the oleylamine solvent. Knowledge of the stability and behaviour of the oleylamine-cation complexes is scarce. The formed complexes are very unstable in the temperature range near the boiling point of the oleylamine solvent. Another issue is the stabilization of the oleylamine-cation complexes after the addition of sulphur-oleylamine precursor solution into the solution of the cation precursors and oleylamine. The control over morphology, elemental composition and phase composition of CZTS nano-powders in the solution-based synthesis depends on the control of complex formation and surface stabilization of nano-powders [64]. The molecule of oleylamine has two functional groups - a double bond and an amine group (see section 1.4.2.). In [68], it was shown that cesium hydroxide promotes alkylation of primary amines and suppresses over-alkylation of the produced secondary amines, being highly chemo-selective to favour mono-N-alkylation over dialkylation. Therefore, it would be important to study the effect of alkali ions on the complex formation and on the morphology, elemental and phase composition of CZTS nano-powders in more detail.

1.6 Sol-gel Method

Sol-gel processing is a wet chemical route for the synthesis of colloidal dispersions of inorganic and organic-inorganic hybrid materials [59]. Sol-gel processing offers low processing temperatures and homogeneity of the material at molecular level [59]. This method is particularly useful for making complex metal oxides, temperature sensitive organic-inorganic hybrid materials and thermodynamically unfavourable or meta-stable materials [59]. Environmentally friendly aqueous or organic solvents may be used to dissolve the cation and anion precursors in the sol-gel process [59]. There are several organic solvents available for the sol-gel method e.g. methanol, ethanol, propanol.

1.6.1 Methanol as Solvent in the Sol-gel Method

Methanol is a low-cost solvent and a good polar liquid for the preparation of individual precursor solutions as sources of cations and sulphur. The CZTS thin films were deposited by the dip coating method using precursors copper chloride, zinc chloride, tin chloride and thiourea dissolved in methanol [69]. In this thesis, the solution-based method was chosen for the synthesis of CZTS thin films as it is a simple and low-temperature deposition method. Methanol is preferred over ethanol due to higher purity and lower water contents.

1.6.2 CZTS Thin Films by the Sol-gel Method

The advantage of the sol-gel method with methanol as solvent is the possibility to deposit the colloidal solution directly onto the substrate by dip coating, doctor blading or spin coating. The nucleation and growth of CZTS nano-materials occur in the following pre-annealing and annealing stages. The sol-gel method provides direct thin

film preparation, but on the other hand, residual impurities remain in the resulting films. In the nano-powder synthesis in oleylamine the impurities are removed during purification and centrifugation stages.

The sol-gel deposition in methanol is a low temperature process (at RT) in comparison with solution-based synthesis in oleylamine (above 200 °C). Thiourea is a popular source of sulphur that can easily form complexes with Cu, Zn and Sn, which yield to sulphides on thermal decomposition [69]. Tanaka *et al.* [70] deposited CZTS thin films by spin coating of sol-gel solution of Cu (II), Zn (II) and Sn (II) salts in methoxy-ethanol with mono-ethanol amine as stabilizer. Yeh and Jiang *et al.* [71] used copper, zinc and tin chlorides and thiourea in ethanol-water sol-gel to deposit CZTS thin films by direct liquid coating method [71]. Jiang *et al.* [72] reached 0.63 % and Su *et al.* [73] gained 5.1 % of solar cell PCE. Lei Cao *et al.* [74] successfully synthesized $\text{Cu}_2\text{ZnSn}(\text{S}_{1-x}\text{Se}_x)_4$ thin films by the simple ethanol-thermal method. Chaudhari with co-authors [69] reported a simple process for deposition of pure CZTS films from a methanol solution of metal–thiourea complexes.

1.7 Summary of the Literature Overview and Aim of the Study

The studies of the synthesis of CZTS nano-powders by the hot-injection method and CZTS thin film deposition by the sol-gel method can be summarized as follows:

1. The solution-based synthesis of CZTS nano-powders has been performed at different temperatures. Different solvents used in these studies are toxic or/and non-toxic, and a wide range of different precursors have been implemented. Solid nano-particles can be separated from the liquid part of the synthesis mixture through purification and centrifugation. However, there is a need for more detailed understanding of the influence of the factors affecting the CZTS nano-powders synthesis process in order to improve their properties.
2. It is useful to study the synthesis of CZTS nano-powders in an extended range of the initial $[\text{Cu}]/([\text{Zn}] + [\text{Sn}])$ concentration ratio and the effect of it on the elemental and phase compositions and morphology of the synthesized CZTS nano-powder particles.
3. To the best of our knowledge, there is no information about the complex formation of oleylamine and alkali ions and its impact on the morphology, phase and elemental composition of CZTS nano-powders. From other studies, however, beneficial effect of the alkali ions on the homogeneous growth of nano-powders could be expected.
4. Sol-gel method is a low cost synthesis method that requires minimum experimental setup. According to our knowledge, the influence of pre-annealing in controlled gas atmosphere on the quality of CZTS thin films deposited by dip coating on different glass substrates has not been thoroughly studied. A comparative study of the CZTS thin film growth on soda lime glass, Mo or ITO substrates would be of interest. In addition, more information is needed on the effect of annealing in different environments to the properties of sol-gel deposited CZTS thin films.

Based on the main conclusions listed above, the objectives of the current doctoral thesis research were:

1. To study the influence of the initial $[\text{Cu}]/([\text{Zn}] + [\text{Sn}])$ concentration ratio on the morphology, phase composition and elemental composition of CZTS nano-powders at different synthesis temperatures.
2. To investigate the effect of oleylamine complex formation with different alkali ions (Na^+ , K^+ and Cs^+) on the CZTS nano-particles growth.
3. To analyze the influence of pre-annealing and post annealing conditions as well as the influence of used substrates (soda lime glass, Mo or ITO) on the morphology, phase and elemental composition of the resulting CZTS thin films prepared by the sol-gel method using methanol as a solvent.

2. Experimental

The experimental details of the CZTS nano-powder synthesis by the hot-injection method and the deposition of CZTS thin films by the sol-gel method in methanol are described in the following sub-sections together with the characterization methods used in this study.

2.1 Synthesis of CZTS Nano-powders by the Hot-injection Method

The solution-based hot-injection method was used in this study for the synthesis of CZTS nano-powders [I, II]. The schematic presentation of the experimental setup is shown in Figure 3.

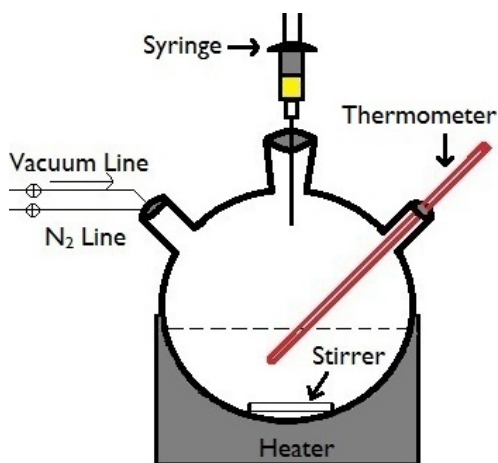


Figure 3 Experimental setup for the hot-injection method

Oleylamine (OAm) was purchased from Sigma Aldrich and used as a solvent without purification. Suitable cation precursors were selected by their solubility in oleylamine to obtain easy release of cations into the solution. The analytical grade chemicals from Sigma Aldrich - zinc acetate, copper (II) acetylacetonate, tin (II) chloride and elemental sulphur - were used as sources for Zn, Cu, Sn and S, respectively [I, II]. The initial composition of precursor mixtures -1.7 mmol of Cu, 1.08 mmol of Zn, 0.9 mmol of Sn, and 4.5 mmol of S - was kept constant for all synthesis temperatures: 215 °C, 225 °C, 235 °C and 280 °C [I, II]. The precursors of metal elements were mixed in 12 ml of oleylamine in a three-neck flask at 25 °C (see Figure 3). The temperature of the mixture was increased to the required synthesis temperature under inert gas and then sulphur component was added. For the preparation of S precursor, 0.32 g of sulphur was added to 10 ml of oleylamine and sonicated for 30 min at 70 °C. From this freshly prepared sulphur solution, 4.5 ml was taken and added to the flask containing the preheated solution of other components at required temperature. The solution mixture was continuously stirred and kept for 30 min at each synthesis temperature [I, II]. The solution mixtures were cooled down naturally to room temperature in N₂ gas environment. CZTS nano-powders were separated from the solution and cleaned by repeated centrifugation with ethanol, hexane and isopropanol, where hexane was used

for removing non-polar impurities and isopropanol for polar impurities [75]. Nano-powders were dried in a thermostat at 40 °C for 30 min [I, II].

2.2 Preparation of Precursor Solutions with Alkali Metal Compounds

The initial precursor composition of 1.7 mmol of Cu, 1.08 mmol of Zn, 0.9 mmol of Sn and 4.5 mmol of S was used for all the syntheses in this series of experiments [II]. Alkali metal containing compounds NaCl, NaOH, KCl, KOH and CsOH in amount of 0.1 mmol were used as precursors of Na⁺, K⁺ and Cs⁺ ions in the experiments. KOH (85%) and NaOH granules (98%) bought from Lach-ner, analytical grade CsOH·H₂O from Fluka and high purity NaCl (99.5%) from Merck and KCl from company REAHM were used without any purification. The effect of CsOH concentration on the morphology, phase and elemental composition of CZTS nano-powders was studied by using 0.1 mmol and 0.5 mmol additives of CsOH to see whether the influence could be enhanced with higher concentration. The used alkali containing precursor compound and Cu, Zn and Sn precursors were mixed in 25 ml of oleylamine in a three-neck flask at 25 °C (see Figure 3). The temperature of the solution was increased up to 280 °C under inert gas conditions. 4.5 ml of freshly prepared sulphur solution (preparation is described in section 2.1) was added to the flask containing oleylamine solution of other precursors at 280 °C [II].

2.3 CZTS Thin Films by the Sol-gel Method

The scheme of the thin film preparation process by the sol-gel method is shown in Figure 4.

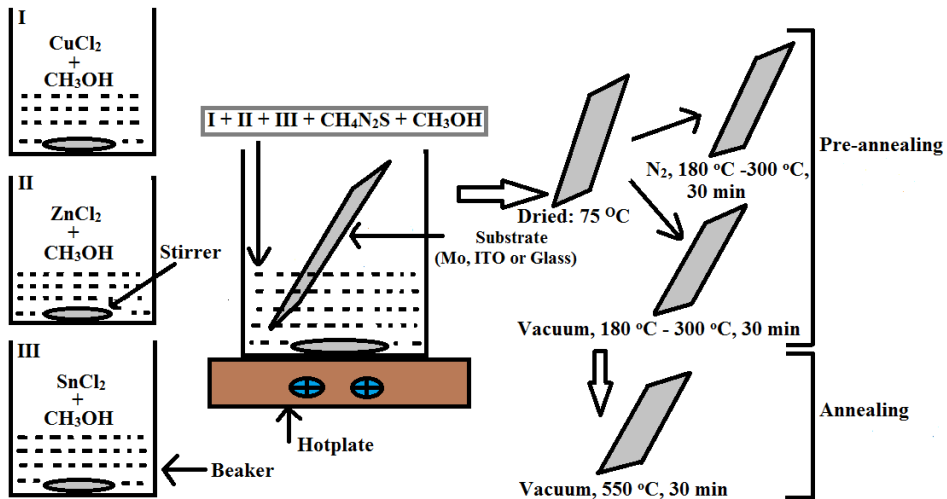


Figure 4 Scheme of the thin film preparation process by the sol-gel method

The analytical grade CuCl₂, ZnCl₂, and SnCl₂ purchased from Sigma Aldrich were used as precursor materials for metal elements. Separate precursor solutions were prepared at room temperature (25 °C) using methanol as solvent and CuCl₂, ZnCl₂, SnCl₂ and CH₄N₂S as solutes. Individually prepared precursor solutions were mixed together in a small beaker at 25 °C. Proper stirring of the solution was performed at 25 °C using a magnetic

stirrer. After 10 minutes of stirring, the substrates were dip coated in the solution and dried in air at 75 °C under ventilation. The process was repeated multiple times to increase the thickness of thin films. Three types of substrates were used: a) indium tin oxide (ITO) coated, b) molybdenum coated, and c) bare soda lime glasses. The bare soda lime glass substrates were degreased in hot sulphuric acid (45 °C). The ITO glasses were activated in the mixture of HCl, HNO₃ and H₂O (47.5, 5.0, and 47.5% by volume, respectively) [76]. The degassing of quartz ampoules was performed at room temperature [III]. The sequence and conditions of post deposition heat treatments in a horizontal tube furnace are presented in Table 1.

Table 1 Precursors' concentrations in methanol solution and post deposition heat-treatment conditions of CZTS thin films [III]

Concentration of precursors in methanol				
Precursors	CuCl ₂	ZnCl ₂	SnCl ₂	Thiourea
Concentration	0.1 mol/L	0.05 mol/L	0.05 mol/L	0.5 mol/L
Heat-treatment conditions in different environments				
Drying	In air at 75 °C			
Pre-annealing	Nitrogen atmosphere (760 Torr)		Vacuum sealed ampoules (10 ⁻² Torr)	
	180 °C, 210 °C, 240 °C, 270 °C, 300 °C for 30 min;		180 °C, 210 °C, 240 °C, 270 °C, 300 °C for 30 min;	
	Films on soda lime, Mo or ITO glass substrates		Films on Mo glass substrates	
Post-annealing	Annealing in vacuum at 550 °C for 30 min			

2.4 Characterization Methods

The methods and apparatus used for the characterization of CZTS nano-powders and thin films are summarized in Table 2.

Table 2 Methods used for the characterization of CZTS nano-powders and thin films

Properties	Characterization method	Apparatus	Ref.
Surface morphology, cross sectional view, film thickness, grain size (estimation)	SEM	ZEISS ULTRA 55 FE-SEM	I, II, III
Elemental composition	EDX	ZEISS ULTRA 55 FE-SEM, Röntec EDS XFlash 3001 detector	I, II, III
Phase composition	Raman	Horiba LabRam HR800 spectrometer	I, II, III
Functional groups	FTIR	Perkin-Elmer GX1 spectrophotometer	III

The SEM analysis was performed to investigate the morphological structure and size of the particles of nano-powders and thickness of thin films using a ZEISS ULTRA 55 FE-SEM apparatus [I, II, III]. The EDS analysis using Röntec EDS XFlash 3001 detector was used to determine the elemental composition of the studied nano-powders and thin films. The samples for the EDS analysis were prepared by pressing the nano-powders into pellets. Raman spectra were recorded using a Horiba LabRam HR800 spectrometer equipped with a multichannel CCD detection system in a backscattering configuration. Incident laser light of 532 nm was focused on different spots of the studied sample and an average of five readings was taken for every sample to obtain the objective phase composition of the studied sample [I, II, III].

The oleylamine-cation (Cu, Zn and Sn) complexes and oleylamine-cation-alkali compound complexes were studied by using Raman and FTIR analysis methods [II]. Alkali metal containing compounds NaCl, NaOH, KCl, KOH and CsOH in amount of 0.1 mmol were added to the solutions of 25 ml of oleylamine with different cation precursors (Cu, Sn, Cu-Zn, Cu-Sn and Cu-Zn-Sn) and mixed in a three-neck flask at 25 °C. Temperature of the solutions was increased to 280 °C under inert gas conditions. The solutions were kept for 30 min at 280 °C. The solutions were cooled down naturally to room temperature in inert gas environment. These freshly made solutions were used as samples for Raman and FTIR analysis. FTIR measurements were performed on Perkin Elmer GX-1 spectrophotometer [II].

3. Results and Discussion

3.1 Tailoring the CZTS Nano-particle Formation and Growth by Varying Cu and Zn Concentrations at Different Temperatures [1]

The influence of the [Cu] and [Zn] in the starting solutions on the size and shape of the CZTS nano-particles' was studied in [1]. The results of variation of [Cu]/([Zn] + [Sn]) concentration ratio from 1.0 to 0.90 in [68] showed that a higher initial Zn concentration promotes the formation of quaternary CZTS compound. Thus, we presumed that it would be useful to study the effect of more wide variation of the initial [Cu]/([Zn] + [Sn]) concentration ratio on the morphology, phase and elemental composition of CZTS nano-powders. SEM images of nano-powders synthesized at 235 °C using different [Cu]/([Zn] + [Sn]) concentration ratios are presented in Figure 5.

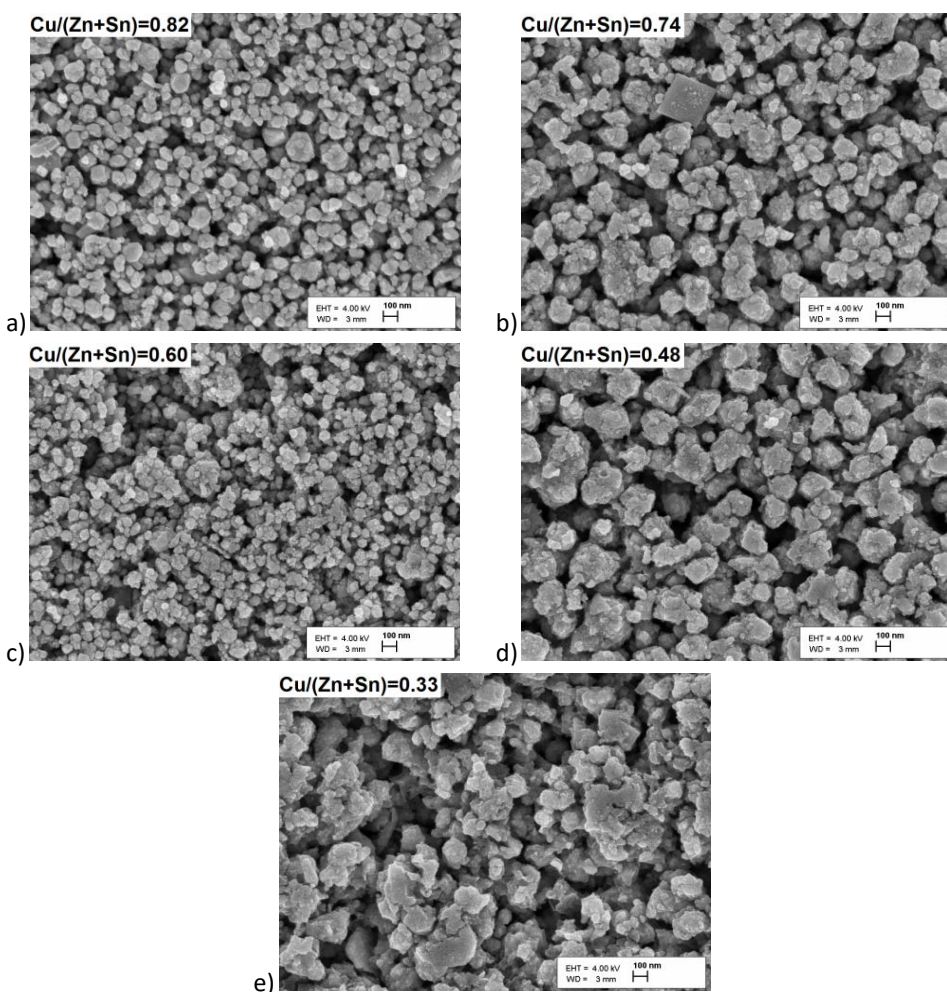


Figure 5 SEM images of the CZTS nano-powders synthesized at 235 °C with varying initial [Cu]/([Zn] + [Sn]) concentration ratio: a) 0.82, b) 0.74, c) 0.60, d) 0.48 and e) 0.33. (A modified version of Figure 3 in [1]).

The CZTS nano-powders were synthesized at 215 °C and 225 °C with varying the initial concentration ratio of precursors $[Cu]/([Zn] + [Sn])$ (i.e. 0.82, 0.74, 0.60 and 0.48) [1]. SEM images of nano-powders are presented in Figure 6 and Figure 7, where large variation in the size of nano-powders from 20 nm to 150 nm can be seen [1]. Decreasing Cu concentration with increasing Zn concentration causes the formation of agglomerated nano-powders with sizes from 2 μm to few μm (see Figure 6f) [1].

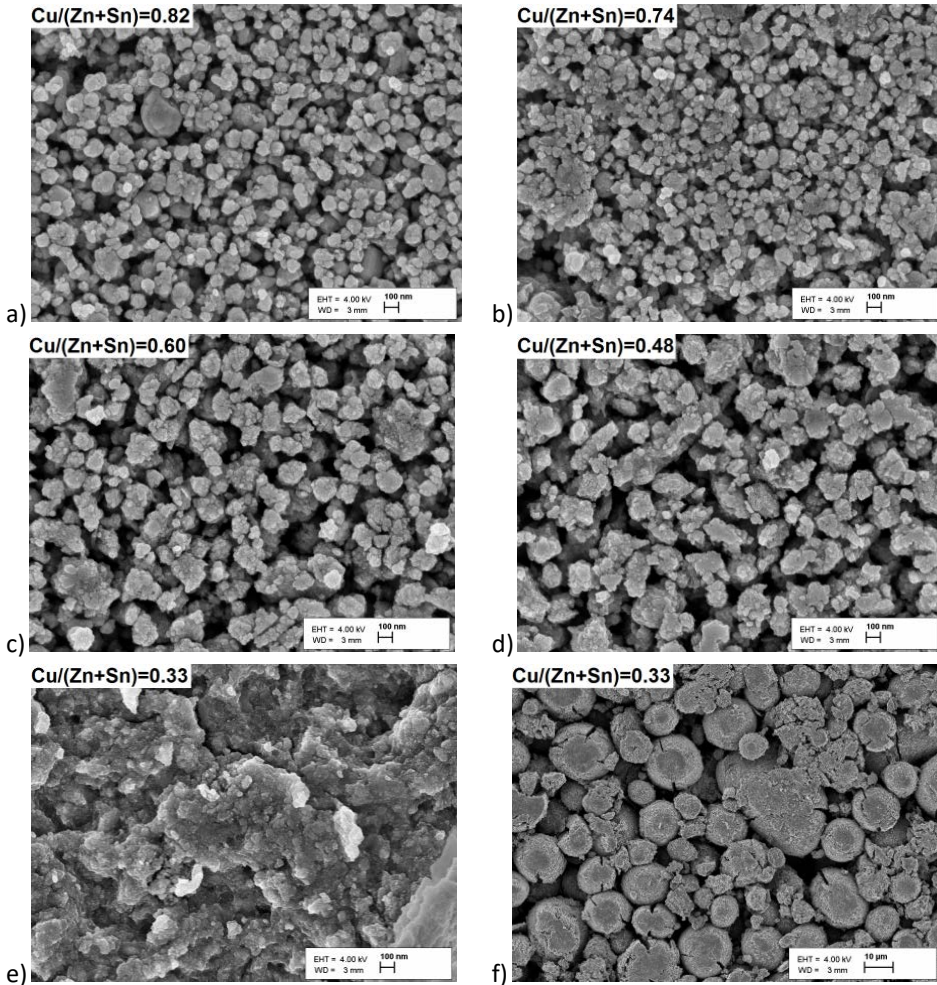


Figure 6 SEM images of CZTS nano-powders synthesized at 215 °C with varying initial $[Cu]/([Zn] + [Sn])$ concentration ratio: a) 0.82, b) 0.74, c) 0.60, d) 0.48, e) 0.33 (Scale: 100 nm) and f) 0.33 (Scale: 10 μm). (A modified version of Figure 1 in [1]).

For the CZTS nano-powders synthesized at 235 °C with initial precursor $[Cu]/([Zn] + [Sn])$ ratio equal to 0.33 the average size of agglomerated nano-powders is few μm (see Figure 5e). The agglomerated nano-powders were synthesized at all three different synthesis temperatures i.e. 215 °C, 225 °C and 235 °C with initial precursor $[Cu]/([Zn] + [Sn])$ ratio lower than 0.82. In the case of $[Cu]/([Zn] + [Sn]) = 0.82$, the size of nano-powders was in the range from 20 nm to 100 nm.

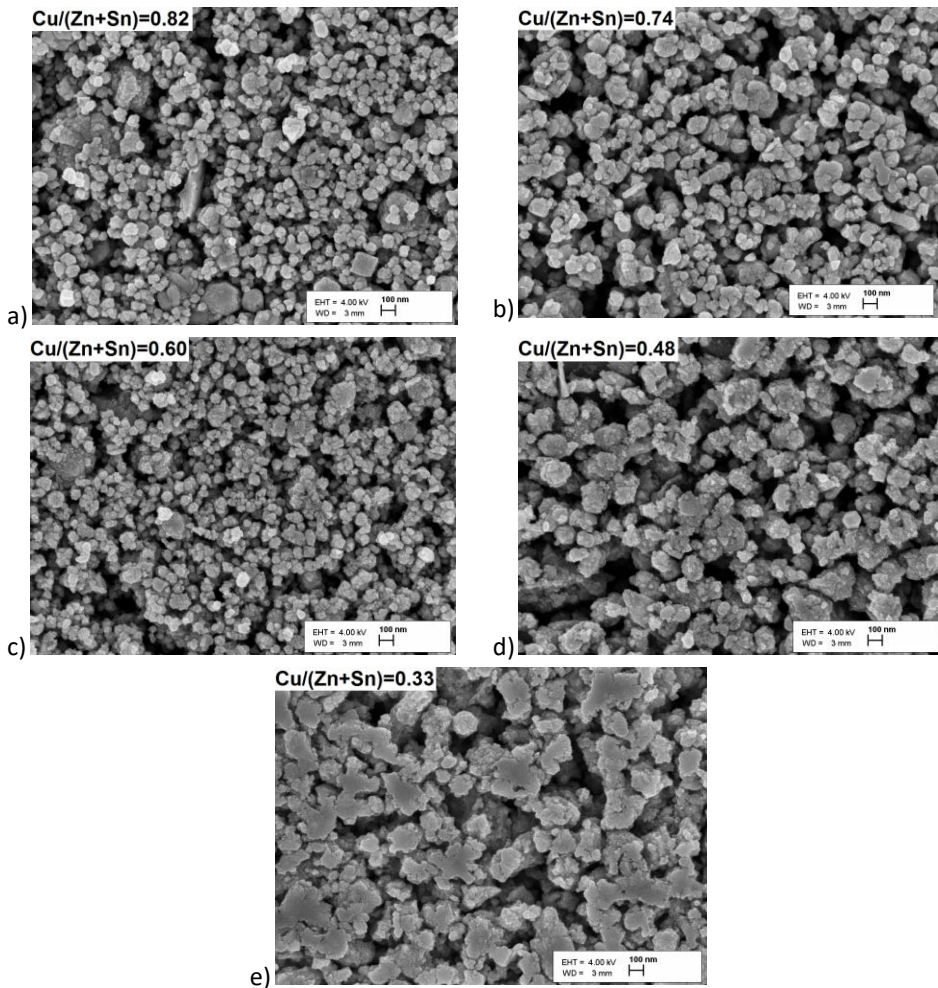


Figure 7 SEM images of CZTS nano-powders synthesized at 225 °C with initial $[\text{Cu}]/([\text{Zn}] + [\text{Sn}])$ concentration ratio: a) 0.82, b) 0.74, c) 0.60, d) 0.48 and e) 0.33. (A modified version of Figure 2 in [1]).

The analysis of EDS results showed that elemental composition of CZTS nano-powders synthesized at 215 °C, 225 °C and 235 °C with initial precursor $[\text{Cu}]/([\text{Zn}] + [\text{Sn}])$ ratios 0.82 and 0.74 was near-stoichiometric. The final concentration of copper varied with the varying initial copper concentration and as initial zinc concentration was increased, a respective increase in the final zinc concentration of nano-powders was detected. The following trends were observed in the elemental composition of the agglomerated nano-powders: with the increase in the initial zinc concentration, the final concentration of tin decreased when the initial $[\text{Cu}]/([\text{Zn}] + [\text{Sn}])$ precursor concentration ratio was equal to 0.82 and 0.74. This shows that the increase in the initial zinc concentration not only increased the chemical potential of zinc but also decreased the chemical potential of tin. With copper-poor initial compositions (relative to stoichiometric composition), the chemical potential of copper stayed unaffected by the increase in the initial zinc concentration. The concentration of sulphur with respect

to the sum of metal ions, $[S]/([Cu] + [Zn] + [Sn])$ remained stoichiometric at all the used initial precursor concentration ratios ($[Cu]/([Zn] + [Sn]) = 0.82, 0.74, 0.60, 0.48$ and 0.33) and at all the used synthesis temperatures ($215\text{ }^{\circ}\text{C}$, $225\text{ }^{\circ}\text{C}$ and $235\text{ }^{\circ}\text{C}$) [1].

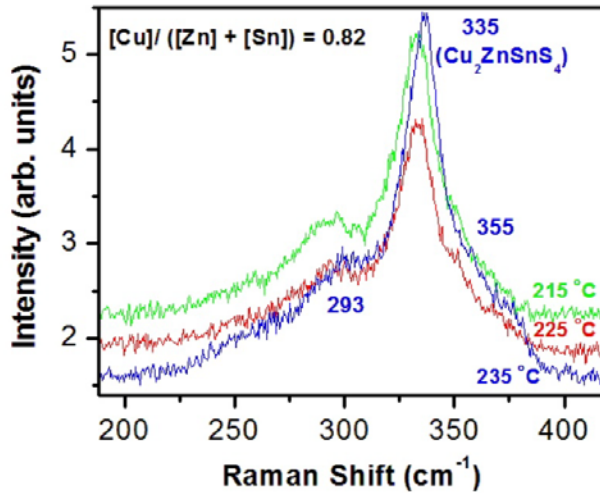


Figure 8 Raman spectra of nano-powders synthesized with initial concentration ratio $[Cu]/([Zn] + [Sn]) = 0.82$ at $215\text{ }^{\circ}\text{C}$, $225\text{ }^{\circ}\text{C}$ and $235\text{ }^{\circ}\text{C}$ (A modified version of Figure 5 in [1]).

Raman spectra of CZTZ nano-powders synthesized from solutions with constant initial concentration ratio of $[Cu]/([Zn] + [Sn]) = 0.82$ at different temperatures are presented in Figure 8 and Raman spectra of powders synthesized at constant temperature of $235\text{ }^{\circ}\text{C}$ with different initial $[Cu]/([Zn] + [Sn])$ concentration ratios are presented in Figure 9. The dominating Raman peak of the nano-powders synthesized with the initial concentration ratio of $[Cu]/([Zn] + [Sn]) = 0.82$ shifted from 333 cm^{-1} to 335 cm^{-1} as the synthesis temperature increased from $215\text{ }^{\circ}\text{C}$ to $235\text{ }^{\circ}\text{C}$ (see Figure 8). Similar Raman shift from 333 to 337 cm^{-1} was also observed when the $[Cu]/([Zn] + [Sn])$ ratio decreased from 0.82 to 0.33 at the synthesis temperature of $215\text{ }^{\circ}\text{C}$. At the same time, with the shift of the most intense Raman peak, the EDS analysis showed higher zinc concentration in the formed nano-powders.

From these findings, the following conclusion can be derived: the insertion of higher Zn concentration into the product nano-powders (on the basis of EDS data) is possible by two ways: first, with higher synthesis temperature, and second, by higher initial zinc concentration in initial precursors creating high chemical potential of zinc in the solution. Raman peaks in the spectra of CZTS nano-powders synthesized at $235\text{ }^{\circ}\text{C}$ for $[Cu]/([Zn] + [Sn])$ ratio of 0.82 (and 0.74) were detected at 335 cm^{-1} , 293 cm^{-1} and 355 cm^{-1} , which correspond to $\text{Cu}_2\text{ZnSnS}_4$ [1, 59, 77, 78]. Raman peaks of nano-powders produced at $235\text{ }^{\circ}\text{C}$ using lower $[Cu]/([Zn] + [Sn])$ ratios ($0.60, 0.48$ and 0.33) were detected at 335 cm^{-1} and 358 cm^{-1} that correspond to $\text{Cu}_2\text{ZnSnS}_4$, and additional Raman peak at 301 cm^{-1} that could correspond to Cu_2SnS_3 or other ternary sulphides [1, 59, 77, 78] that can form in this temperature region according to the phase diagram (see Figure 1).

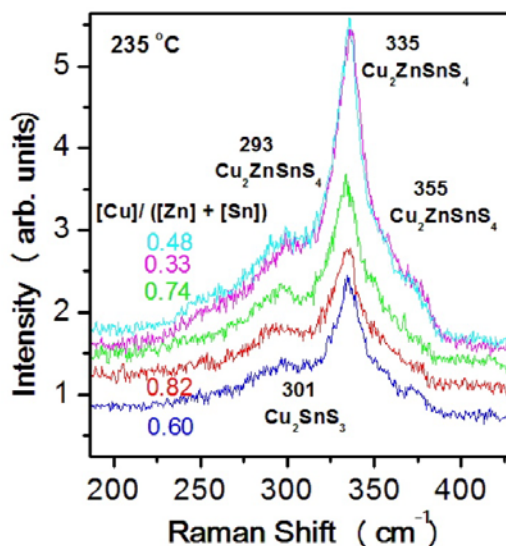


Figure 9 Raman spectra of nano-powders synthesized with different initial $[Cu]/([Zn] + [Sn])$ concentration ratios at 235 °C (A modified version of Figure 6 in [1]).

The shift of the peaks towards a higher wave number side is accompanied with the decrease in the full width at half maxima (FWHM) of the Raman peaks, showing improved crystallinity of nano-powders [1]. The changing positions of the Raman peaks at the wave numbers corresponding to CZTS and Cu_2SnS_3 indicate that most probably the powders are a mixture of these two phases, CZTS prevailing at higher temperatures and at lower $[Cu]/([Zn] + [Sn])$ ratios [1].

By varying the initial precursor concentration ratio $[Cu]/([Zn] + [Sn])$ from 0.82 to 0.33 in the synthesis of CZTS nano-powders in the temperature range from 215 °C to 235 °C, it was found that the average size of the formed nano-powders increased from 20 nm to 1 μm with the decreasing initial $[Cu]/([Zn] + [Sn])$ concentration ratio in the formed mixture of co-existing Cu_2ZnSnS_4 and Cu_2SnS_3 phases where the part of Cu_2ZnSnS_4 was prevailing at higher temperatures [1]. The elemental composition of the formed nano-powders was compatible to near-stoichiometric CZTS at initial $[Cu]/([Zn] + [Sn])$ concentration ratios 0.82 and 0.74 [1].

3.2 Effect of Alkali Ions (Na^+ , K^+ , Cs^+) on the Reaction Mechanism of CZTS Nano-particle Synthesis [II]

3.2.1 Analysis of FTIR Spectra of Oleylamine and Oleylamine-Cation Precursors

The FTIR spectra of oleylamine and solutions of oleylamine with different metal precursors are shown in Figures 10, 11 and 12. The FTIR absorption peak positions together with the corresponding vibrational assignments are presented in Table 4. The FTIR spectrum of oleylamine shows absorption peaks at 722, 794, 967, 1071, 1312, 1378, 1463 and 1651 cm^{-1} (see Figure 13). In the FTIR spectra of oleylamine-metal precursor solutions, peaks at lower wavelength side (below 700 cm^{-1}) due to the components of precursor compounds and oleylamine are also detected. The FTIR

absorption peak of oleylamine at 1071 cm^{-1} corresponds to the bending vibration of carbon-nitrogen (C-N) bond [II, 79, 80, 81].

Table 4 Vibrational assignments of IR absorption peaks [II]

Solution	FTIR peak positions (cm^{-1})												Ref.
Vibrational Modes → Solutions ↓	ν_{as} C-Sn	ν_{s} C-Cu	ν Sn-Cu, Cu-Zn	δ C-C	δ NH ₂ , ν NH ₂	Wagging (NH ₂), δ N-Cs	δ C-N	δ Cu-N	ν C-Sn, Sn-Cu, Sn-Zn	δ CH ₃	δ C=C	ν C-Cu, Sn,Zn ν N-Cu	[II, 85]
OAm				722	795 1593		1071			1465	1647		[79, 80, 81, 82]
OAm				722	794	967	1071			1463	1651		[II]
OAm-Cu		532			795 1605	967		1129				1553 1670	[II]
OAm-Cu+Zn		534	606 618		795	967						1555 1666	[II]
OAm-Sn	528 535 [83]				795	967			1341 1396			1510 1673	[II]
OAm-Cu+Zn+Sn	528 [83]		601 670		795	967			1339 1398			1510 1553 1666- 1673	[II]
OAm-CsOH						967 985							[II]

ν -symmetric or asymmetric vibrations, ν_{s} -symmetric vibrations, ν_{as} -asymmetric vibrations, δ -bending vibrations

The FTIR absorption spectrum of oleylamine-copper precursor solution shows absorption peaks at 532, 721, 795, 967, 1129, 1403, 1553, 1615 and 1670 cm^{-1} (see Figure 10). Instead of the peak at 1071 cm^{-1} , due to the C-N bending vibrations, as was observed in pure oleylamine, a shifted FTIR absorption peak at 1129 cm^{-1} was detected, most probably because of the formation of oleylamine carbon-copper bond and the formed complex of oleylamine-copper-NH₂ group (see Figure 10). The absorption peak at 1593 cm^{-1} corresponds to the bending of the NH₂ group in oleylamine [II, 81, 82]; while in oleylamine copper precursor solution, this peak is broad and less intense and is disappearing due to the weak bond between the copper and NH₂ group. The two additional absorption peaks at 1670 cm^{-1} and 1553 cm^{-1} correspond to the vibrations of oleylamine carbon-copper and oleylamine nitrogen-copper bond. The FTIR absorption spectrum of the oleylamine solution with copper and zinc precursors shows peaks at 534, 606, 618, 721, 795, 967, 1555, and 1666 cm^{-1} (see Figure 10). Peaks at 606 and 618 cm^{-1} appeared with addition of Zn precursor. Probably the mechanisms of complex formation in the oleylamine-copper and oleylamine-copper-zinc solutions are similar.

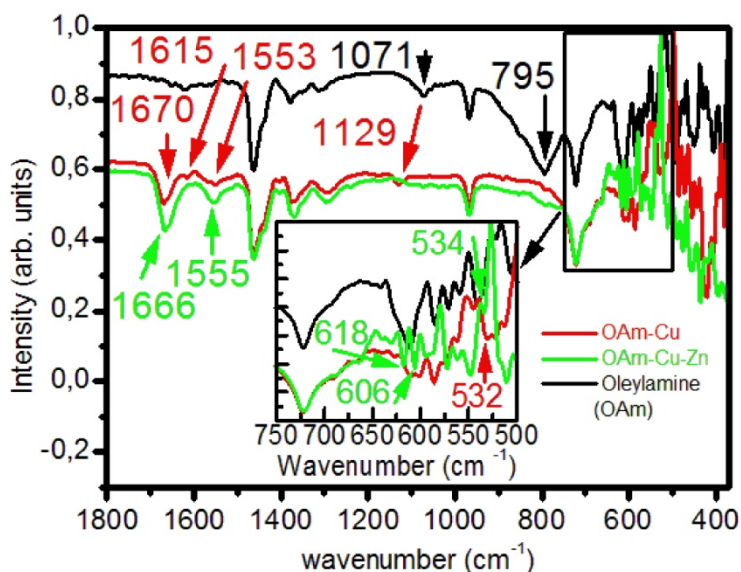


Figure 10 FTIR spectra of oleylamine, oleylamine-copper and oleylamine-copper-zinc precursor solutions.

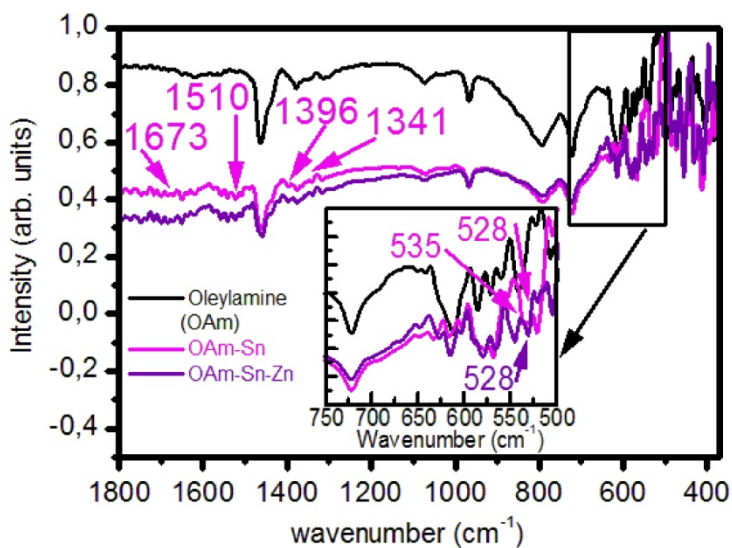


Figure 11 FTIR spectra of oleylamine, oleylamine-tin and oleylamine-tin-zinc precursor solution.

The FTIR absorption spectrum of oleylamine-tin precursor solution shows absorption peaks at 528, 535, 721, 795, 967, 1341, 1396, 1510 and 1673 cm^{-1} (see Figure 11). The new bond forms probably between oleylamine carbon and tin (see Figure 12) without affecting the amine group in oleylamine. The carbon nitrogen bending vibrations (1071 cm^{-1}) and wagging vibrations (967 cm^{-1}) of the amine (NH_2) group in oleylamine

were unaffected [II]. The FTIR absorption peak related to the oleylamine carbon-tin bond in the oleylamine tin precursor solution is at 528 and 535 cm^{-1} [83].

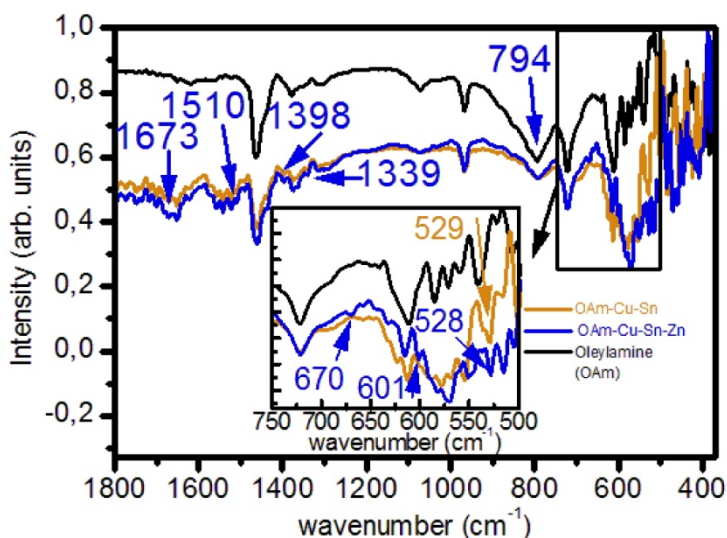


Figure 12 FTIR spectra of oleylamine, oleylamine-copper-tin and oleylamine-copper-tin-zinc precursor solution.

In the presence of zinc and tin precursors in oleylamine, carbon-tin-zinc- NH_2 complex is formed because FTIR spectrum shows no changes in the absorption behaviour of amine group. The FTIR spectrum of the oleylamine-copper-zinc-tin solution shows peaks at 528, 601, 670, 1339, 1398, 1510, 1553 and 1673 cm^{-1} . The FTIR absorption peak at 528 cm^{-1} is related to the oleylamine carbon-tin bond, as it was found in [83] in the oleylamine-tin precursor solution (see Figure 12) [II]. The two additional absorption peaks that appeared at 1666 - 1673 cm^{-1} and 1552 - 1555 cm^{-1} could correspond to the carbon-metal and nitrogen-metal bonds. The changes in the FTIR spectra enable us to conclude that the oleylamine carbon-tin-copper-zinc- NH_2 complex was formed and most probably this is the nuclei for the CZTS crystal formation and growth after the addition of the sulphur-in-oleylamine precursor solution [II].

3.2.2 Analysis of FTIR Spectra of Oleylamine, Oleylamine-Cation Precursors and Oleylamine-Alkali Compounds

The FTIR spectra of oleylamine, oleylamine- NaOH , oleylamine- KOH , oleylamine- CsOH , oleylamine- NaCl and oleylamine- KCl are shown in Figure 13. The addition of NaCl , KCl , NaOH and KOH did not lead to changes in the corresponding FTIR spectra. With the addition of caesium hydroxide absorption peak at 985 cm^{-1} appears. In the case of the solution of oleylamine- CsOH , the absorption peak at 967 cm^{-1} corresponds to NH_2 wagging and the peak at 985 cm^{-1} can be attributed to the complex formation of caesium hydroxide and amine group (see Figure 14) [II, 81, 82]. The FTIR spectra of oleylamine-metal precursor solutions show no absorption peaks at 985 cm^{-1} while this peak is present only in the FTIR spectra of oleylamine- CsOH-Cu-Sn-Zn precursor solution (see Figure 15) [II]. As we can see later, CZTS nano-powders with rather large

nano-particles of uniform size grow from the CsOH containing solution (see Figure 17) [II]. Therefore, we can assume that the formed oleylamine-caesium hydroxide complex improves the stabilizing properties of oleylamine.

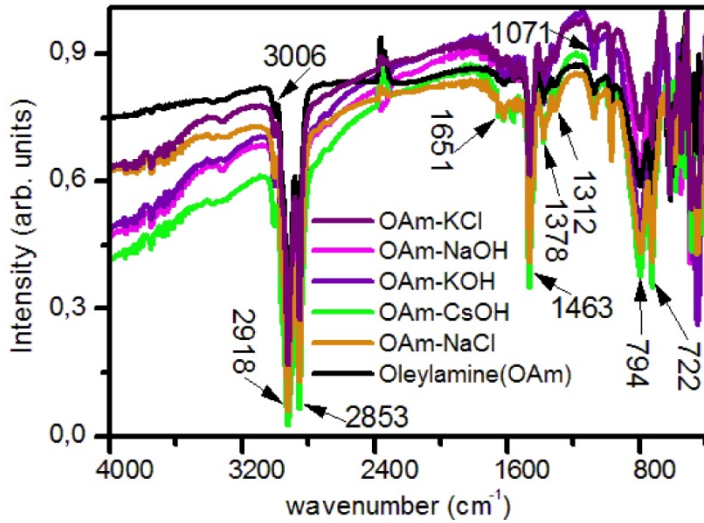


Figure 13 FTIR spectra of Oleylamine (OAm), OAm-CsOH, OAm-NaOH, OAm-KOH, OAm-NaCl, and OAm-KCl precursor solutions (A modified version of Figure 4 in [II]).

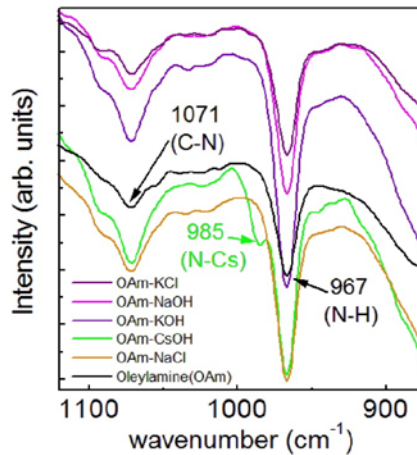


Figure 14 FTIR spectra of Oleylamine (OAm), OAm-CsOH, OAm-NaOH, OAm-KOH, OAm-NaCl, OAm-KCl precursor solutions. The additional absorption peak at 985 cm^{-1} corresponding to caesium hydroxide and amine group complex is observed for the solution of oleylamine-CsOH (A modified version of Figure 4 in [II]).

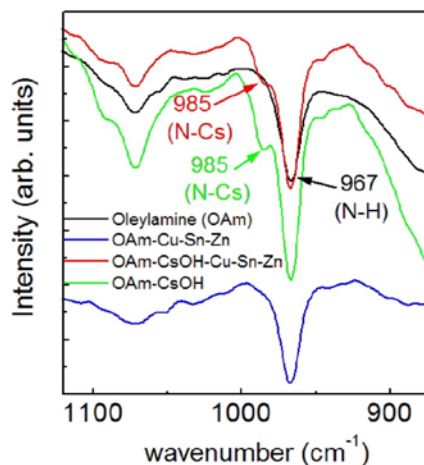


Figure 15 FTIR spectra of Oleylamine (OAm), OAm-CsOH, OAm-Cu-Sn-Zn, OAm-CsOH-Cu-Sn-Zn precursor solutions. The absorption peak at 967 cm^{-1} corresponds to NH_2 wagging and absorption peak at 985 cm^{-1} corresponds to complex of oleylamine-CsOH-Cu-Sn-Zn (A modified version of Figure 5 in [II]).

The FTIR studies show that complexes between oleylamine and cation atoms or groups of cation atoms (Cu, Sn, Cu-Zn, Cu-Sn and Cu-Zn-Sn) in the oleylamine-metal precursor solutions were formed. The oleylamine as solvent and surfactant has been used in different syntheses and it was shown that oleylamine forms complexes with cation and/or anion atoms in the syntheses of nano-particles of pure elements and compounds [80, 81, 84]. Cation atoms or a group of cation atoms can attach to oleylamine nitrogen or oleylamine carbon next to the nitrogen in the oleylamine structure [II]. The FTIR studies of the oleylamine-copper-zinc-tin solution show that the Sn atom is attached to the carbon atom of the oleylamine and the other cation atoms (Cu, Zn) form bonds with Sn atom or carbon atom [II]. At $280\text{ }^\circ\text{C}$ these cation atoms absorbing energy in the form of kinetic or thermal energy can get released into the solution by breaking bonds or are rearranged in the same metal oleylamine complex [II]. The stepwise details of the reaction mechanism of CZTS nucleation and growth will be presented and explained as chemical equations in the next section of this thesis. There are two possible ways of decomposition or deterioration of the metal oleylamine complex: a) formed metal oleylamine complex releases a cation atom or a group of cation atoms into the solution, b) formed metal oleylamine complex releases or reorganizes the cation atom or a group of cation atoms in the same oleylamine complex by changing the coordination with carbon and/or nitrogen [II].

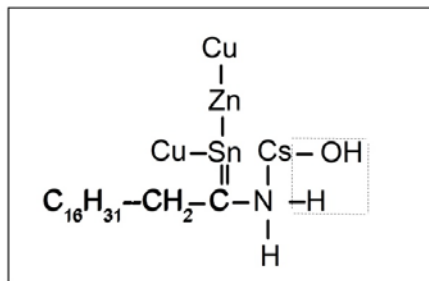


Figure 16 The oleylamine-metal complex with CsOH (Figure 10 in [II])

We propose the formation of the complex of oleylamine-caesium hydroxide and metal precursors (see Figure 16) [II]. If CsOH is present, the oleylamine nitrogen site is blocked by forming the bond between the caesium and nitrogen atoms [II]. When the oleylamine nitrogen atom is blocked due to the caesium nitrogen bond formation, the Cu, Zn and Sn cation atoms attach to the carbon atom [II]. The cation atoms attached to the oleylamine carbon atom give higher stability to the cation metal-oleylamine complex [II]. The cation metal-oleylamine complex is stabilized and the number of nuclei of different phases is reduced, leading towards the growth of the limited phases [II]. This is the nuclei for the CZTS crystal formation and growth after the addition of the sulphur-in-oleylamine precursor solution [II].

3.2.3 Analysis of CZTS Nano-powders Synthesized in the Presence of Alkali Compounds

SEM images of CZTS nano-powders synthesized in the oleylamine solvent in the presence of alkali salts (NaCl and KCl), alkali hydroxides (NaOH, KOH and CsOH) and without any salt are presented in Figure 17 [II]. Nano-powders synthesized in the presence of Na⁺ and K⁺ ions show two size ranges - small nano-powders with medium size around 18 nm, large aggregates of nano-powders larger than 100 nm (see Figure 17) [II].

Nano-powders synthesized in the presence of Cs⁺ ions (CsOH) show only one size range of nano-powders - uniform nano-powders in the range of 100 nm - 200 nm [II]. The nano-powders formed in the presence of sodium and potassium compounds show large agglomerates of nano-particles (see Figure 17) whereas no such agglomeration was observed in the powders synthesized in the presence of caesium hydroxide [II]. The above described observation could be interpreted as an effect of enhanced stabilization ability of oleylamine in the presence of intermediate caesium-oleylamine complex, supporting the diffusion limited growth (i.e. formation of homogeneous nano-powders) and reducing the further poly-nucleation and aggregation of nano-particles [II].

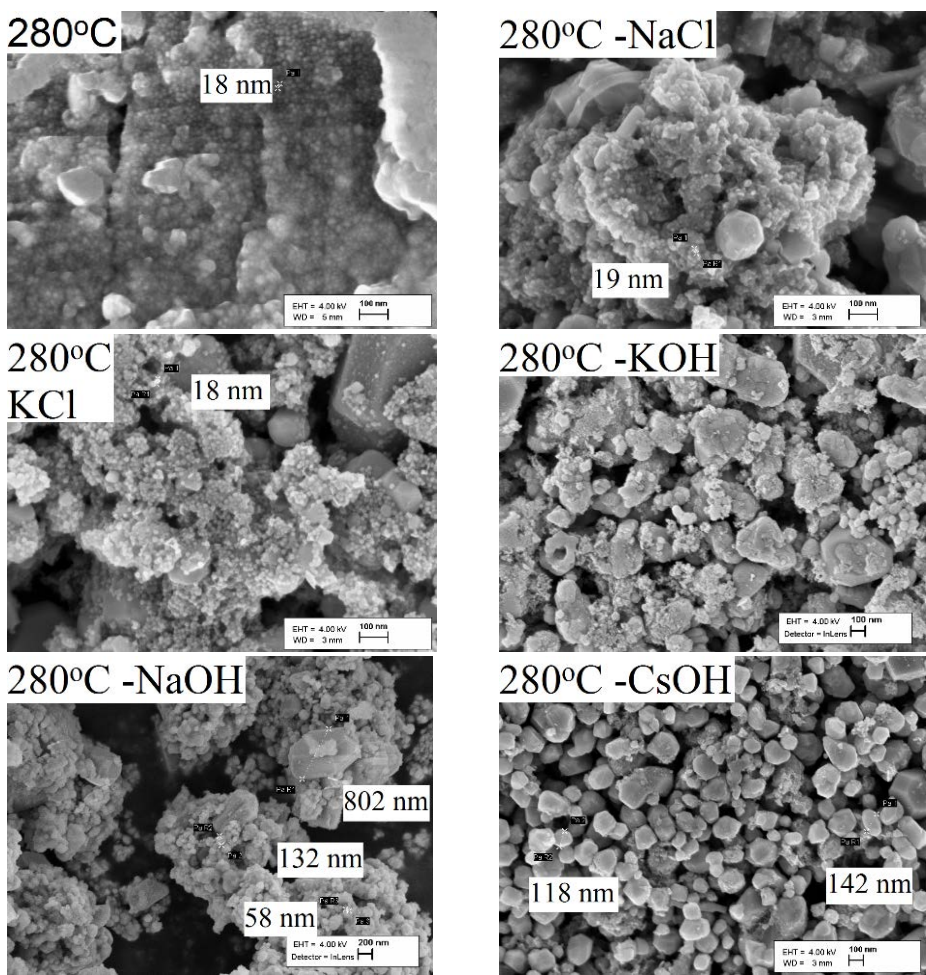


Figure 17 SEM images of CZTS nano-powders synthesized in the oleylamine solvent in the presence of 0.1 mmol of alkali salts and/or alkali hydroxides (Figure 8 in [II]).

3.2.4 Effect of Concentration of CsOH

To see whether the beneficial effect of CsOH could be enhanced with increased amount of CsOH in the synthesis solution, different initial concentrations of CsOH (0.1 mmol and 0.5 mmol of CsOH) were added into oleylamine in the synthesis of CZTS nano-powders at 280 °C [II]. Figure 18 shows SEM images of the resulting CZTS nano-powders [II]. It can be observed that higher concentration of CsOH enhances the homogeneous growth of nano-powders [II].

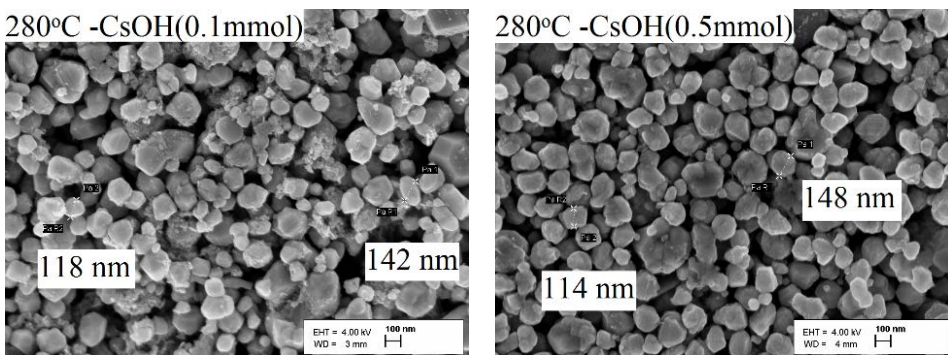
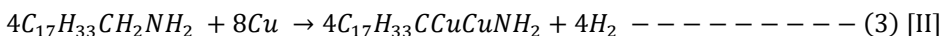
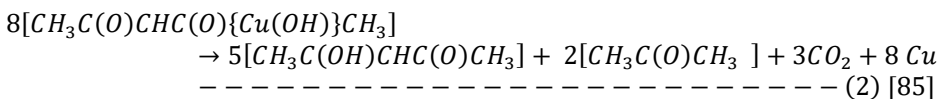
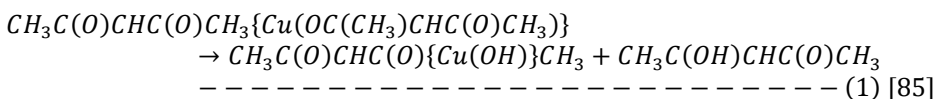
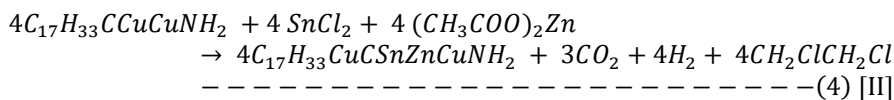


Figure 18 CZTS nano-powders synthesized at 280 °C with 0.1 mmol and 0.5 mmol of Caesium hydroxide in oleylamine (Figure 11 in [II]).

We have proposed the possible chemical equations for the interactions and complex formation between solvent oleylamine, copper 2, 4-pentanedionate, zinc acetate and tin (II) chloride before addition of the sulphur precursor solution [II]. As shown by the thermal decomposition studies in the work [85], copper 2, 4-pentanedionate (copper (II) acetylacetonate) decomposes in two steps in the temperature region from 170 °C to 250 °C. In the first step, acetyl-acetone ($C_5H_8O_2$) separates and the remained part of the molecule ($C_5H_8O_3$) decomposes with the reduction of Cu(II) to Cu(0) and oxidation of the ligands to CO_2 and produces acetone ($H_4C_6O_2$) by the reactions (1) and (2) [85]:

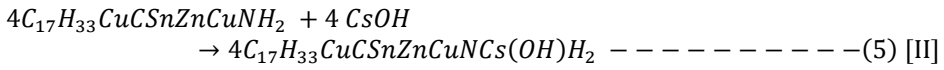


Cu(0) atoms attach to carbon in the chain of oleylamine by replacing 2 hydrogen atoms and Cu(0) is changed to Cu(I) as is described by the chemical equation (3) [II]. In the next stage, Sn(II) forms a single bond with oleylamine carbon and copper (C-Sn-Cu) [II]. Atoms are rearranged and Sn(II) state is converted to Sn(IV), forming a double bond with carbon atom (C=Sn), because of very high coordinating power of Sn and high stability of the formed complex [II]. In the next stage, zinc atom is inserted into the oleylamine chain as Zn(II) forms a metal-oleylamine complex (see Figure 16) [II].

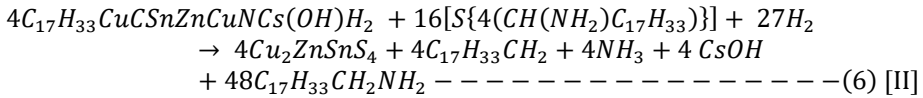


The amine group in the oleylamine is still active in the metal-oleylamine complex and needs to be further stabilized. The CsOH plays the role of an amine group stabilizer in such a complex of oleylamine-metal-caesium hydroxide (see structure of a complex

in Figure 16) [II]. There is a high possibility that CsOH forms a complex with oleylamine before any attachment of Cu, Zn, Sn elements; in this way, it maximizes the possibility of forming a bond with carbon not nitrogen in oleylamine [II]:



After addition of the oleylamine-sulphur solution into the three-neck flask, the formed metal nuclei react with sulphur to form CZTS nano-crystals:



To summarize, the influence of alkali compound additives in oleylamine on the morphology, phase and elemental composition of CZTS nano-powders was studied [II]. The formation of an oleylamine-alkali hydroxide-cation complex is proposed [II]. We found that only CsOH had effective influence on the CZTS nano-particle growth, leading to the formation of nano-particles of homogeneous size [II]. It was found that the increased concentration of CsOH further enhanced the homogeneous growth of CZTS nano-powders [II].

3.3 CZTS Thin Films by the Sol-gel Method [III]

The influence of pre-annealing and post annealing conditions as well as the influence of used substrates (soda lime glass, Mo or ITO) on the morphology, phase and elemental composition of the resulting thin films prepared by the sol-gel method using methanol as solvent was studied.

3.3.1 Morphology and Elemental Composition of Films Pre-annealed in Nitrogen

The thickness of uniform as-deposited CZTS thin films could be increased by multiple dip coating of thin films, as shown in Figure 19 [III].

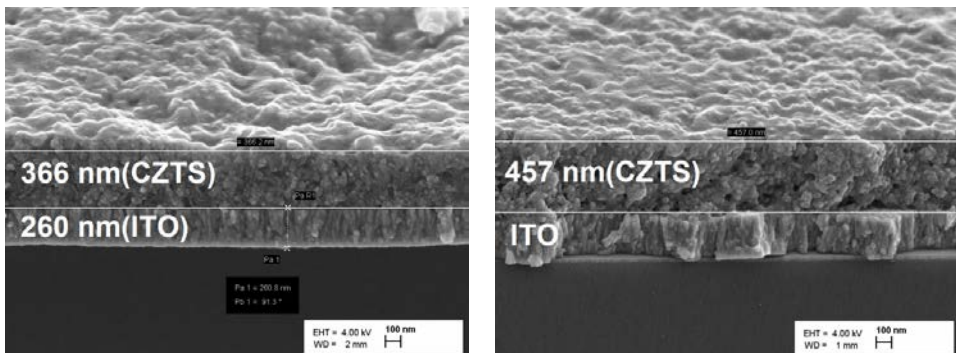


Figure 19 Thickness of as-deposited thin films on ITO: left – dipping for 1 min into solution; right – 3 times for 1 min dip coated (A modified version of Figure 1 in [III]).

The EDS results show that the compositions of CZTS thin films on different substrates (ITO and Mo covered glass - Cu: Zn: Sn: S = 2.09: 1: 1.1: 4.8) and soda lime glass (Cu: Zn: Sn: S = 1.7: 1: 1.4: 3.2) are different probably due to more effective adhesion of the metal thiourea complex gel with Mo and ITO covered glass substrates [III]. The compositions of the CZTS thin films deposited on Mo and ITO coated glass substrates and pre-annealed in nitrogen atmosphere at 240 °C are close to the stoichiometric composition of Cu_2ZnSnS_4 in comparison with the films deposited onto the bare soda-lime glass substrate [III].

3.3.2 Raman Studies of CZTS Thin Films Pre-annealed in Nitrogen

Raman spectra of CZTS thin films deposited onto Mo and ITO coated glass substrates and pre-annealed at 240 °C in nitrogen atmosphere consisted of peaks at 328 cm^{-1} , 293 cm^{-1} and 352 cm^{-1} that correspond to Cu_3SnS_4 and ZnS phases, respectively (see Figure 20) [III, 28, 72, 86].

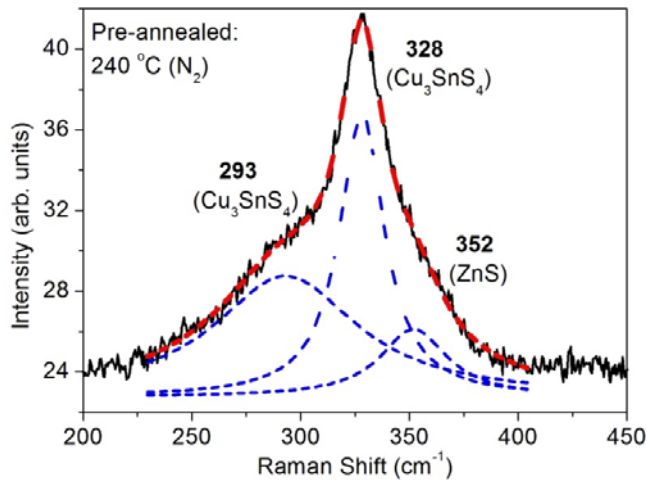
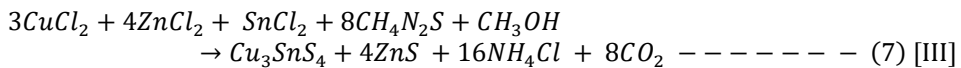


Figure 20 Raman spectra of thin films on Mo coated glass substrate and pre-annealed in nitrogen atmosphere at 240 °C (A modified version of Figure 5 in [III]).

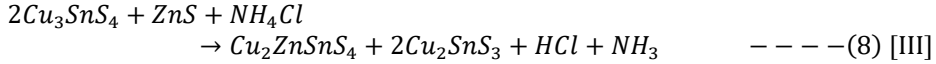
Therefore, the chemical reaction taking place during the pre-annealing of as-deposited thin films on ITO and Mo coated glass substrates in nitrogen atmosphere could be given as shown below, resulting in the formation of Cu_3SnS_4 and ZnS phases (Eq. 7) [III]. The decomposition of ammonium chloride into ammonia and hydrogen chloride gases removes the salt from thin films above 338 °C [87]. The formed gaseous carbon dioxide is easily evaporated from thin films.



Raman spectra of CZTS thin films deposited onto Mo and ITO covered glass substrates followed by pre-annealing at 240 °C in nitrogen atmosphere and post-annealing at 550 °C in vacuum sealed ampoules consisted of peaks at 338 cm^{-1} , 349 cm^{-1}

and 301 cm⁻¹ that correspond to Cu₂ZnSnS₄ (338 cm⁻¹, 349 cm⁻¹) and Cu₂SnS₃ phases, respectively (see Figure 21) [III, 28, 72].

The probable chemical reaction in thin films during the annealing at 550 °C is the conversion of ternary Cu₃SnS₄ and binary ZnS phase into quaternary Cu₂ZnSnS₄ and ternary Cu₂SnS₃ phases (Eq. 8) [III]:



The following formation pathway of Cu₂ZnSnS₄ thin films in nitrogen atmosphere on Mo and ITO coated glass substrates can be proposed [III]:

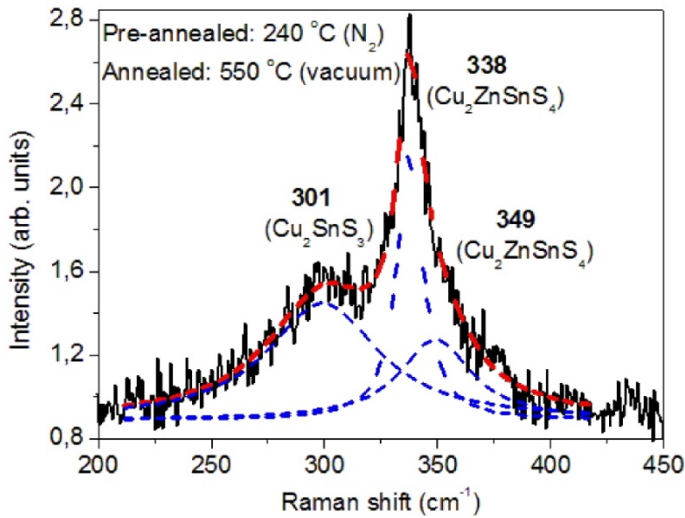
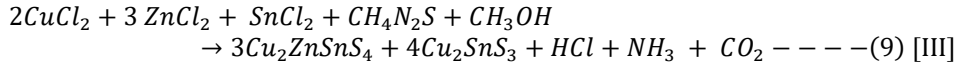


Figure 21 Raman spectrum CZTS thin film on Mo glass substrate pre-annealed in nitrogen atmosphere and post-annealed at 550 °C in vacuum sealed ampoules (A modified version of Figure 6 in [III]).

3.3.3 Vacuum Annealed CZTS Thin Films

The as-deposited CZTS thin films were dried and pre-annealed at various temperatures: 180 °C, 210 °C, 240 °C, 270 °C and 300 °C in vacuum sealed ampoules followed by the second step annealing at 550 °C in the same closed ampoules [III]. The SEM images of thin films are shown in paper [III]. Thin films on Mo covered glass substrates pre-annealed and post-annealed in vacuum sealed ampoules showed lots of cracks on the surface while thin films prepared in nitrogen atmosphere showed few cracks and uniform morphology [III]. Raman spectra of thin films pre-annealed at different temperatures are presented in paper [III]. Raman peak positions observed in CZTS thin films on Mo, pre-annealed at 180 °C and 210 °C in vacuum sealed ampoules are at 306 - 309 cm⁻¹ and 330 cm⁻¹, which could correspond to binary and ternary sulphides of

copper and tin [III, 28, 78]. Raman peak positions observed in CZTS thin films on Mo covered glass substrates, pre-annealed at 240 °C and 270 °C in vacuum sealed ampoules are at 317 cm^{-1} and 321 cm^{-1} , which could correspond to ternary sulphide of copper and tin [III, 28, 78].

To summarize, the formation pathway of CZTS thin films on Mo or ITO covered glass and soda lime glass substrates by the sol-gel method was explained in [III]. The thickness of as-deposited thin films could be increased by repeated dip coating [III]. CZTS thin films deposited on Mo and ITO glass and pre-annealed at 240 °C under nitrogen atmosphere showed the ternary Cu_3SnS_4 phase and binary ZnS phase that was converted to quaternary $\text{Cu}_2\text{ZnSnS}_4$ and ternary Cu_2SnS_3 phases during annealing at 550 °C in vacuum sealed ampoules [III].

Conclusions

Resulting from the study of the synthesis of CZTS nano-powders in oleylamine by varying the process parameters – synthesis temperature, initial composition of precursors, and by modifying the chemical nature of the solvent by adding alkali metal containing compounds into oleylamine - the main conclusions can be formulated as follows:

1. A narrow temperature range 215 °C - 235 °C at the initial precursor concentration ratio $[Cu]/([Zn] + [Sn]) = 0.82$ was found to be optimal for the synthesis of CZTS nano-powders because of the formation of dominating near-stoichiometric CZTS phase with the average size of the formed nano-powder crystals of 20 nm in these conditions. With a decreasing ($[Cu]/([Zn] + [Sn])$) ratio the average size of formed nano-powders increased from 20 nm to 1 μm in the formed mixture of co-existing $\text{Cu}_2\text{ZnSnS}_4$ and Cu_2SnS_3 phases. The higher initial zinc concentration, i.e. higher chemical potential at specific temperature reduced the final tin concentration in the formed nano-powders.
2. In the studies of oleylamine-cation complex formation in the presence of alkali metal containing compounds to the oleylamine-metal precursor solutions it was found that only CsOH had an effective influence on CZTS nano-particle growth, leading to the formation of nano-particles of homogeneous size and shape. This finding confirms for the first time that caesium hydroxide is highly chemo-selective also when oleylamine as a solvent is used, suppressing the over-alkylation of the produced secondary amines. The formation of an oleylamine-caesium hydroxide complex is proposed. It was found that the increased concentration of CsOH (from 0.1 mmol to 0.5 mmol) further enhanced the homogeneous growth of CZTS nano-particles with narrow size distribution in comparison with very large size distribution characteristic to the powders grown in solutions containing Na^+ and K^+ ions - from small nano-particles to large aggregated nano-particles (1 μm).

Sol-gel method was used for the deposition of CZTS thin films. The formation of CZTS thin films on Mo and ITO covered glass and on soda lime glass substrates in controlled nitrogen atmosphere and in vacuum conditions was studied. Following conclusions can be drawn:

3. It was found that the thickness of the as-deposited thin films could be increased by repeated dip coating. CZTS thin films deposited on Mo and ITO covered glass substrates and pre-annealed at 240 °C under nitrogen atmosphere showed the ternary Cu_3SnS_4 phase and binary ZnS phase that were converted to quaternary $\text{Cu}_2\text{ZnSnS}_4$ and ternary Cu_2SnS_3 phases during the annealing at 550 °C in vacuum sealed ampoules. The corresponding chemical reactions were proposed. Due to the formation of a multiphase thin film, it is required to optimise the initial composition.

References

- [1] First solar reports on 23 February 2016. <http://www.greentechmedia.com/articles/read/first-solar-hits-record-22-1-conversion-efficiency-for-cdte-solar-cell>. (Accessed 12 February 2018)
- [2] Solar Frontier announced in 20 December 2017. http://www.solar-frontier.com/eng/news/2017/1220_press.html. (Accessed 20 March 2018)
- [3] J. Kim, B. Shin, Strategies to Reduce the Open-Circuit Voltage Deficit in $\text{Cu}_2\text{ZnSn}(\text{S},\text{Se})_4$ Thin Film Solar Cells, *Electron Mater Lett* 13-5 (2017) 373-392.
- [4] H. Katagiri, K. Jimbo, W.S. Maw, K. Oishi, M. Yamazaki, H. Araki, A. Takeuchi, Development of CZTS- based thin film solar cells, *Thin Solid Films* 517 (2009) 2455-2460.
- [5] C. X. Xu, J. X. Su, X. H. Xu, P. P. Liu, H.J. Zhao, F. Tian, Y. Ding, Low temperature oxidation over unsupported nano-porous gold, *J. Am. Chem. Soc.* 129 (2009) 42.
- [6] V. Zielasek, B. Jurgens, C. Schulz, J. Biener, M. M. Biener, A. V. Hamza, M. Baumer, Gold catalysts: Nano-porous gold foams, *Angew Chem. Int. Ed.* 45 (2006) 8241.
- [7] W. Wang, M. T. Winkler, O. Gunawan, T. Gokmen, T. K Todorov, Y. Zhu, D. B. Mitzi, Device characteristics of CZTSSe thin-film solar cells with 12.6% efficiency, *Advanced Energy Materials* 4 (2013) 1301465.
- [8] Q. Guo, G. M. Ford, W.C. Yang, C. J. Hages, H. W. Hillhouse, R. Agarwal, Enhancing the performance of CZTSSe solar cells with Ge alloying, *Solar Energy Materials & Solar Cells* 105 (2012) 132–136.
- [9] S. C. Riha, B. A. Parkinson, A. L. Prieto, Solution based synthesis and characterization of $\text{Cu}_2\text{ZnSnS}_4$ nano-crystals, *J. Am. Chem. Soc.* 131 (2009) 12054-12055.
- [10] J. Madarasz, P. Bombicz, M. Okuya, S. Kaneb, Thermal decomposition of thiourea complexes of Cu(I), Zn(II) and Sn(II) chlorides as precursors for the spray pyrolysis deposition of sulphide thin films, *Solid State Ionics* 141-142 (2001) 439.
- [11] S. Schorr, The crystal structure of kesterite type compounds: A neutron and X-ray diffraction study, *Solar Energy Materials & Solar Cells* 95 (2011)1482-1488.
- [12] Q. Guo, H. W. Hillhouse, R. Agrawal, Synthesis of $\text{Cu}_2\text{ZnSnS}_4$ nano-crystal ink and its use for solar cells, *J. Am. Chem. Soc.* 131 (2009) 11672–11673.
- [13] X. Yu, A. Shavel, X. An, Z. Luo, M. Ibáñez, A. Cabot, $\text{Cu}_2\text{ZnSnS}_4$ -Pt and $\text{Cu}_2\text{ZnSnS}_4$ -Au hetero-structured nano-particles for photo-catalytic water splitting and pollutant degradation, *J. Am. Chem. Soc.* 136 (2014) 9236–9239.
- [14] X. Yu, X. An, A. Genc, M. Ibáñez, J. Arbiol, Y. Zhang, A. Cabot, $\text{Cu}_2\text{ZnSnS}_4$ -PtM (M= Co, Ni) nano hetero-structures for photo-catalytic hydrogen evolution, *J. Phys. Chem. C* 119 (2015) 21882–21888.
- [15] C. Xiao, K. Li, J. Zhang, W. Tong, Y. Liu Z. Li, P. Huang, B. Pan, H. Su, Y. Xie, Magnetic ions in wide band gap semiconductor nano-crystals for optimized thermoelectric properties, *Materials Horizons* 1 (2014) 81–86.
- [16] S. Kumar, M. Z. Ansari, N. Khare, Enhanced thermoelectric power factor of $\text{Cu}_2\text{ZnSnS}_4$ in the presence of Cu_{2-x}S and SnS_2 secondary phase, *AIP Conference Proceedings* 1832 (2017) 120033.
- [17] J. Lin, J. Guo, C. Liu, H. Guo, Ultrahigh-performance $\text{Cu}_2\text{ZnSnS}_4$ thin film and its application in micro-scale thin-film lithium-ion battery: comparison with SnO_2 , *ACS Appl. Mater. Interfaces* 8 (2016) 34372.

- [18] A. Walsh, S. Chen, X.G. Gong, S. H. Wei, Defect physics of the kesterite thin-film solar cell absorber $\text{Cu}_2\text{ZnSnS}_4$, *Physics of Semiconductors AIP Conf. Proc.* 1399 (2011) 63-64.
- [19] M. Grossberg, J. Krustok, J. Raudoja, T. Raadik, The role of structural properties on deep defect states in $\text{Cu}_2\text{ZnSnS}_4$ studied by photoluminescence spectroscopy, *Appl. Phys. Lett.* 101 (2012) 102.
- [20] J. Krustok, T. Raadik, M. Grossberg, M. Kauk-Kuusik, V. Trifiletti, S. Binetti, Photoluminescence study of deep donor- deep acceptor pairs in $\text{Cu}_2\text{ZnSnS}_4$, *Material Science in Semiconductor Processing* 80 (2018) 52-55.
- [21] M. Grossberg, T. Raadik, J. Raudoja, J. Krustok, Photoluminescence study of defect clusters in $\text{Cu}_2\text{ZnSnS}_4$ poly-crystals, *Current Applied Physics* 14 (2014) 447.
- [22] T. K. Todorov, K. B. Reuter, D. B. Mitzi, High-efficiency solar cell with Earth-abundant liquid-processed absorber, *Adv. Mater.* 22(20) (2010) E156.
- [23] A. Khare, B. Himmetoglu, M. Johnson, D. J. Norris, M. Cococcioni, E. S. Aydil, Calculation of the lattice dynamics and Raman spectra of copper zinc tin chalcogenides and comparison to experiments, *J. Appl. Phys.* 111 (2012) 083707.
- [24] C. Persson, Electronic and optical properties of $\text{Cu}_2\text{ZnSnS}_4$ and $\text{Cu}_2\text{ZnSnSe}_4$, *J. Appl. Phys.* 107 (2010) 053710.
- [25] S. Botti, D. Kammerlander, M. A. L. Marques, Band structures of $\text{Cu}_2\text{ZnSnS}_4$ and $\text{Cu}_2\text{ZnSnSe}_4$ from many-body methods, *Appl. Phys. Lett.* 98 (2011) 241915.
- [26] Y. B. K. Kumar, G. S. Babu, P. U. Bhaskar, V. S. Raja, Preparation and characterization of spray-deposited $\text{Cu}_2\text{ZnSnS}_4$ thin films, *Solar Energy Materials and Solar Cells* 93-8 (2009) 1230.
- [27] J. J. Scragg, P. J. Dale, L. M. Peter, Towards sustainable materials for solar energy conversion: Preparation and photo-electro-chemical characterization of $\text{Cu}_2\text{ZnSnS}_4$, *Electrochemistry Communications* 10 (4) (2008) 639-642.
- [28] H. Katagiri, N. Sasaguchi, S. Hando, S. Hoshino, J. Ohashi, T. Yokota, Preparation and evaluation of $\text{Cu}_2\text{ZnSnS}_4$ thin films by sulphurization of $\text{E}\overline{\text{B}}$ evaporated precursors, *Solar Energy Materials and Solar Cells* 49 (1-4) (1997) 407-414.
- [29] S. Chen, H.G. Gong, A. Walsh, S. H. Wei, Crystal and electronic band structure of $\text{Cu}_2\text{ZnSnX}_4$ (X=S and Se) photovoltaic absorbers: First-principles insights, *Appl. Phys. Lett.* 94 (2009) 041903.
- [30] I. D. Olekseyuk, I. V. Dudchak and L. V. Piskach, Phase equilibrium in the $\text{Cu}_2\text{S}-\text{ZnS}-\text{SnS}_2$ system, *Journal of Alloys and Compounds* 368 (2004) 135-143.
- [31] K. Muska, Doctoral Thesis, Study of Composition and Thermal Treatments of Quaternary Compounds for Monograin Layer Solar Cells, Tallinn (2012).
- [32] European Commission Cosmetics Directive, Regulation no 1223/2009 of the European parliament and of the council on cosmetic products (2009).
- [33] G. A. Silva, Neuroscience nanotechnology: progress, opportunities and challenges, *Nat. Rev. Neuroscience* 7 (2006) 65-74.
- [34] Q. Guo, G. M. Ford, W. C. Yang, B. C. Walker, E. A. Stach, Hillhouse H W, Agrawal R. Fabrication of 7.2% efficient CZTSSe solar cells using CZTS nano-crystals, *J. Am. Chem. Soc.* 132(49) (2010) 17384-17386.
- [35] T. Taskesen, J. Neerken, J. Schoneberg, D. Pareek, V. Steininger, J. Parisi, L. Gütay, Device characteristics of an 11.4% CZTSe solar cell fabricated from sputtered precursors, *Adv. Energy Mater. Commun. Solar Cells* (2018) 1703295.
- [36] Unit 2: Solutions, Chemistry part I, Textbook for Class XII, NCERT, New Delhi, 2012.

- [37] Q. Guo, G. M. Ford, W. C. Yang, C. J. Hages, H. W. Hillhouse, R. Agrawal, Enhancing the performance of CZTSSe solar cells with Ge alloying, *solar energy materials and solar cells* 105 (2012) 132-136.
- [38] D. Wang, Y. Li, D. Z. Liao, Slow magnetic relaxation in lanthanide complexes with chelating nitronyl nitroxide radical, *Inorganic Chemistry* 50 (2011) 5196-50202.
- [39] S. Mourdikoudis, L. M. Liz-Marzan, Oleylamine in nano-particle synthesis, *Chem. Mater.* 25 (2013) 1465-1476.
- [40] K. M. Nam, J. H. Shim, H. Ki, S. I. Choi, G. Lee, J. K. Jang, Y. Jo, M.H. Jung, H. Song, J.T. Park, Single-crystalline hollow face-centred-cubic cobalt nano-particles from solid face-centred-cubic cobalt oxide nano-particles, *Angew Chem, Int. Ed.* 47 (2008) 9504.
- [41] A. C. Johnston-Peck, J. Wang, J. B. Tracy, Synthesis and structural and magnetic characterization of Ni(core)/NiO(shell) nano-particles, *ACS Nano* 3 (2009) 1077.
- [42] J. G. Railsback, A. C. Johnston-Peck, J. Wang, J. B. Tracy, Size-dependent nano-scale kirkendall effect during the oxidation of nickel nano-particles, *ACS Nano* 4 (2010) 1913.
- [43] C. Wang, H. Daimon, Y. Lee, J. Kim, S. Sun, Synthesis of mono-disperse Pt nano-cubes and their enhanced catalysis for oxygen reduction, *J. Am. Chem. Soc.* 129 (2007) 6974.
- [44] B. Wu, N. Zheng, G. Fu, Small molecules control the formation of Pt nano-crystals: a key role of carbon monoxide in the synthesis of Pt nano-cubes, *J. Chem. Comm.* 47 (2011) 1039.
- [45] J. Wu, A. Gross, H. Yang, Shape and composition-controlled platinum alloy nano-crystals using carbon monoxide as reducing agent, *Nano Lett* 11 (2011) 798.
- [46] S. Zhou, G.S. Jackson, B. Eichhom, AuPt alloy nano-particles for CO-tolerant hydrogen activation: Architectural effects in Au-Pt bimetallic nano-catalysts, *Advanced Functional Materials* 17 (2007) 3099.
- [47] Y. C. Lu, Z. Xu, H. A. Gasteiger, S. Chen, K. H. Schifferli, Y. Shao-Hom, Platinum-gold nano-particles: a highly active bi-functional electro-catalyst for rechargeable lithium-air batteries, *J. Am. Chem. Soc.* 132 (2010) 12170.
- [48] Z. Peng, H. You, H. Yang, Composition-dependent formation of platinum silver nano-wires, *ACS nano* 4 (2010) 1501.
- [49] Z. Niu, Q. Peng, M. Gong, H. Rong, Y. Li, Oleylamine-mediated shape evolution of palladium nano-crystals, *Angew Chem. Int. Ed.* 50 (2011) 6315.
- [50] N. Li, X. Zhang, S. Chen, X. Hou, Y. Liu, X. Zhai, Synthesis and optical properties of CdS nano-rods and CdSe nano-crystals using oleylamine as both solvent and stabilizer, *Mater. Sci. Eng. B* 176 (2011) 688.
- [51] L. Cademartiri, J. Bertolotti, R. Sapienza, D.S. Wiersma, G. Freymann, G. A. Ozin, Multi-gram scale, solvent-less, and diffusion-controlled route to highly mono-disperse PbS nano-crystals, *A. J. Phys. Chem. B* 110 (2006) 671.
- [52] A. Ghezelbash, B.A. Korgel, Nickel sulphide and copper sulphide nano-crystal synthesis and polymorphism, *Langmuir* 21 (2005) 9451.
- [53] X. Zhai, X. Zhang, S. Chen, W. Yang, Z. Gong, Oleylamine as solvent and stabilizer to synthesize shape-controlled ZnS nano-crystals with good optical properties, *Colloid Surf. A* 409 (2012) 126.
- [54] Y. Xia, Y. Xiong, B. Lim, S. E. Skrabalak, Shape-controlled synthesis of metal nano-crystals: Simple chemistry meets complex physics, *Angew Chem Int. Ed. Engl.* 48 (1) (2009) 60-103.

- [55] V. K. La Mer, R. H. Dinegar, Theory, production and mechanism of formation of mono-dispersed hydrosols, *J. Am. Chem. Soc.* 72 (1950) 4847.
- [56] L. C. Ciacchi, M. Mertig, W. Pompe, S. Meriani, A. De Vita, Growth of platinum clusters via addition of Pt(II) complexes: A first principles investigation, *Platinum Met. Rev* 47 (2003) 98.
- [57] L. C. Colombi, W. Pompe, A. De Vita, Initial nucleation of platinum clusters after reduction of K_2PtCl_4 in aqueous solution: A First Principles Study, *J. Am. Chem. Soc.* 123 (2001) 7371.
- [58] M. Mertig, L. C. Colombi, R. Seidel, W. Pompe, A. D. Vita, DNA as a selective metallization template, *Nano Lett* 2 (2002) 841.
- [59] Chapter 3, Fundamentals of homogeneous nucleation, [Depts.washington.edu/solgel/documents/class-docs/MSE502/ch-3-Section-3.2.1-3.2.5.3.pdf](https://depts.washington.edu/solgel/documents/class-docs/MSE502/ch-3-Section-3.2.1-3.2.5.3.pdf). (Accessed on 12 February 2018)
- [60] M. Karimi, M. J. Eshraghi, V. Jahangir, A facile and green synthetic approach based on deep eutectic solvents toward synthesis of CZTS nano-particles, *Materials Lett.* 171 (2016) 100-103.
- [61] R. Ahmad, M. Brandl, M. Distaso, P. Herre, E. Spiecker, R. Hock, W. Peukert, A comprehensive study on the mechanism behind formation and depletion of Cu_2ZnSnS_4 , *Cryst. Eng. Comm.* 17 (2015) 6972.
- [62] R. Ahmad, M. Distaso, H. Azimi, J. Brabec, W. Peukert, Facile synthesis and post processing of eco-friendly, highly conductive CZTS nano-particle, *Journal Nano-scale res.* 15 (2013) 1-16.
- [63] T. Nguyen, From formation mechanisms to synthetic methods toward shape-controlled oxide nano-particles, *Nanoscale* 5 (2013) 9455.
- [64] C. Coughlan, K.M. Ryan, Complete study of the composition and shape evolution in the synthesis of Cu_2ZnSnS_4 semiconductor nano-crystals, *Cryst. Eng. Comm.* 17 (2015) 6914.
- [65] A. Ping, Z. Liang, X. Xu, X. Wang, H. Jin, N. Wang, J. Wang, F. Zhu, Heating up method for the synthesis of pure phase kesterite Cu_2ZnSnS_4 nano-crystals using simple coordinating sulphur precursor, *RSC Adv.* 5 (2015) 6879.
- [66] S. Gupta, T. J. Whittles, Y. Batra, V. Satsangi, S. Krishnamurthy, V. R. Dhanak, B. R. Mehta, A low cost sulphurization free approach to control optical and electronic properties of Cu_2ZnSnS_4 via precursor variation, *Solar Energy Materials & Solar Cells* 157 (2016) 820-830.
- [67] J. J. Scragg, P. J. Dale, L. M. Peter, G. Zoppi, I. Forbes, New routes to sustainable photo-voltaics: evaluation of Cu_2ZnSnS_4 as an alternative absorber material, *Phys. Stat. Sol. B* 9 (2008) 1772.
- [68] R. N. Salvatore, A. S. Nalge, K. W. Jung, Caesium Effect: High Chemo-selectivity in Direct N-alkylation of Amines, *J. Org. Chem.* 67 (2002) 674-683.
- [69] T. Chaudhari, D. Tiwari, Earth-abundant non-toxic Cu_2ZnSnS_4 thin films by direct liquid coating from metal-thiourea, *Solar Energy Materials and Solar Cells* 101 (2012) 46-50.
- [70] K. Tanaka, Y. Fukui, N. Moritake, H. Uchikih, Chemical composition dependence of morphological and optical properties of Cu_2ZnSnS_4 thin films deposited by sol-gel sulphurization and Cu_2ZnSnS_4 thin film solar cell efficiency, *Solar Energy Materials and Solar Cells* 95 (2011) 838.

- [71] M. Y. Yeh, C. Lee, D. S. Wu, Influence of synthesizing temperatures on the properties of $\text{Cu}_2\text{ZnSnS}_4$ prepared by sol gel spin coated deposition, *J. Sol Gel Sci. Technol.* (2009) 52-65.
- [72] M. Jiang, Y. Li, R. Dhakal, P. Thapaliya, M. Mastro, J. D. Caldwell, F. Kub, X. Yan, $\text{Cu}_2\text{ZnSnS}_4$ polycrystalline thin films with large densely packed grains prepared by sol-gel method, *Journal of Photonics for Energy* 1 (2011) (019501-1-6).
- [73] Z. Su, K. Sun, Z. Han, H. Cui, F. Liu, Y. Lai, J. Li, X. Hao, Y. Liua, M. A. Green, Fabrication of $\text{Cu}_2\text{ZnSnS}_4$ solar cells with efficiency 5.1% via thermal decomposition and reaction using a non-toxic sol-gel route, *J. Mater. Chem. A* 2 (2004) 500.
- [74] L. Cao, S. Ma, J. Sui, J. Bai, H. Dong, Q. Zhang, L. Dong, Kesterite $\text{Cu}_2\text{ZnSn}(\text{S}_{1-x}\text{Se}_x)_4$ film synthesis through ethanol-thermal route with sulphurization/selenization treatments, *Materials Letters* 139 (2015) 101-103.
- [75] Unit 10-11, Chemistry part II, Textbook for Class XII, NCERT, New Delhi, 2012.
- [76] M. Altosaar, T. Varema, E. Mellikov, Surface degreasing and activation as important factor for Cu electroplating on ITO substrates, DAAM Proceedings of the 2nd International Conference, Tallinn (2000) 233.
- [77] P. A. Fernandes P A, Salome P M P, Cunha A F, $\text{Cu}_x\text{SnS}_{x+1}$ ($x=2, 3$) thin films grown by sulphurization of metallic precursors deposited by DC magnetron sputtering, *Phys. Status Solidi C* 7 (3-4) (2010) 901.
- [78] P. A. Fernandes, P. M. P. Salome, A. F. da Cunha, Study of polycrystalline $\text{Cu}_2\text{ZnSnS}_4$ films by Raman scattering, *Journal of Alloys and Compounds* 509 (2011) 7600-7606.
- [79] S. Mourdikoudis, L. M. Liz-Marzan, Oleylamine in nano-particle synthesis, *Chem. Mater.* 25 (2013) 1465-1476.
- [80] X. Lu, H. Y. Tuan, B. A. Korgel, Y. Xia, Facile synthesis of gold nano-particles with narrow size distribution by using AuCl or AuBr as the precursor, *Chemistry* 14 (5) (2008) 1584-1591.
- [81] N. Shukla, C. Liu, P. M. Jones, D. Weller, FTIR study of surfactant bonding to Fe-Pt nano-particles, *J. Magn. Mater.* 266 (2003) 178-184.
- [82] J. L. Zhang, R. S. Srivastava, R. D. K. Mishra, Core-shell magnetite nano-particles surface encapsulated with smart stimuli-responsive polymer: synthesis, characterization and LCST of viable drug targeting delivery system, *Langmuir* 23 (11) (2007) 6342-6351.
- [83] R. J. Greenwald, S. Tom, W. Zucconi, J. C. Cochran, Carbon Tin vibrational frequencies in substituted trimethyl vinyl stannanes, *Main Group Metal Chemistry* 17 (1994) 435.
- [84] W. H. Hsu, H. I. Hsiang, Y. L. Chang, D. T. Ray, F. S. Yen, Formation mechanisms of $\text{Cu}(\text{In}_{0.7}\text{Ga}_{0.3})\text{Se}_2$ nano-crystallites synthesized using hot injection and heating up processes, *J. Am. Ceram. Soc.* 94 – 9 (2011) 3030-3034.
- [85] S. Yoda, Y. Takebayashi, K. Sue, T. Furuya, K. Otake, Thermal decomposition of copper (II) acetylacetonate in supercritical carbon dioxide: In situ observation via UV-vis spectroscopy, *The Journal of Supercritical Fluids* 123 (2017) 82-91.
- [86] U. Chalapathi, Y. B. K. Kumar, S. Uthana, V. S. Raja, Investigations on Cu_3SnS_4 thin films prepared by spray pyrolysis, *Thin Solid Films* 556 (2014) 61-67.
- [87] E. Wiberg, N. Wiberg, *Inorganic Chemistry*, 2001, Academic Press, 614, ISBN 0-12-352651-5.

Acknowledgements

I sincerely appreciate the guidance, support and the positive attitude of my supervisors Dr. Mare Altsaar, senior research scientist and Dr. Maarja Grossberg, Professor. I value the advice you gave and constructive discussions we had.

I am thankful to all my senior colleagues, senior researchers: Dr. Tiit Varema, Dr. Jaan Raudoja, Dr. Valdek Mikli, Prof. Jüri Krustok, Dr. Marit Kauk-Kuusik, Dr. Kristi Timmo, Dr. Taavi Raadik, Dr. Mati Danilson, Dr. Enn Mellikov, Dr. Revathi Naidu, colleagues: Dr. God'swill Nkwusi, Mr. Mihkel Loorits and Dr. Ilona Oja Acik for allowing me to use the spectrometer for FTIR measurements.

I wish to thank Dr. Malle Krunks, Head of Department of Materials and Environmental Technology and Prof. Andres Öpik, the Director of the Doctoral school "Functional materials and technologies" for providing the opportunity to participate in the PhD studies of the School of Engineering and in the graduate school.

This work was supported by the institutional research funding IUT 19–28 of the Estonian Ministry of Education and Research, the European Union through the European Regional Development Fund, Project TK141, the Estonian Science Foundation grant ETF9369, ETF9425 and the doctoral school (ASTRA "TUT Institutional Development Program" Graduate School of Functional Materials and Technologies (2014-2020.4.01.16-0032)).

My warmest gratitude belongs to my family, to my sons Virat and Vihan.

Abstract

Synthesis of $\text{Cu}_2\text{ZnSnS}_4$ Nano-powders and Nano-structured Thin Films

The thesis is focused on the solution-based synthesis of $\text{Cu}_2\text{ZnSnS}_4$ nano-powders in oleylamine by the hot-injection method. The influence of the initial $[\text{Cu}]/([\text{Zn}] + [\text{Sn}])$ concentration ratio (from 0.82 to 0.33) on the morphology, phase and elemental composition of nano-powders was studied. It was found that the average size of nano-powders of CZTS nano-powders increased from 20 nm to few μm with the decreasing initial $[\text{Cu}]/([\text{Zn}] + [\text{Sn}])$ concentration ratio at the synthesis temperature (215 °C, 225 °C and 235 °C). The elemental composition of the formed nano-powders was compatible to near-stoichiometric CZTS at initial $[\text{Cu}]/([\text{Zn}] + [\text{Sn}])$ concentration ratios 0.82 and 0.74. Higher initial zinc concentration i.e. higher chemical potential at specific temperature reduces the final tin concentration component in the nano-powders.

The control of morphology, elemental and phase composition of $\text{Cu}_2\text{ZnSnS}_4$ (CZTS) nano-powders depends on the control of the complex formation and surface stabilization of nano-materials in the solution-based synthesis in oleylamine. At temperatures ≥ 280 °C, the control of nano-particles morphology and homogeneous growth is difficult because of fast poly-nuclear growth occurring at higher temperatures. The effect of oleylamine complex formation with different alkali ions (Na^+ , K^+ and Cs^+) on nano-particle growth at the synthesis temperature of 280 °C was studied. It was found that nano-powders synthesized in the presence of Na^+ and K^+ ions showed the formation of crystals of different sizes - small nano-powders, large aggregated crystals and large single crystals. The presence of Cs^+ ions in the nano-powder synthesis in the oleylamine-metal precursor- CsOH solution promoted growth of nano-powders of homogeneous size. It is proposed that the formed oleylamine- Cs complexes a) enhance the formation and stabilization of oleylamine-metal (Cu , Zn and Sn) complexes before the injection of sulphur precursor into the oleylamine-metal precursor solution and b) after addition of sulphur stabilize the fast nucleated nano-particles and promote diffusion limited growth.

$\text{Cu}_2\text{ZnSnS}_4$ thin films on Mo and/or ITO covered glass substrates were prepared by the dip coating method using methanol as solvent for CuCl_2 , ZnCl_2 , SnCl_2 and $\text{CH}_4\text{N}_2\text{S}$ as precursors. The influence of pre-annealing and post-annealing conditions as well as the influence of used substrate on the morphology, phase composition and elemental composition of the resulting films was studied. It was found that thin films deposited onto Mo and ITO substrates and pre-annealed at 240 °C in nitrogen atmosphere and post heated at 550 °C showed Raman dominating peak at 338 cm^{-1} characteristic of $\text{Cu}_2\text{ZnSnS}_4$. These films were continuous, with good crystallinity and had near-stoichiometric composition.

Kokkuvõte

Cu₂ZnSnS₄ nano-pulbrite ja nano-struktuursete kilede süntees

Käesolev dissertatsioon on uurimistöö, mis on fokuseeritud Cu₂ZnSnS₄ nanopulbrite sünteesile oleüülamiinis vedeliksadestuse meetodil. Cu₂ZnSnS₄ katioonkomponente sisaldavad lähteühendid lahustati oleüülamiinis ja kuumutati lämmastiku keskkonnas sünteesitemperatuurile. Kuumale katioonkomponente sisaldavale lahusele lisati väevli lahus oleüülamiinis. Uuriti alglahuse metallkomponentide kontsentratsioonide suhete [Cu]/([Zn] + [Sn]) (0,82-0,33) mõju tekkivate nanoosakeste morfoloogiale ja faasikoostisele. Leiti, et sünteesitemperatuuridel 215 °C, 225 °C ja 235 °C kasvas CZTS keskmine nanoosakeste suurus [Cu]/([Zn] + [Sn]) suhte vähenedes 20 nm-lt paarile mikromeetrile. [Cu]/([Zn] + [Sn]) kontsentratsioonisuhtel 0,82 ja 0,74 moodustusid peaaegu stöhhiomeetrilise koostisega CZTS nano-pulbrid. Kõrgem algne tsingi kontsentratsioon (s.o kõrgem keemiline potentsiaal) vähendas tina kontsentratsiooni moodustunud nanopulbris.

CZTS nanokristallide morfoloogia, element- ja faasikoostis sõltuvad keemiliste komplekside moodustumisest ning nanoosakeste pinna stabiliseerimisest sünteesil oleüülamiinis. Temperatuuridel ≥ 280 °C on nanokristallide morfoloogia ja homogeense kasvu kontrollimine keeruline, kuna kõrgetel temperatuuridel leiab aset kiire mitmetuumaline kasv. Oleüülamiin-kompleksi moodustumist erinevate leelismetallide ioonidega (Na⁺, K⁺ ja Cs⁺) uuriti sünteesitemperatuuril 280 °C. Leiti, et Na⁺ ja K⁺ ioonide juuresolekul näitasid sünteesitud nanopulbrid erineva suurusega kristallide moodustumist - väikesed nanoosakesed, suured agregeeritud kristallid ja suured monokristallid. Cs⁺ -ioonide (CsOH) juuresolek oleüülamiin-katioon alglahuses soodustas homogeense suurusega nanokristallide kasvu nanopulbri sünteesis. Leiti, et moodustunud oleüülamiin-Cs kompleksid a) tugevdavad oleüülamiin-metall-komplekside (Cu, Zn ja Sn) moodustumist ja stabiliseerumist enne väevlilahuse lisamist oleüülamiin-katioon lahusesse ja b) pärast väevli lisamist stabiliseerib moodustunud nanoosakeste pinna ning soodustab difusiooniga-limiteeritud kristallide kasvu.

Cu₂ZnSnS₄ õhukeste kilede sadestamiseks Mo- ja / või ITO-ga kaetud klaasalustele kasutati pindtilgutamise meetodit, kasutades lähteainete CuCl₂, ZnCl₂, SnCl₂ ja CH₄N₂S lahust metanoolis. Uuriti eel- ning järellõõmutuse mõju ja kasutatud klaasaluste pinnakatete mõju moodustunud CZTS kilede morfoloogiale, faasi- ning elementkoostisele. Leiti, et pidevad ja stöhhiomeetrilise koostisega CZTS-kiled moodustusid Mo ja ITO-ga kaetud klaasile pärast vahelõõmutust lämmastiku atmosfääris temperatuuril 240 °C ning järelkuumutamist temperatuuril 550 °C.

Appendix

Publication I

Suresh Kumar, Vikash Kumar, Valdek Mikli, Tiit Varema, Mare Altosaar, Maarja Grossberg, Study of CZTS nano-powder synthesis by hot injection method by variation of Cu and Zn concentrations, *Energy Procedia* 102 (2016) 136-143.



E-MRS Spring Meeting 2016 Symposium T - Advanced materials and characterization techniques for solar cells III, 2-6 May 2016, Lille, France

Study of CZTS nano-powder synthesis by hot injection method by variation of Cu and Zn concentrations

Suresh Kumar*, Vikash Kumar, Valdek Mikli, Tiit Varema, Mare Altosaar, Maarja Grossberg

Tallinn University of Technology, Institute of Materials Science, Ehitajate tee 5, 19086, Tallinn, Estonia

Abstract

Copper Zinc Tin Sulphide (CZTS) nano-powders were synthesized by solution based method in oleylamine at 215°C, 225°C and 235°C using copper pentane2, 4-dionate, zinc acetate, tin (II) chloride and elemental sulphur as precursors. The influence of initial Cu/ (Zn + Sn) concentration ratio (from 0.82 to 0.33) on the morphology, phase composition and elemental composition of nano-powders was studied. It was found that the average size of colloidal nano-particles of CZTS nano-powders increased from 20 nm to 10 µm with decreasing initial Cu/ (Zn + Sn) concentration ratio at every used synthesis temperature. The elemental composition of the formed nano-powders was compatible to near-stoichiometric CZTS if initial Cu/ (Zn + Sn) concentration ratios were 0.82 and 0.74. Higher initial zinc concentration i.e. higher chemical potential at specific temperature reduces the final tin concentration component in the colloidal nano-powders.

© 2016 The Authors. Published by Elsevier Ltd. This is an open access article under the CC BY-NC-ND license (<http://creativecommons.org/licenses/by-nc-nd/4.0/>).

Peer-review under responsibility of The European Materials Research Society (E-MRS).

Keywords: CZTS; nano-powders; copper zinc tin sulphide; solution based synthesis; Cu and Zn concentration;

1. Introduction

First prerequisite for solar energy conversion is a good absorber material composed from earth abundant elements with least toxicity, and having high absorption coefficient and direct band gap. Copper zinc tin sulphide (selenide)

* Corresponding author. Tel.: +3726203367.

E-mail address: sureshkumamara@gmail.com

215 °C / 225 °C / 235 °C	1.8	1.2	1.0	4.5	1.5	0.82	1.2
215 °C / 225 °C / 235 °C	1.7	1.3	1.0	4.5	1.3	0.74	1.3
215 °C / 225 °C / 235 °C	1.5	1.5	1.0	4.5	1.0	0.60	1.5
215 °C / 225 °C / 235 °C	1.3	1.7	1.0	4.5	0.8	0.48	1.7
215 °C / 225 °C / 235 °C	1.0	2.0	1.0	4.5	0.5	0.33	2.0

ZEISS ULTRA 55 FE-SEM apparatus was used to investigate the morphological structure and to estimate the size of particles of nano-powders and to perform the energy dispersive x-ray spectroscopy (EDS) analysis to determine the elemental composition of nano-powder samples. The samples for the EDS analysis were prepared by pressing the nano-powders into pellets. Raman spectroscopy was performed using Horiba Jobin Yvon HR800 micro-Raman spectrometer.

3. Results and Discussion

3.1. SEM and EDS Analysis of Nano-powders

3.1.1. SEM analysis of nano-powders

SEM images of nano-powders are presented in Figures 1-3. The CZTS nano-powders synthesised at 215 °C with varying the initial concentration ratio of precursors Cu/ (Zn + Sn) (i.e. 0.82, 0.74, 0.60 and 0.48) show large variation in the size of nano-particles from 20 nm to 150 nm (Figure 1). Decreasing copper concentration with increasing zinc concentration causes the formation of colloidal nano-particles with sizes from 2 μm to 10 μm (Figure. 1).

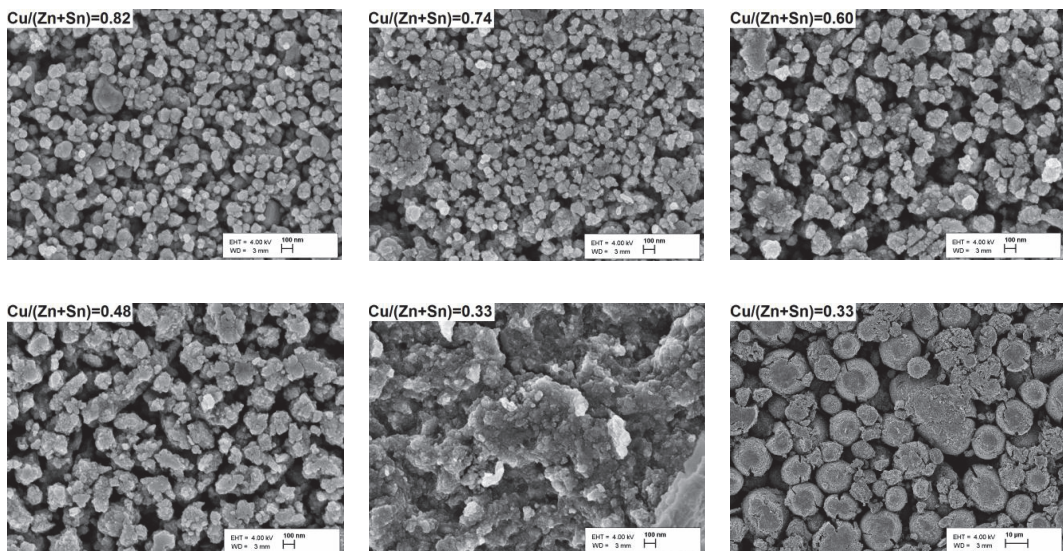


Figure 1. Colloidal nano-particles synthesised at 215 °C with initial Cu/ (Zn + Sn) ratio equal to 0.82, 0.74, 0.60, 0.48, 0.33 and 0.33 (10 μm scale) respectively.

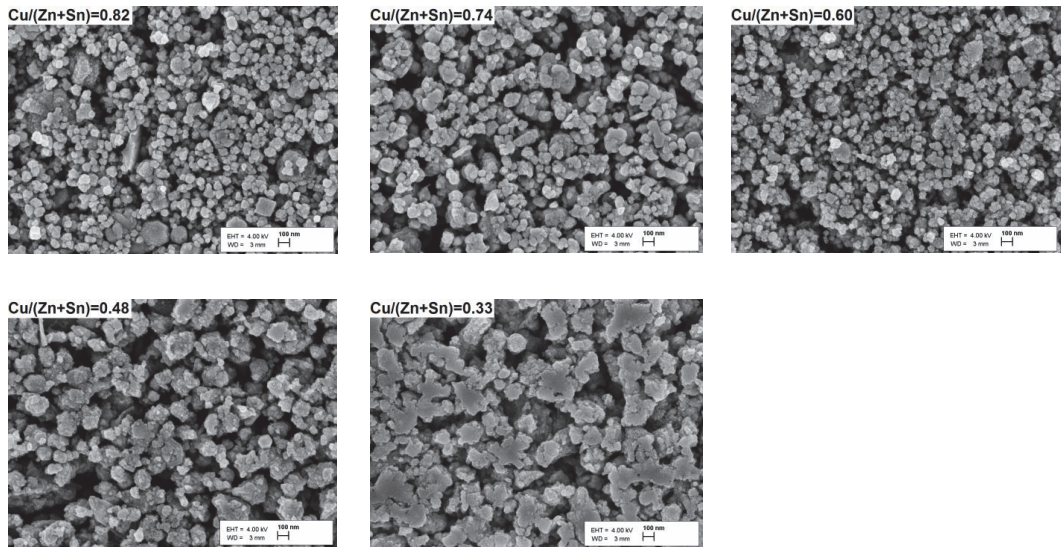


Figure 2. Colloidal nano-particles synthesised at 225°C with initial Cu/ (Zn + Sn) equal to 0.82, 0.74, 0.60, 0.48 and 0.33 respectively.

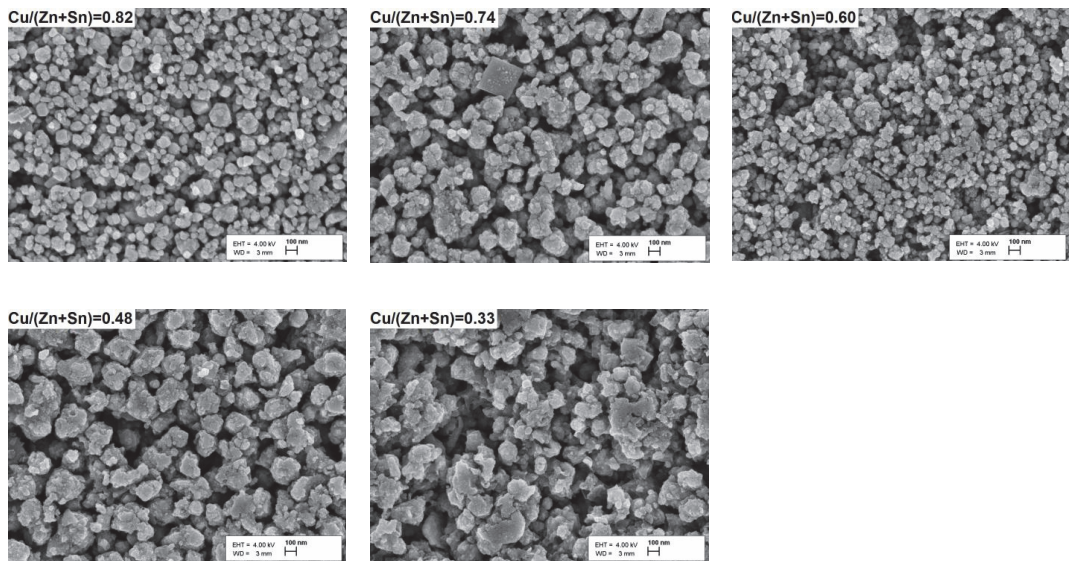


Figure 3. Colloidal nano-particles synthesised at 235°C with initial Cu/ (Zn + Sn) equal to 0.82, 0.74, 0.60, 0.48 and 0.33 respectively.

For the CZTS nano-powders synthesised at 215°C with initial precursor Cu/(Zn + Sn) ratio equal to 0.33 the average size of agglomerated colloidal nano-particles is 10 μm . According to thermodynamics, as the synthesis temperature decreases then the chemical potentials of the elements increases. Therefore, at a particular synthesis temperature with high initial zinc concentration higher chemical potential of zinc in the solution is expected. The crystals in colloidal nano-powders synthesised at three different synthesis temperatures i.e. 215°C, 225°C and 235°C with initial precursor Cu/(Zn + Sn) ratio equal to 0.82 and 0.74 have size in the range 20 nm to 100 nm.

3.1.2. EDS analysis of nano-powders

The analysis of EDS results show that elemental composition of CZTS colloidal nano-powders synthesised at 215°C, 225°C and 235°C with initial precursor Cu/ (Zn + Sn) ratio equal to 0.82 and 0.74 are near-stoichiometric. The final concentration of copper varies with the initial copper concentration and as initial zinc concentration was increased, a respective increase in the final zinc concentration of colloidal nano-powders was detected.

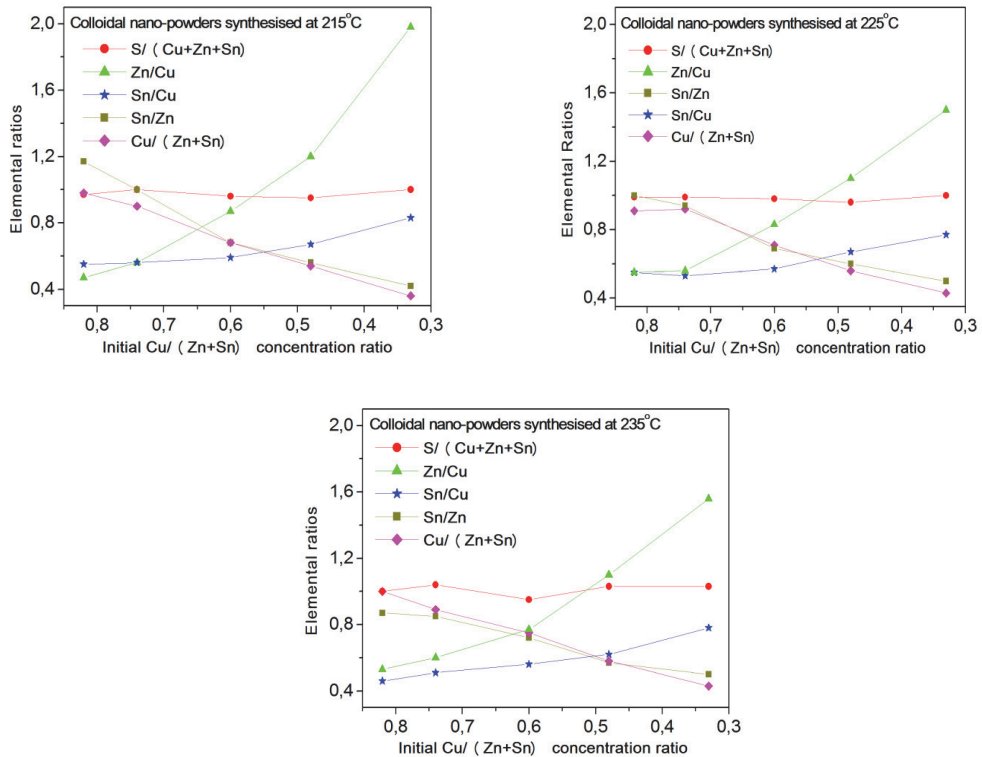


Figure 4. Concentration ratios determined by EDS of components in colloidal nano-particles synthesised with different initial concentrations at 215°C, 225°C and 235°C respectively.

Following trends were observed in the colloidal nano-particles: with the increase in initial zinc concentration final concentration of tin decreases with initial precursor Cu/ (Zn + Sn) ratio equal to 0.82 and 0.74. This shows that the increase in initial zinc concentration not only increases the chemical potential of zinc but also decreases the chemical potential of tin state. The chemical potential of copper is unaffected by the increase in initial zinc concentration. The concentration of sulphur with respect to the sum of metal ions, S/ (Cu + Zn + Sn) remains stoichiometric at the all used initial precursor concentration ratios (Cu/ (Zn + Sn) = 0.82, 0.74, 0.6, 0.48 and 0.33) and at all used synthesis temperatures (215°C, 225°C and 235°C).

3.2. Raman analysis

3.2.1. Raman spectra analysis of nano-powders with near stoichiometric composition synthesised at different temperatures (215°C, 225°C and 235°C)

Raman spectra of CZTS colloidal nano-powders synthesised at 215°C, 225°C and 235°C with initial precursor ratios

Cu/ (Zn + Sn) equal to 0.82 and 0.74 are shown in Figure 5.

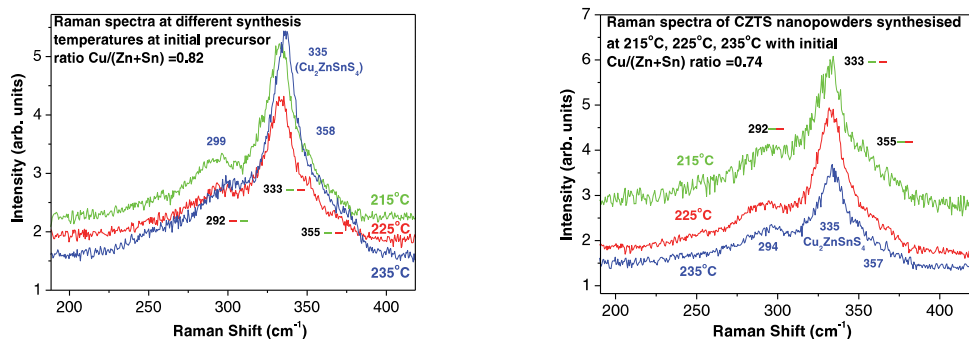


Figure 5. Raman spectra of colloidal nano-powders synthesised with initial Cu/(Zn + Sn) concentration ratios equal to 0.82 (a) and 0.74 (b) at 215°C (green), 225°C (red) and 235°C (blue line)

The Raman peak positions were determined from the fittings of the spectra by using Lorentzian curves. Raman peaks observed in CZTS colloidal nano-powders synthesized at 215°C and 225°C are at 333 cm⁻¹, 292 cm⁻¹ and 355 cm⁻¹ which could correspond to Cu₂SnS₃ or some other ternary sulphide [17, 18 and 19]. Dominating Raman peaks observed in CZTS nano-powders synthesised at 235°C are at 335 cm⁻¹ and 358 cm⁻¹ which could correspond to Cu₂ZnSnS₄, and at 299 cm⁻¹ which could correspond to Cu₂SnS₃ or other ternary sulphide [17, 18 and 19].

Katagari et al showed that Cu/(Zn+Sn) ratio equal to 0.69 or less results in binary phases of Sn and S (SnS and SnS₂) and ratio Cu/(Zn+Sn) above 1.09 results in binary compound of copper and sulphur (i.e. Cu₂S) [20]. The highest photocurrent and solar cell efficiency was observed with Cu/(Zn+Sn) ratio equal to 0.85 [20]. The Cu/(Zn+Sn) ratio equal to 0.8 shows CZTS and CTS phase whereas Cu/(Zn+Sn) ratio equal to 1.19 shows CZTS phase with 7-10 nm diameter nano-particles were concluded by Pal et al [21]. Raman spectra of CZTS nano-powders synthesised in this study at 215°C, 225°C and 235°C with initial precursor ratio Cu/ (Zn + Sn) equal to 0.82 and 0.74 show dominating Raman peak shift from 333 cm⁻¹ to 335 cm⁻¹. Shoulder at the lower wave number side of this peak and also the shift of the second peak from 292 cm⁻¹ to 299 cm⁻¹ indicates that there is a coexistence of Cu₂ZnSnS₄ and Cu₂SnS₃ phases. Katagari et al showed that Cu/(Zn+Sn) ratio equal to 0.69 or less results in binary phases of Sn and S whereas our results show CZTS and CTS phases and in agreement with Pal et al. The shift of the peaks is probably caused by the changing in the ratio of the two phases, CZTS prevailing at higher temperatures.

3.2.2. Raman spectra analysis of nano-powders synthesised with big difference in Cu/(Zn + Sn) concentration ratios at particular temperatures (215°C, 225°C and 235°C)

The most intense Raman peaks of colloidal nano-particles shift from 333 cm⁻¹ to 335 cm⁻¹ as the synthesis temperature increases from 215°C to 235°C (Figure 5). Similar Raman shift of most intense peak from 333 cm⁻¹ to 337 cm⁻¹ is also observed when the Cu/ (Zn + Sn) ratio decreases from 0.82 to 0.33 at synthesis temperature 215°C (Figure 6). The insertion of Zn ions into the CZTS is possible by two ways: first, with higher synthesis temperature, and second, by high initial zinc concentration by creating high chemical potential of zinc in the solution (EDS shows high zinc concentration in colloidal nano-powders). Raman spectra of CZTS nano-powders synthesised at 235°C with different Cu/ (Zn + Sn) ratios (i.e. 0.82, 0.74, 0.60, 0.48 and 0.33) are presented in Fig.6. Raman peaks observed in CZTS nano-powders at 235°C are for Cu/(Zn + Sn) ratios 0.82 and 0.74 are 335 cm⁻¹, 292-294 cm⁻¹ and 355 cm⁻¹ which could correspond to Cu₂ZnSnS₄ [15, 16 and 17]. Raman peaks observed in CZTS nano-powders at 235°C for Cu / (Zn + Sn) ratios 0.60, 0.48 and 0.33 are at 335 cm⁻¹ and 360 cm⁻¹ which could correspond to Cu₂ZnSnS₄ and Raman peak at 299-300 cm⁻¹ which could correspond to Cu₂SnS₃ or other ternary sulphide [15, 16 and 17].

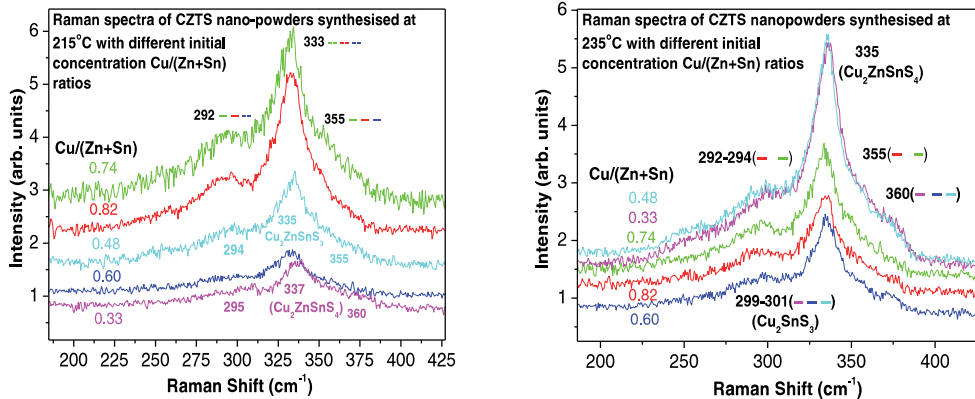


Figure 6. Raman spectra of colloidal nano-powders as synthesised with different initial concentration Cu/(Zn + Sn) ratios at 215°C and 235°C

The shift of the peaks towards higher wave number side is accompanied with the decrease in the peak half-width shows improved crystalline nature. The changing positions of the Raman peaks at the wave numbers corresponding to CZTS and Cu_2SnS_3 indicate that most probably the powders are a mixture of these two phases, CZTS prevailing at higher temperatures and at lower Cu/ (Zn + Sn) ratios.

4. Conclusions

The CZTS colloidal nano-powders were synthesised at 215°C, 225°C and 235°C by solution based hot injection method. The CZTS colloidal nano-powders synthesised with varying initial precursor concentration ratio Cu/ (Zn + Sn) (i.e. 0.82, 0.74, 0.60, 0.48 and 0.33) at each synthesis temperature. It was found that the average size of colloidal nano-particles of CZTS nano-powders increased from 20 nm to 10 μm with decreasing initial Cu/ (Zn + Sn) concentration ratio at every used synthesis temperature. The most intense peak of Raman spectra shifted towards higher wave number probably because of high zinc component in the CZTS colloidal nano-powders with increase in the synthesis temperature from 215°C to 235°C. The changing positions of the Raman peaks at the wave numbers corresponding to CZTS and Cu_2SnS_3 indicate that most probably the powders are a mixture of these two phases, CZTS prevailing at higher temperatures and at lower Cu/ (Zn + Sn) ratios. At synthesis temperature 215°C, main Raman peak is shifted from 333 cm^{-1} to 337 cm^{-1} with variation of initial precursor Cu/(Zn + Sn) concentration ratio from 0.82 to 0.33. Shoulder at the lower wave number side of this peak and also the shift of the second peak from 292 cm^{-1} to 299 cm^{-1} indicates that there is a coexistence of $\text{Cu}_2\text{ZnSnS}_4$ and Cu_2SnS_3 phases. The shift of the peaks is probably caused by the changing ratio of the two phases, CZTS prevailing at higher temperatures. Higher initial zinc concentration i.e. higher chemical potential at specific temperature reduces the final tin concentration in the colloidal nano-powders.

Acknowledgment

This work was supported by the Estonian Science Foundation grant ETF9369, ETF9425, by the institutional research funding IUT 19–28 of the Estonian Ministry of Education and Research, and by the European Union through the European Regional Development Fund, Project TK141, Advanced materials and high-technology devices for energy recuperation systems.

References

- [1] Schorr S, Gonzalez-Aviles G. In situ investigation of the structural phase transition in kesterite, *Phys Status Solidi*, A 206, No.5, 1054- 1058 (2009) /DOI 10.1002/pssa.200881214.

- [2] Wang W, Winkler M T, Gunawan O, Gokmen T, Todorov T K, Zhu Y & Mitzi D B. Device characteristics of CZTS_{Se} thin-film solar cells with 12.6% efficiency, *Advanced Energy Materials*, (2013), 4(7), doi: 10.1002/aenm.201301465.
- [3] Brammertz G., Buffière M, Oueslati S, ElAnzeery H, Ben Messaoud H, Sahayaraj S, Köble C, Meuris M, Poortmans J. Characterization of defects in 9.7% efficient Cu₂ZnSnSe₄-CdS-ZnO solar cells, *Applied Physics Letters*, 2013, 103(16), 163904.
- [4] Guo Q, Hillhouse H W, Agrawal R. Synthesis of Cu₂ZnSnS₄ nano-crystal ink and its use for solar cells, *Journal of American Chemical Society*, 2009, 131, 11672–11673.
- [5] Guo Q, Ford G M, Yang W C, Walker B C, Stach E A, Hillhouse H W, Agrawal R. Fabrication of 7.2% efficient CZTS_{Se} solar cells using CZTS nano-crystals. *Journal of American Chemical Society*, 2010, 132(49), 17384–17386.
- [6] Riha S C, Parkinson B A, Prieto A L. Solution based synthesis and characterization of Cu₂ZnSnS₄ nano-crystals, *J. Am. Chem. Soc.* 2009, 131, 12054-12055.
- [7] Collard A D, Hillhouse H W. Composition control and formation pathway of CZTS and CZTGS₄ nano-crystal inks for solar cells, *Chem. Mater.*, 2015, 27, 1855-1862.
- [8] Chernomordik B D, Beland A E, Trejo N D, Gunawan A A, Deng D D, Mkhoyan K A, Ayedil E S. Rapid Facile synthesis of Cu₂ZnSnS₄ nano-crystals, *J. Mater. Chem. A*, 2014, 2, 10389-10395.
- [9] Coughlan C & Ryan K M. Complete study of the composition and shape evolution in the synthesis of Cu₂ZnSnS₄ (CZTS) semiconductor nano-crystals, *CrystEngComm*, 2015, 17, 6914.
- [10] Karimi M, Eshraghi M J, Jahangir V. A facile and green synthetic approach based on deep eutectic solvents toward synthesis of CZTS nano-particles, *Materials Letters*, 171, 15 May 2016, 100-103.
- [11] Ping An, Liang Z, Xu X, Wang X, Jin H, Wang N, Wang J, Zhu F. Heating up method for the synthesis of pure phase kesterite Cu₂ZnSnS₄ nano-crystals using simple coordinating sulphur precursor, *RSC Adv.*, 2015, 5, 6879.
- [12] Gupta S, Whittles T J, Batra Y, Satsangi V, Krishnamurthy S, Dhanak V R, Mehta B R. A low cost sulphurization free approach to control optical and electronic properties of Cu₂ZnSnS₄ via precursor variation, *Solar Energy Materials & Solar Cells*, 157 (2016), 820-830.
- [13] Scragg J J, Dale P J, Peter L M, Zoppi G, Forbes I. New routes to sustainable photo-voltaics: evaluation of Cu₂ZnSnS₄ as an alternative absorber material, *Phys Status Solidi*, B9 (2008), 1772.
- [14] Mourdikoudis S, Liz-Marzan L M. Oleylamine in nano-particle synthesis, dx.doi.org/10.101021/cm4000476/ *Chem. Mater.* 2013, 25, 1465-1476.
- [15] Ahmad R, Brandl M, Distaso M, Herre P, Spiecker E, Hock R, Peukert W. A comprehensive study on the mechanism behind formation and depletion of Cu₂ZnSnS₄ (CZTS) phases, *Cryst Eng Comm*, 2015, 17, 6972.
- [16] Chemistry Part II textbook for class XII, NCERT, November 2012, ISBN 81-7450-716-7(Part II).
- [17] Fernandes P A, Salome P M P, da Cunha A F. Study of polycrystalline Cu₂ZnSnS₄ films by Raman scattering, *Journal of Alloys and Compounds* 509 (2011)7600-7606.
- [18] Chalapathi U, Kumar Y B K, Uthanna S, Raja V S. Investigations of Cu₂SnS₄ thin films prepared by spray pyrolysis, *Thin Solid Films* 556 (2014) 61-67.
- [19] Price L S, Parkin P I, Hardy M E A, Clark J H, Hibbert T G, Molloy K C. Atmospheric pressure chemical vapour deposition of tin sulphides (SnS, Sn₂S₃ and SnS₂) on glass, *Glass. Chem. Mater.* 1999, 11, 1792-1799.
- [20] Kobayashi T, Jimbo K, Tsuchida K, Oyanagi T, Katagari H. Investigation of Cu₂ZnSnS₄ based thin film solar cells using abundant materials, *Jpn. J. Appl. Phys.*, 44 (2005), 783.
- [21] Pal M, Mathews N R, Gonzalez R S, Mathew X. Synthesis of Cu₂ZnSnS₄ nano-crystals by solvo-thermal method, *Thin Solid Films*, 535 (2013), 78-82.

Publication II

Suresh Kumar, Mare Altosaar, Maarja Grossberg, Valdek Mikli, Effect of Alkali ions (Na^+ , K^+ , Cs^+) on Reaction Mechanism of CZTS Nano-particles Synthesis, *Superlattices and Microstructures* 116 (2018) 54-63.



Effect of alkali ions (Na^+ , K^+ , Cs^+) on reaction mechanism of CZTS nano-particles synthesis



Suresh Kumar^{*}, Mare Altosaar, Maarja Grossberg, Valdek Mikli

Department of Materials and Environmental Technology, Tallinn University of Technology, Ehitajate tee 5, 19086, Tallinn, Estonia

ARTICLE INFO

Article history:

Available online 14 February 2018

Keywords:

$\text{Cu}_2\text{ZnSnS}_4$
Nano-crystal synthesis
Growth/reaction mechanism
Complexes
Alkali ions
FTIR

ABSTRACT

The control of morphology, elemental composition and phase composition of $\text{Cu}_2\text{ZnSnS}_4$ (CZTS) nano-crystals depends on the control of complex formation and surface stabilization of nano-particles in solution-based synthesis in oleylamine. At temperatures $\geq 280^\circ\text{C}$, the control of nano-crystal's morphology and homogenous growth is difficult because of fast poly-nuclear growth occurring at higher temperatures. In the present work the effect of oleylamine complex formation with different alkali ions (Na^+ , K^+ and Cs^+) on nano-crystals growth at synthesis temperature of 280°C was studied. It was found that nano-powders synthesized in the presence of Na^+ and K^+ ions showed the formation of crystals of different sizes - small nano-particles (18 nm–30 nm), large aggregated crystals (few nm to $1\ \mu\text{m}$) and large single crystals ($1\ \mu\text{m}$ - $4\ \mu\text{m}$). The presence of Cs^+ ions in the nano-powder synthesis in oleylamine-metal precursor- CsOH solution promoted growth of nano-crystals of homogenous size. It is proposed that the formed oleylamine- Cs complexes a) enhance the formation and stabilization of oleylamine-metal (Cu, Zn and Sn) complexes before the injection of sulphur precursor into the oleylamine-metal precursor solution and b) after addition of sulphur stabilize the fast nucleated nano-particles and promote diffusion limited growth.

© 2018 Published by Elsevier Ltd.

1. Introduction

The direct production of electricity from solar energy using photovoltaic cell is renewable and non-polluting method. Besides the prevailing silicon, the main PV inorganic compound absorber materials used in solar cell mass production are CdTe and $\text{Cu}(\text{InGa})\text{Se}_2$ showing record power conversion efficiencies 22.1% [1] and 22.6% [2], respectively. However, there are concerns with toxicity (Cd) and/or scarcity (In and Te) of the constituent elements. Therefore, kesterite compound $\text{Cu}_2\text{ZnSnS}_4$ (CZTS) has drawn significant attraction as an alternative for CdTe and CIGS because of the non-toxic and earth-abundant constituent elements [3]. CZTS has high absorption coefficient ($\geq 10^4\ \text{cm}^{-1}$) and direct band gap (1.5 eV) [4]. The low cost nano-powder ink technology motivates photovoltaic research to achieve cost-efficient CZTS solar cells production technology. The control of morphology, elemental composition and phase composition of CZTS nano-crystals in solution-based synthesis depends on the control of complex formation and surface stabilization of nano-particles [5]. We performed a series of experiments of CZTS nano-powders synthesis at temperatures from 190°C to 340°C and found that CZTS phase dominated at synthesis temperature of 280°C (the work will be published). We found that the control of nano-crystals morphology and

^{*} Corresponding author.

E-mail address: sureshkumarnara@gmail.com (S. Kumar).

homogenous nano-crystals growth in solution-based method is very difficult at higher temperatures (i.e. $\geq 280^\circ\text{C}$) because of fast poly-nuclear growth occurring at this temperature. In this work, the CZTS nano-powders were synthesised by solution-based hot injection method using oleylamine as solvent. The effect of a complex of oleylamine and alkali (Na^+ , K^+ and Cs^+) ion on nano-crystals growth at synthesis temperature (280°C) was studied. In Ref. [6] it was shown that caesium hydroxide promoted alkylation of primary amines and suppressed over-alkylation of the produced secondary amines being highly chemo-selective to favour mono-N-alkylation over dialkylation. Best to our knowledge, no group have studied such a complex formation with oleylamine and its impact on the morphology, phase and elemental composition of CZTS nano-powders. The alkali (Na^+ , K^+ and Cs^+) ions were used to promote and stabilize the complex formation of oleylamine-metal (Cu, Zn and Sn) complex by forming an intermediate oleylamine-alkali ion complex. In the present work Raman and Fourier Transform Infrared (FTIR) spectroscopy were used for studying the complex formation in oleylamine-alkali ion containing solutions.

2. Experimental

2.1. CZTS nano-powder synthesis

The analytical grade chemicals copper 2, 4-pentanedionate, zinc acetate, tin (II) chloride and elemental sulphur were used as precursors (Sigma Aldrich) for Cu, Zn, Sn and S, respectively. All chemicals were used as received without any further purification or treatment. Oleylamine is used as solvent, surfactant and capping ligand in the solution-based synthesis of CZTS nano-powders [7]. The initial precursor composition of 1.9 mmol of Cu, 1.08 mmol of Zn, 0.9 mmol of Sn and 4.5 mmol of S was used for all synthesis. Alkali metal containing compounds NaCl, NaOH, KCl, KOH and CsOH in amount of 0.1 mmol were used as precursors of Na^+ , K^+ and Cs^+ ions for respective experiments. KOH (85%) and NaOH granules (98%) bought from Lach:ner, analytical grade $\text{CsOH}\cdot\text{H}_2\text{O}$ from Fluka and high purity NaCl (99.5%) from Merck and KCl from company REAHM were used without any purification. The effect of CsOH concentration was studied by using 0.1 mmol and 0.5 mmol additives of caesium hydroxide. The used alkali compound and Cu, Zn and Sn precursors were mixed in 25 ml of oleylamine in three-neck flask at 25°C . Temperature of the solution was increased to 280°C under inert gas condition. Separately, 0.32 g of sulphur was added to 10 ml of oleylamine and sonicated for 30 min at 70°C . 4.5 ml of this freshly prepared sulphur solution was added to the flask containing oleylamine solution of other precursors at 280°C . The required synthesis temperature is easier to maintain if to inject the sulphur-oleylamine precursor solution into the pre-heated metal-oleylamine solution at the required synthesis temperature. In this case, the nucleation and growth of nano-particles start immediately without further intermediate reaction steps that are possible if temperature is lower or higher than needed. The solution was kept for 30 min at 280°C . The synthesis time and temperature were kept constant for every test as both of the synthesis parameters have impact on the CZTS nano-crystals structure, growth and nucleation [8,9]. The solution was cooled down naturally to room temperature in inert gas environment. The synthesized CZTS nano-powders were separated from solution and cleaned by repeated centrifugation with ethanol, hexane and isopropanol, where hexane was used for removing non-polar impurities and isopropanol for polar impurities [10]. The nano-powders were dried in thermostat at 40°C for 30 min. The scanning electron microscopy (SEM) was performed to investigate the morphological structure and size of particles of nano-powders using a ZEISS ULTRA 55 FE-SEM apparatus. The energy dispersive X-ray spectroscopy (EDS) was performed on the same set-up for determining the elemental composition of nano-powder samples. The samples for the EDS analysis were prepared by pressing the nano-powders into pellets. The formation of complexes of oleylamine-alkali salt and oleylamine-alkali hydroxide were studied using Raman and FTIR spectroscopy. The samples were prepared by mixing 4 ml of oleylamine and 0.1 mmol of respective alkali salt or alkali hydroxide followed by sonication at 70°C for 60 min for dissolution of alkali salts and alkali hydroxides. The FTIR and Raman analysis of samples of oleylamine cation complexes and oleylamine cation alkali compound complexes were performed. Alkali metal containing compounds NaCl, NaOH, KCl, KOH and CsOH in amount of 0.1 mmol with different cation precursors (Cu, Sn, Cu-Zn, Cu-Sn and Cu-Zn-Sn) were mixed in 25 ml of oleylamine in three-neck flask at 25°C . Temperature of the solutions was increased to 280°C under inert gas condition. The solutions were kept for 30 min at 280°C . The solutions were cooled down naturally to room temperature in inert gas environment. These freshly made solutions were used as samples for Raman and FTIR analysis. Raman spectroscopy was performed at room temperature using Horiba Jobin Yvon HR800 micro-Raman spectroscope with 532 nm laser as excitation source. FTIR measurements were performed on Perkin Elmer GX-1 spectrometer.

3. Results and discussion

3.1. FTIR spectra analysis of oleylamine and oleylamine-metal precursors

The FTIR spectra of oleylamine and solutions of oleylamine with different metal precursors are shown in Figs. 1–3 and the FTIR absorption peak positions are presented in Table 1 together with corresponding vibrational assignments. The FTIR spectrum of oleylamine shows absorption peaks at 722, 794, 967, 1071, 1312, 1378, 1463 and 1651 cm^{-1} (Fig. 4). In the FTIR spectra of oleylamine-metal precursor solutions (Figs. 1–3) peaks at lower wavelength side (below 700 cm^{-1}) due to the components of precursor compounds and oleylamine are also detected. The FTIR absorption peak of oleylamine at 1071 cm^{-1} corresponds to the bending vibration of carbon-nitrogen (C-N) bond [7,11,12].

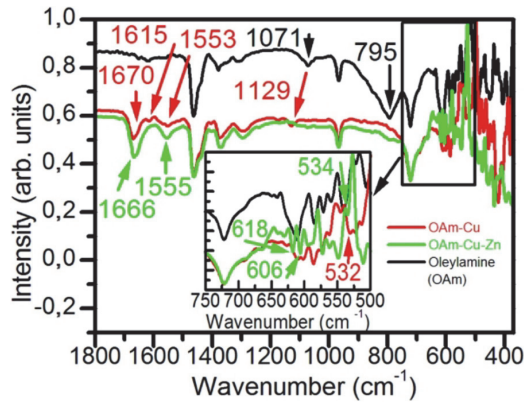


Fig. 1. FTIR spectra of oleylamine, oleylamine-copper, oleylamine-copper-zinc precursor solution.

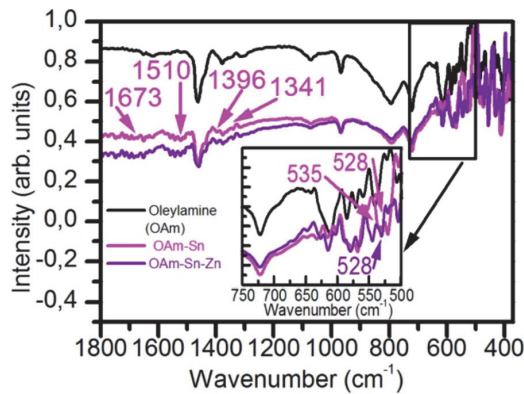


Fig. 2. FTIR spectra of oleylamine, oleylamine-tin, oleylamine-tin-zinc precursor solution.

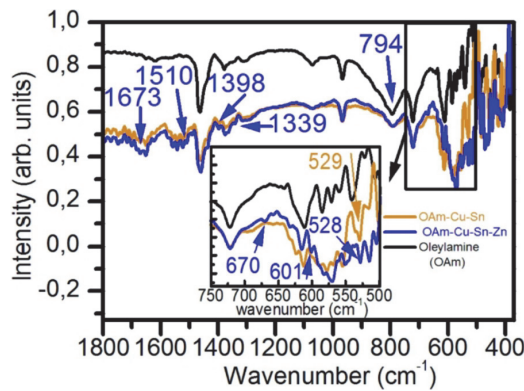


Fig. 3. FTIR spectra of oleylamine, oleylamine-copper-tin, oleylamine-copper-tin-zinc precursor solution.

The FTIR absorption spectrum of oleylamine-copper precursor solution shows absorption peaks at 532, 721, 795, 967, 1129, 1403, 1553, 1615 and 1670 cm^{-1} (see Fig. 1). Instead of the peak at 1071 cm^{-1} as it was observed in pure oleylamine, a shifted FTIR absorption peak at 1129 cm^{-1} is detected, most probably because of formation of oleylamine carbon–copper bond and

Table 1
Vibrational assignments of IR absorption peaks.

Solution	FTIR peak positions (cm^{-1})											Ref.	
Vibrational Modes	ν_{as} C-Sn	ν_{s} C-Cu	ν Sn-Cu, Cu-Zn	δ C-C	δ NH_2 , ν NH_2	Wagging (NH_2), δ N-Cs	δ C-N	δ Cu-N	ν C-Sn, Sn-Cu, Sn-Zn	δ CH3	δ -C=C	ν C-Cu,Sn,Zn ν N-Cu	[4] This work
OAm				722	795		1071			1465	1647		[4,8–10]
OAm				722	794	967	1071			1463	1651		This work
OAm-Cu		532			795	967		1129				1553	This work
					1605							1670	
OAm-Cu + Zn		534	606		795	967						1555	This work
			618									1666	
OAm-Sn	528 [11]				795	967			1341			1510	This work
	535 [11]								1396			1673	
OAm-Cu + Zn + Sn	528 [11]		601		795	967			1339			1510	This work
			670						1398			1553	
												1666–1673	
OAm-CsOH						967							This work
						985							

ν -symmetric or asymmetric vibrations, ν_{s} -symmetric vibrations, ν_{as} -asymmetric vibrations, δ -bending vibrations.

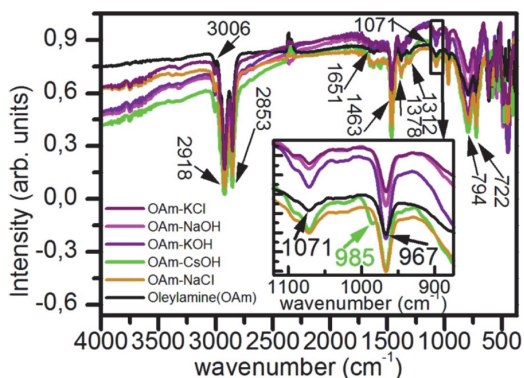


Fig. 4. FTIR spectra of Oleylamine (OAm), OAm-CsOH, OAm-NaOH, OAm-KOH, OAm-NaCl, OAm-KCl precursor solution. The additional absorption peak at 985 cm^{-1} corresponding to complex formation of caesium hydroxide and amine group is observed for the solution of oleylamine-CsOH.

formed complex of oleylamine-copper- NH_2 group (Fig. 1). The absorption peak at 1593 cm^{-1} corresponds to the bending of the NH_2 group in oleylamine [12,13]; while in oleylamine copper precursor solution this peak is broad and less intense and is disappearing due to weak bond between copper and NH_2 group. The two additional absorption peaks at 1670 cm^{-1} and 1553 cm^{-1} correspond to vibrations of oleylamine carbon-copper and oleylamine nitrogen-copper bond.

The FTIR absorption spectrum of oleylamine solution with copper and zinc precursors shows peaks at 534, 606, 618, 721, 795, 967, 1555, and 1666 cm^{-1} (see Fig. 1). Peaks at 606 and 618 cm^{-1} appeared with addition of Zn precursor. Probably the mechanism of complex formation in the oleylamine-copper and oleylamine-copper-zinc solutions is similar to each other.

The FTIR absorption spectrum of oleylamine-tin precursor solution shows absorption peaks at 528, 535, 721, 795, 967, 1341, 1396, 1510 and 1673 cm^{-1} (Fig. 2). The new bond forms probably between oleylamine carbon and tin (see Fig. 10) without affecting the amine group in oleylamine. The carbon nitrogen stretching vibrations (1071 cm^{-1}) and nitrogen hydrogen bending vibrations (967 cm^{-1}) of amine (NH_2) group in oleylamine were unaffected. The FTIR absorption peak related to oleylamine carbon-tin bond in the oleylamine tin precursor solution is at 528 and 535 cm^{-1} [14].

In the presence of zinc and tin precursors in oleylamine, there forms carbon-tin-zinc- NH_2 complex because FTIR spectrum shows no changes in the absorption behaviour of amine group. The FTIR spectrum of oleylamine-copper-zinc-tin solution shows peaks at 528, 601, 670, 1339, 1398, 1510 1553 and 1673 cm^{-1} . The FTIR absorption peak at 528 cm^{-1} is related to oleylamine carbon-tin bond as it was found in Ref. [14] in the oleylamine-tin precursor solution. The two additional absorption peaks appearing at $1666\text{--}1673 \text{ cm}^{-1}$ and $1552\text{--}1555 \text{ cm}^{-1}$ could correspond to carbon-metal and nitrogen-metal bonds. The changes in FTIR spectra let us conclude that the oleylamine carbon-tin-copper-zinc- NH_2 complex was formed and this is the nuclei for the CZTS crystal formation and growth after the addition of the sulphur-in-oleylamine precursor solution.

3.2. FTIR spectra analysis of oleylamine, oleylamine-metal precursors, oleylamine-alkali salts and oleylamine-alkali hydroxides

The FTIR spectra of oleylamine, oleylamine-NaOH, oleylamine-KOH, oleylamine-CsOH, oleylamine-NaCl and oleylamine-KCl are shown in Figs. 4 and 5. As we can recognize, no big changes in FTIR spectra accompany with addition of NaCl, KCl, NaOH and KOH. With addition of caesium hydroxide adsorption peak at 985 cm^{-1} appears. The FTIR spectra of solutions of oleylamine-metal precursors show no absorption peaks at 985 cm^{-1} while this peak is present in oleylamine-CsOH-Cu-Sn-Zn precursor solutions. In the case of solution of oleylamine-CsOH the absorption peak at 967 cm^{-1} corresponds to NH_2 wagging and absorption peak at 985 cm^{-1} corresponds to complex formation of caesium hydroxide and amine group (Fig. 4) [12,13]. As we can see later, CZTS nano-powders with rather big nano-crystals of uniform size grow from the CsOH containing solution (Fig. 8). Therefore, we can assume that the formed oleylamine-caesium hydroxide complex improves the stabilizing properties of oleylamine.

The FTIR studies show that complexes between oleylamine and cation atoms or groups of cation atoms (Cu, Sn, Cu-Zn, Cu-Sn, Cu-Zn-Sn) were formed. The oleylamine as solvent and surfactant has been used in different syntheses and it was shown that oleylamine forms complexes with cation and/or anion atoms in the syntheses of nano-particles of pure elements and compounds [11,12,15]. Cation atoms or a group of cation atoms can attach to oleylamine nitrogen or oleylamine carbon next to the nitrogen. The FTIR studies of the oleylamine-copper-zinc-tin solution show that the Sn atom is attached to the carbon atom of the oleylamine and the other cation atoms (Cu, Zn) form bonds with Sn atom or carbon atom. At 280°C these cation atoms absorbing energy in the form of kinetic or thermal energy can get released into the solution by breaking bonds or rearrange in the same metal oleylamine complex. The stepwise details of reaction mechanism of CZTS nucleation and growth will be presented and explained as chemical equations in the latter part of the paper. There are two possible ways of decomposition or deterioration of metal oleylamine complex: a) formed metal oleylamine complex release cation atom or group of cation atoms into the solution, b) formed metal oleylamine complex release or reorganise the cation atom or group of cation atoms in the same oleylamine complex by changing the coordination with carbon and/or nitrogen. If CsOH is present, the oleylamine nitrogen site is blocked by forming the bond between the caesium and nitrogen atoms. When the oleylamine nitrogen atom is blocked due to the caesium nitrogen bond formation, the Cu, Zn and Sn cation atoms attach to the carbon atom. The cation atoms attached to the oleylamine carbon atom give higher stability to cation metal-oleylamine complex. The cation metal-oleylamine complex is stabilized and the number of nuclei of different phases is reduced, leading towards the growth of limited phases. This is the nuclei for the CZTS crystal formation and growth after the addition of the sulphur-in-oleylamine precursor solution.

3.3. Raman analysis of oleylamine and oleylamine-alkali salts or oleylamine-alkali hydroxide

The room-temperature Raman spectra of oleylamine, CsOH and oleylamine-CsOH solution in the region from 50 to 2300 cm^{-1} are plotted in Fig. 6 and in the regions from 2200 cm^{-1} and from 2300 cm^{-1} to 8000 cm^{-1} in Fig. 7. For better comparison the normalised Raman spectra are presented.

The Raman spectrum of oleylamine shows Raman peak at 1070 cm^{-1} (Fig. 6) which corresponds to carbon nitrogen bond movement [7]. The Raman spectrum of oleylamine-caesium hydroxide solution shows additional Raman peak at 649 cm^{-1} corresponding to caesium hydroxide and amine complex (Fig. 6). Oleylamine forms with alkali hydroxides a complex which improves the stabilizing properties of oleylamine by forming a nitrogen caesium bond and stabilizing the amine functional group [6]. The influence of the formed Cs-oleylamine complex to the CZTS crystal growth can be seen in the changed

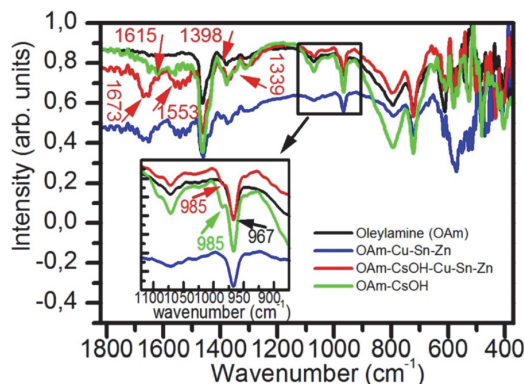


Fig. 5. FTIR spectra of Oleylamine (OAm), OAm-CsOH, OAm-Cu-Sn-Zn, OAm-CsOH-Cu-Sn-Zn precursor solution. The absorption peak at 967 cm^{-1} corresponds to NH_2 wagging and absorption peak at 985 cm^{-1} corresponds to complex of oleylamine-CsOH-Cu-Sn-Zn.

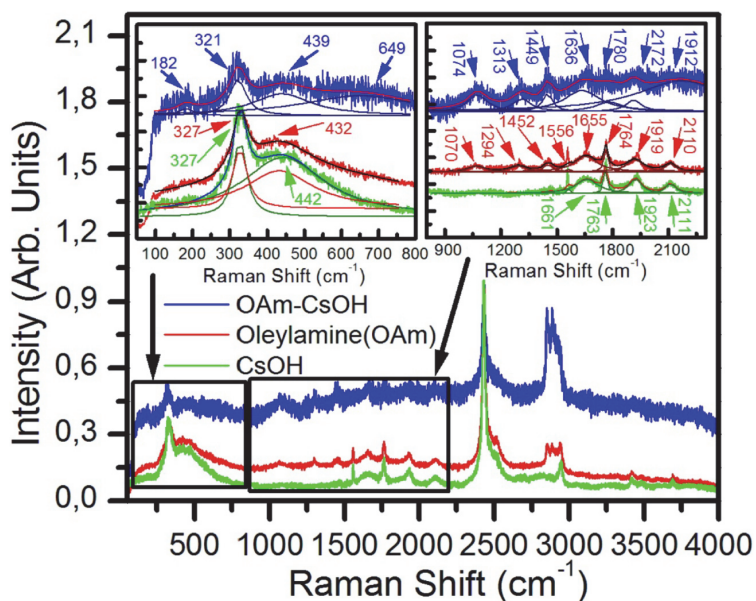


Fig. 6. Raman spectra of oleylamine (OAm), OAm-CsOH and CsOH. The inset graphs show the fittings of the spectrum in the spectral region from 50 cm^{-1} to 2300 cm^{-1} .

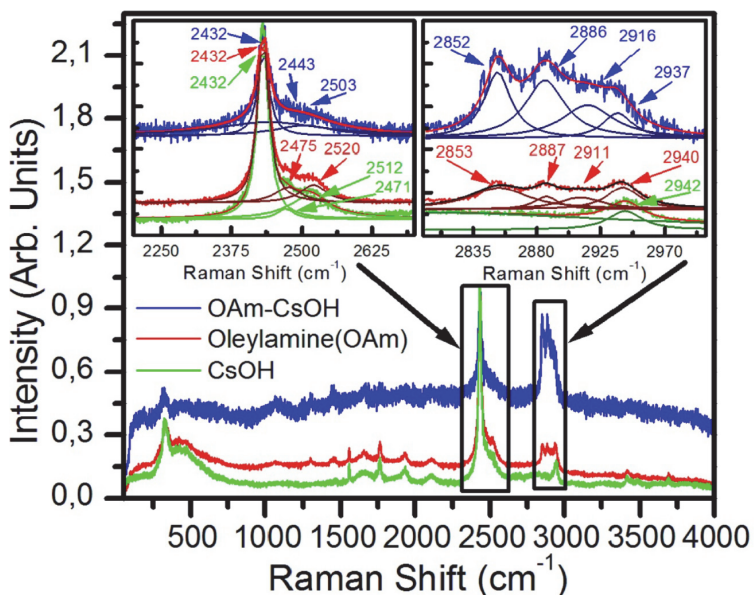


Fig. 7. Raman spectra of oleylamine (OAm), OAm-CsOH and CsOH. The inset graphs show the fitting of the spectrum in the spectral region from 2200 cm^{-1} to 3000 cm^{-1} .

morphology of the formed nano-powders synthesized in the presence of CsOH showing non-aggregated big uniform nano-crystals with a similar size. The other used hydroxides (NaOH, KOH) do not give a similar effect.

3.4. SEM, EDS and Raman analysis of CZTS nano-powders

SEM images of CZTS nano-powders synthesised in oleylamine solvent in the presence of alkali salts (NaCl and KCl), alkali hydroxides (NaOH, KOH and CsOH) and without any salt are presented in Fig. 8. Nano-powder crystals synthesised in the presence of Na⁺ and K⁺ ions show three size ranges - small nano-particles with medium size around 18 nm, large aggregates of crystals and nano-crystals bigger than 100 nm (Fig. 8).

Nano-powders synthesised in the presence of Cs⁺ ions (CsOH) show only one size range of nano-particles - uniform nano-crystals in the range of 100 nm–200 nm. The nano-powders formed in the presence of sodium and potassium compounds show large agglomerates of nano-crystals (Fig. 8) whereas no such agglomeration was observed in the powders synthesised in the presence of caesium hydroxide. The above described observation could be interpreted as an effect of enhanced stabilization ability of oleylamine in the presence of intermediate caesium-oleylamine complex supporting the diffusion limited growth (i.e. formation of homogenous nano-crystals) and reducing the further poly-nucleation and aggregation of nano-particles.

The composition of CZTS nano-powders synthesised in the presence of alkali salts (Na, K and Cs) was analysed by EDS. The sulphur concentration and tin to copper concentration ratio in the formed powders are decreased in comparison with the initial elemental composition in all experiments. Nano-powders synthesised in the presence of sodium salt are slightly zinc rich and copper poor. Nano-powders synthesised with addition of caesium hydroxide had zinc poor, tin and copper rich elemental composition.

The Raman spectra of nano-powders synthesised in the presence of caesium hydroxide show two main peaks at 337 and 286 cm⁻¹ which correspond to CZTS (Fig. 9). The full width at the half maximum (FWHM) of the dominating Raman peak is small (7.7 cm⁻¹) showing the high crystallinity of the nano-powders.

The effect of different initial concentrations of CsOH was studied by adding different amounts - 0.1 mmol and 0.5 mmol of CsOH into oleylamine in the synthesis of CZTS nano-powders at 280 °C. Fig. 11 shows SEM images of these CZTS nano-powders. It can be observed that higher concentration of CsOH enhances the homogeneous growth of nano-crystals.

We propose the possible chemical equations for the interactions and complex formation between solvent oleylamine, copper 2, 4-pentanedionate, zinc acetate and tin (II) chloride before addition of the sulphur precursor solution. As shown by thermal decomposition studies in the work [16] copper 2, 4-pentanedionate (copper (II) acetylacetonate) decomposes in two steps in the temperature region of 443–523 K. In the first step acetyl-acetone (C₅H₈O₂) separates and the remained part of molecule (C₅H₈O₃) decomposes with reduction of Cu(II) to Cu(0) and oxidation of the ligands to CO₂ and produces acetone (H₁₄C₆O₂) by the reactions (1, 2) [16].

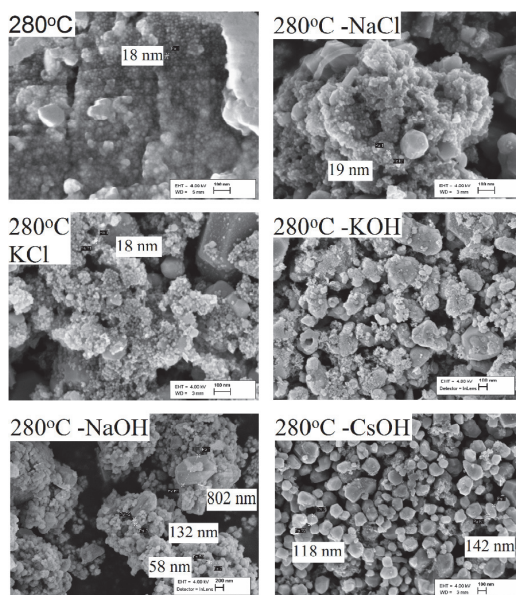


Fig. 8. SEM images of CZTS nano-powders synthesised in oleylamine solvent in the presence of 0.1 mmol of alkali salts and/or alkali hydroxides.

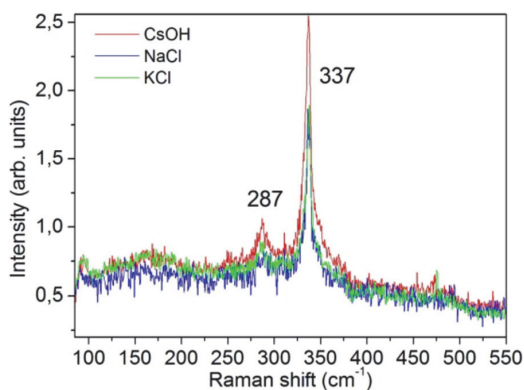


Fig. 9. Raman spectra of CZTS nano-powders synthesized in oleylamine at 280 °C with added NaCl, KCl and CsOH.

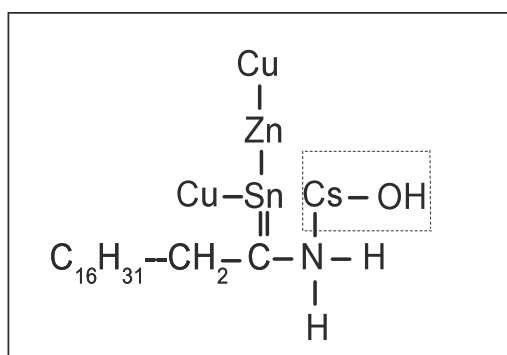


Fig. 10. The oleylamine-metals complex with CsOH.

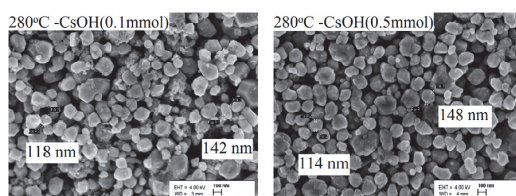
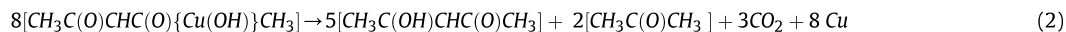
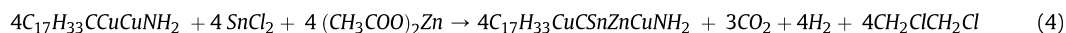


Fig. 11. CZTS nano-powders synthesized at 280 °C with 0.1 mmol and 0.5 mmol of Caesium hydroxide in oleylamine.



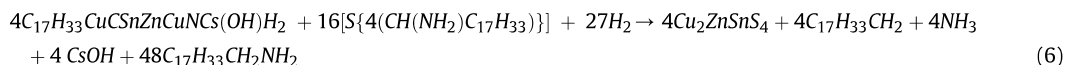
Cu(0) atoms attach to carbon in the chain of oleylamine by replacing 2 hydrogen atoms and Cu(0) is changed to Cu(I), this reaction is shown in chemical equation (3). In the next stage Sn(II) forms a single bond with oleylamine carbon and copper (C-Sn-Cu). There occurs a rearrangement of atoms and Sn(II) state is converted to Sn(IV) forming a double bond with carbon atom (C=Sn) because of very high coordinating power of Sn and high stability of the formed complex. In the next stage zinc atom is inserted into the oleylamine chain as Zn(II) forms a metal-oleylamine complex (see Fig. 10).



The amine group in the oleylamine is still active in the metal-oleylamine complex and needs to be further stabilized. The CsOH plays the role as an amine group stabilizer in such a complex of oleylamine-metal-caesium hydroxide (see structure of a complex in Fig. 10). There is high possibility that CsOH forms a complex with oleylamine before any attachment of Cu, Zn, Sn elements; in this way it maximises the possibility of forming a bond with carbon not nitrogen in oleylamine.



After addition of the oleylamine-sulphur solution into the three-neck flask, the formed metal nuclei react with sulphur to form CZTS nano-crystals.



Raman analysis of oleylamine and caesium hydroxide shows the formation of complex between oleylamine and alkali hydroxide whereas alkali salts did not show any complex formation. The hydroxide of potassium or sodium effectively modifies the complex formation, nucleation and nano-crystals' growth whereas hydroxide of caesium effectively promotes formation of stable nuclei, homogenous poly-nuclear growth by diffusion limited process. Analysis of Raman and FTIR spectra of oleylamine-metal precursor solutions and analysis of EDS results of synthesised CZTS nano-powders show the non-effectiveness of oleylamine-potassium hydroxide and oleylamine-sodium hydroxide complexes. Only oleylamine-caesium hydroxide complex plays a crucial role stabilizing the oleylamine-metal complexes in the Cu, Zn and Sn precursor solutions and enhances the homogeneous growth of nano-crystals. The measured pH values of oleylamine, oleylamine-NaOH, oleylamine-KOH and oleylamine-CsOH were 11.40, 11.60, 10.90 and 12.56, respectively. The basic character of solutions is higher when CsOH is added showing higher dissolution of it in oleylamine and therefore higher ability to form a stable complex. Based on the results and discussion, we propose that the formed oleylamine-caesium hydroxide complex a) enhances the formation and stabilization of oleylamine-metal (Cu, Zn and Sn) complexes before injection of sulphur precursor, b) after addition of sulphur it stabilizes the fast nucleated nano-particles and promotes homogenous nano crystal growth.

4. Conclusions

The CZTS synthesis solutions of oleylamine (as solvent) with precursor salts and with or without added alkali hydroxides or alkali chlorides (i.e. oleylamine, oleylamine + individual precursors, those with KCl, KOH, NaCl, NaOH and CsOH) were studied by FTIR and Raman spectroscopy. According to our knowledge, the FTIR spectra of these solutions were investigated in detail for the first time. The fine understanding of these spectra led us to probable reaction mechanism and reaction steps in the CZTS nano-crystals formation and growth in oleylamine with and without some alkaline additives. We have been successful in developing the effective influence of CsOH on CZTS nano-crystal growth at different stages leading to homogenous growth. We have proposed the formation of complex of oleylamine-alkali hydroxide and metal precursors. Raman, SEM and EDS studies of CZTS nano-powders synthesised at 280 °C confirmed that from oleylamine-alkali hydroxide complexes only CsOH had an effective influence in stabilization and promotion of homogeneous nano-crystal growth. The increased concentration of CsOH (0.1 mmol–0.5 mmol) further enhanced the homogeneous growth of nano-crystals with narrow size distribution in comparison with very large size distribution that was characteristic to powders grown in the solutions with Na⁺ and K⁺ ions - from small nano-particles (18 nm–30 nm) to large aggregated crystals (few nm to 1 μm) and large single crystals (1 μm - 4 μm).

Acknowledgement

This work was supported by the institutional research funding IUT 19–28 of the Estonian Ministry of Education and Research, and by the European Union through the European Regional Development Fund, Project TK141.

References

- [1] First solar reports on 23 February 2016. <http://www.greentechmedia.com/articles/read/first-solar-hits-record-22-1-conversion-efficiency-for-cdte-solar-cell>. (Accessed 12 February 2018).
- [2] ZSW press release 09/2016. http://www.zsw-bw.de/fileadmin/user_upload/PDFs/Pressemitteilungen/2016/pr09-2016-ZSW-WorldRecordCIGS.pdf. (Accessed 12 February 2018).
- [3] J. Kim, B. Shin, Strategies to reduce the open-circuit voltage deficit in Cu₂ZnSn(S,Se)₄ thin film solar cells, *Electron. Mater. Lett.* 13 (5) (2017) 373–392, <https://doi.org/10.1007/s13391-017-7118-1>.
- [4] H. Katagiri, K. Jimbo, W.S. Maw, K. Oishi, M. Yamazaki, H. Araki, A. Takeuchi, Development of CZTS- based thin film solar cells, *Thin Solid Films* 517 (2009) 2455–2460, <https://doi.org/10.1016/j.tsf.2008.11.002>.
- [5] Fundamentals of homogenous nucleation, [Depts.washington.edu/solgel/documents/class-docs/MSE502/ch-3-Section-3.2.1-3.2.5.3.pdf](https://depts.washington.edu/solgel/documents/class-docs/MSE502/ch-3-Section-3.2.1-3.2.5.3.pdf).
- [6] R.N. Salvatore, A.S. Nalge, K.W. Jung, Caesium effect: high chemo-selectivity in direct N-alkylation of amines, *J. Org. Chem.* 67 (2002) 674–683, <https://doi.org/10.1021/jo010643c>.
- [7] S. Mourdikoudis, L.M. Liz-Marzan, Oleylamine in nano-particle synthesis, *Chem. Mater.* 25 (2013) 1465–1476, <https://doi.org/10.1021/cm4000476>.
- [8] S.C. Riha, B.A. Parkinson, A.L. Prieto, Solution based synthesis and characterization of Cu₂ZnSnS₄ nano-crystals, *J. Am. Chem. Soc.* 131 (2009) 12054–12055, <https://doi.org/10.1021/ja9044168>.

- [9] R. Ahmad, M. Brandl, M. Distaso, P. Herre, E. Spiecker, R. Hock, W. Peukert, A comprehensive study on the mechanism behind formation and depletion of $\text{Cu}_2\text{ZnSnS}_4$, *CrystEngComm* 17 (2015) 6972, <https://doi.org/10.1039/C5CE00661A>.
- [10] J. Kim, H. Hiroi, T.K. Todorov, O. Gunawan, M. Kuwahara, T. Gokmen, D. Nair, M. Hopstaken, B. Shin, Y.S. Lee, W. Wang, H. Sugimoto, D.B. Mitzi, High efficiency $\text{Cu}_2\text{ZnSn}(\text{SSe})_4$ solar cells by applying a double $\text{In}_2\text{S}_3/\text{CdS}$ emitter, *Adv. Mater.* 26 (2014) 7427–7431, <https://doi.org/10.1002/adma.201402373>.
- [11] X. Lu, H.Y. Tuan, B.A. Korgel, Y. Xia, Facile synthesis of gold nano-particles with narrow size distribution by using AuCl or AuBr as the precursor, *Chemistry* 14 (5) (2008) 1584–1591, <https://doi.org/10.1002/chem.200701570>.
- [12] N. Shukla, C. Liu, P.M. Jones, D. Weller, FTIR study of surfactant bonding to Fe-Pt nano-particles, *J. Magn. Magn. Mater.* 266 (2003) 178–184, [https://doi.org/10.1016/S0304-8853\(03\)00469-4](https://doi.org/10.1016/S0304-8853(03)00469-4).
- [13] J.L. Zhang, R.S. Srivastava, R.D.K. Mishra, Core-shell magnetite nano-particles surface encapsulated with smart stimuli-responsive polymer: synthesis, characterization and LCST of viable drug targeting delivery system, *Langmuir* 23 (11) (2007) 6342–6351, <https://doi.org/10.1021/la0636199>.
- [14] R.J. Greenwald, S. Tom, W. Zucconi, J.C. Cochran, Carbon Tin vibrational frequencies in substituted trimethyl vinyl stannanes, *Main Group Met. Chem.* 17 (1994) 435, <https://doi.org/10.1515/MGMC.1994.17.6.435>.
- [15] W.H. Hsu, H.I. Hsiang, Y.L. Chang, D.T. Ray, F.S. Yen, Formation mechanisms of $\text{Cu}(\text{In}_{0.7}\text{Ga}_{0.3})\text{Se}_2$ nano-crystallites synthesized using hot injection and heating up processes, *J. Am. Ceram. Soc.* 94–9 (2011) 3030–3034, <https://doi.org/10.1111/j.1551-2916.2011.044881.x>.
- [16] S. Yoda, Y. Takebayashi, K. Sue, T. Furuya, K. Otake, Thermal decomposition of copper (II) acetylacetonate in supercritical carbon dioxide: in situ observation via UV–vis spectroscopy, *J. Supercrit. Fluids* 123 (2017) 82–91, <https://doi.org/10.1016/j.supflu.2016.12.017>.

Publication III

Suresh Kumar, Bharath Kasubosula, Mihkel Loorits, Jaan Raudoja, Valdek Mikli, Mare Altosaar, Maarja Grossberg, Synthesis of $\text{Cu}_2\text{ZnSnS}_4$ Solar Cell Absorber Material by Sol-Gel Method, *Energy Procedia* 102 (2016) 102-109.



E-MRS Spring Meeting 2016 Symposium T - Advanced materials and characterization techniques for solar cells III, 2-6 May 2016, Lille, France

Synthesis of $\text{Cu}_2\text{ZnSnS}_4$ solar cell absorber material by sol-gel method

Suresh Kumar*, Bharath Kasubosula, Mihkel Loorits, Jaan Raudoja, Valdek Mikli, Mare Altosaar, Maarja Grossberg

Tallinn University of Technology, Institute of Materials Science, Ehitajate tee 5, 19086, Tallinn, Estonia

Abstract

$\text{Cu}_2\text{ZnSnS}_4$ thin films on Mo and/or ITO covered glass substrates were prepared by dip coating method using methanol as solvent for CuCl_2 , ZnCl_2 , SnCl_2 and $\text{CH}_4\text{N}_2\text{S}$ as precursors. The influence of pre-annealing and post annealing conditions as well as the influence of used substrate on the morphology, phase composition and elemental composition of the resulting films was studied. It was found that thin films deposited onto Mo and ITO substrates and pre-annealed at 240°C in nitrogen atmosphere and post heated at 550°C showed Raman dominating peak at 338 cm^{-1} characteristic to $\text{Cu}_2\text{ZnSnS}_4$. These films were continuous, with good crystallinity and they had near-stoichiometric composition.

© 2016 The Authors. Published by Elsevier Ltd. This is an open access article under the CC BY-NC-ND license (<http://creativecommons.org/licenses/by-nc-nd/4.0/>).

Peer-review under responsibility of The European Materials Research Society (E-MRS).

Keywords: CZTS; copper zinc tin sulphide; sol-gel; thin film; heat treatment;

1. Introduction

Kesterite semiconductor compound $\text{Cu}_2\text{ZnSnS}_4$ (CZTS) is a promising absorber candidate for low cost, non toxic and sustainable thin film solar cell devices. The band gap of CZTS is close to 1.5 eV [1], being therefore

* Corresponding author. Tel.: +3726203367.

E-mail address: sureshkumarnara@gmail.com

optimal for solar energy conversion. Moreover, CZTS has a high absorption coefficient (10^4 cm^{-1}) [2]. $\text{Cu}_2\text{ZnSnS}_4$ thin films can be prepared by using several techniques such as spray pyrolysis [3], spin coating method [4], dc magnetron sputtering [5], sol gel sulphurization method [6], pulsed laser deposition [7], co-evaporation [8], and electron beam evaporation technique [9]. Tanaka et al. [9] deposited CZTS films by spin coating precursor films from sol gel solution of Cu (II), Zn (II) and Sn (II) salts in methoxy ethanol with mono-ethanol amine as stabiliser. Yeh and Jiang et al. [4, 5] used copper, zinc and tin chlorides and thiourea in ethanol-water sol gel to deposit CZTS thin films by direct liquid coating method [4] and Jiang et al. [5] reached 0.63 % of solar cell power conversion efficiency (PCE). Lei Cao et al. [6] synthesized successfully $\text{Cu}_2\text{ZnSn}(\text{S}_{1-x}\text{Se}_x)_4$ thin films by simple ethanol-thermal method. T. Chaudhuri with co-authors [7] reported a simple process for deposition of pure CZTS films from a methanol solution of metal–thiourea complexes. In the present work, the growth of CZTS thin films on bare glass, Mo or ITO substrates was studied and compared. The $\text{Cu}_2\text{ZnSnS}_4$ thin films were deposited by dip coating method using precursors copper chloride, zinc chloride, tin chloride and thiourea dissolved in methanol. The solution based method was chosen for the synthesis of CZTS thin films as it is simple and low-temperature deposition method. Methanol is a low cost solvent and a good polar liquid for preparation individual precursor solutions as sources of cations and sulphur. Thiourea is a popular source of sulphur that can easily form complexes with Cu, Zn and Sn which yield sulphides on thermal decomposition [3]. The aim of this work was to investigate the influence of pre-annealing in controlled gas atmosphere on the quality of CZTS thin films deposited by dip coating on different glass substrates. The structural properties and composition of the thin films were characterized by Raman, SEM and EDS methods.

2. Experimental

The analytical reagent grade copper chloride, zinc chloride and tin chloride were used as precursor materials for metal elements. Separate precursor solutions were prepared at room temperature (25°C) using methanol as solvent and CuCl_2 , ZnCl_2 , SnCl_2 and $\text{CH}_4\text{N}_2\text{S}$ as solutes. Separately prepared precursor solutions were mixed together in a small beaker at 25°C . The proper stirring of solution was performed at 25°C using a magnetic stirrer. After 10 minutes of stirring, the substrates were dip coated in the solution and dried in air at 75°C under ventilation. The process was repeated multiple times to increase the thickness of thin films on substrate. Three types of substrates were used: a) indium tin oxide (ITO) coated, b) molybdenum coated and c) bare soda lime glasses. The bare soda lime glass substrates were degreased in hot sulphuric acid (45°C). The ITO glasses were activated in the mixture of HCl, HNO_3 and H_2O (47.5, 5.0, and 47.5% by volume, respectively) [10]. The sequence and conditions of post deposition heat treatments in a horizontal tube furnace are presented in Table 1. The degassing of vacuum ampoules was performed at room temperature.

Table 1 Precursor concentrations in methanol solution and heat-treatment conditions of thin films.

Concentration of precursors in methanol				
Precursors	CuCl_2	ZnCl_2	SnCl_2	Thiourea
Concentration	0.1 mol/L	0.05 mol/L	0.05 mol/L	0.5 mol/L
Heat-treatment conditions in different environments				
Drying	In air at 75°C			
Pre-annealing	Nitrogen atmosphere (760 Torr)		Vacuum sealed ampoules (10^{-2} Torr)	
	180°C, 210°C, 240°C, 270°C, 300°C for 30 minutes;		180°C, 210°C, 240°C, 270°C, 300°C for 30 minutes;	
	Films on soda lime / Mo / ITO glass substrates		Films on Mo glass substrates	
Post annealing	Annealing in vacuum sealed ampoules at 550°C for 30 minutes			

ZEISS ULTRA 55 FE-SEM apparatus was used to investigate the morphological structure and to estimate the thickness of thin films and to perform the energy dispersive x-ray spectroscopy (EDS) analysis to determine the elemental composition of thin film samples. Raman spectroscopy was performed using Horiba Jobin Yvon HR800 micro-Raman spectrometer.

3. Results and Discussion

3.1 Thin films annealed in nitrogen

3.1.1 Morphology and elemental composition of films pre-annealed in nitrogen

The aim of the study was to investigate the influence of pre-annealing on the quality of CZTS thin films deposited by dip coating on different glass substrates on the structural properties and composition of the thin films.

The thickness of as-deposited thin films could be increased by multiple dip coating of thin films like it is shown in Figure 1. The EDS results show that the compositions of films on different substrates ITO and Mo (Cu:Zn:Sn:S = 2.09:1:1.1:4.8) and soda lime glass (Cu:Zn:Sn:S = 1.7:1:1.4:3.2) is different probably due to more effective adhesion of metal thiourea complex gel with Mo and ITO substrates. The thin films deposited on Mo and ITO coated glass substrates and pre-annealed in nitrogen atmosphere at 240°C are close to the stoichiometric composition of $\text{Cu}_2\text{ZnSnS}_4$ in comparison with the films deposited onto the bare glass substrate.

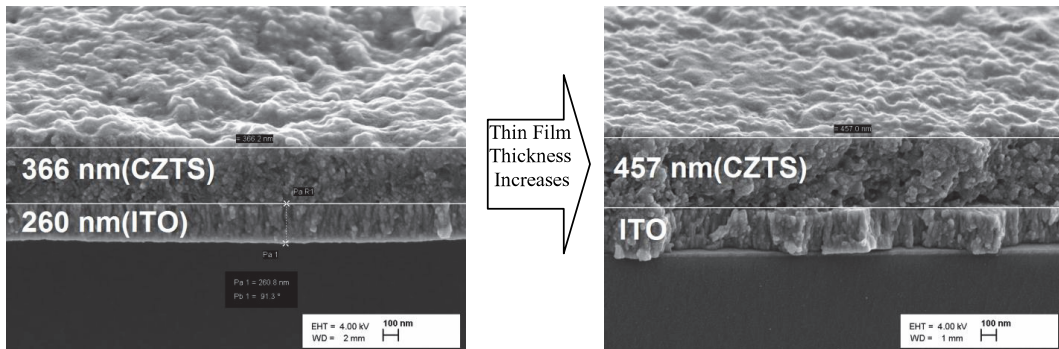


Figure 1. Thickness of as deposited thin films on ITO: left – dipping for 1 minute into solution; right – 3 times for 1 minute dip coated.

SEM images of thin films on different substrates, after drying and pre-annealing in nitrogen atmosphere, are presented in Figure 2. All the as-deposited films on different substrates are porous. On soda lime glass they have uniform morphology. Thin films on ITO and on Mo substrates show some signs of coagulation of nano-particles (see Figures 2B and 2C). Post heat-treated films on Mo glass have uniform morphology with some holes (Figure 4).

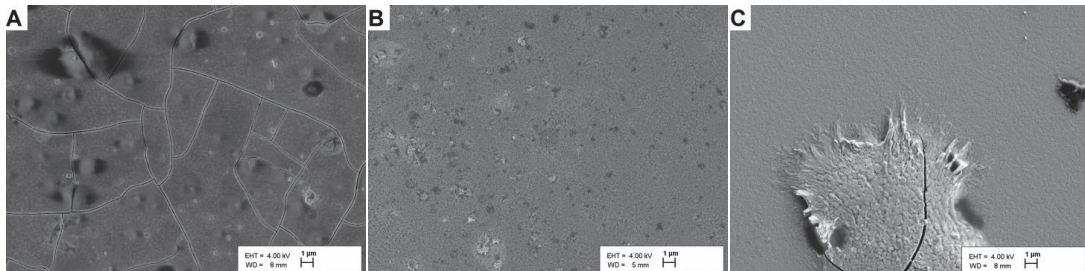


Figure 2 SEM images of pre-annealed in nitrogen atmosphere CZTS thin films on soda lime (A), on ITO (B) and on Mo (C) glass substrates

Thin films pre-annealed at 240°C have continuous uniform surface and the films are tightly bound with substrate (Figure 3).

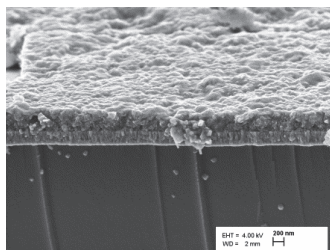


Figure 3. SEM image of thin films on Mo glass pre-annealed at 240°C in nitrogen.

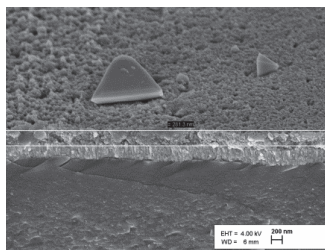


Figure 4. Cross-sectional SEM image (left) and overview (right) of thin film on Mo pre-annealed at 240°C in nitrogen and post-annealed at 550°C in closed ampoule.

Thin films annealed at 550°C in closed ampoules show uniformly grown grains and homogenous thin film surface as could be seen in the figure 4. Thin films also show some cracks on the surface.

3.1.2 Raman studies of thin films pre-annealed in nitrogen

Raman peak positions observed in thin films on Mo and ITO substrates pre-annealed at 240°C in nitrogen atmosphere are at 327-328 cm⁻¹, 293-294 cm⁻¹ and 352 cm⁻¹ which could correspond to Cu₃SnS₄ and ZnS phases respectively (Figure 7) [5, 11,12]. Therefore the chemical reaction taking place during pre-annealing of as-deposited thin films on ITO and Mo glass substrates in nitrogen atmosphere could be given as shown below, resulting in formation of Cu₃SnS₄ and ZnS phases (Eq. 1). The decomposition of ammonium chloride into ammonia and hydrogen chloride gases removes the salt from thin films above 338°C [17]. The formed gaseous carbon dioxide easily evaporates from thin films.

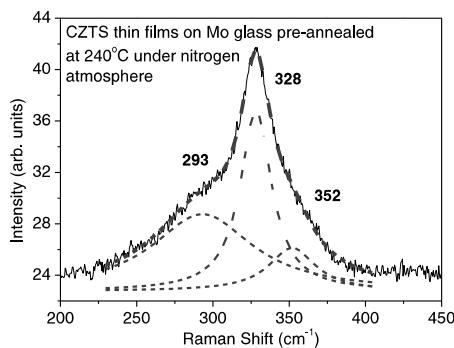
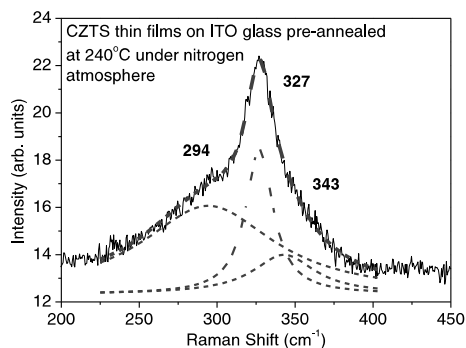
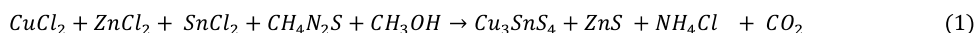


Figure 5. Raman spectra of thin films on ITO (left) and Mo (right) pre-annealed in nitrogen atmosphere

Raman peak positions observed in CZTS thin films on Mo and ITO substrates pre-annealed at 240°C in nitrogen atmosphere and post-annealed at 550°C in vacuum sealed ampoules are at 338 cm⁻¹ and 299-300 cm⁻¹ which could correspond to Cu₂ZnSnS₄ and Cu₂SnS₃ phases, respectively (Figure 6) [5,11,12].

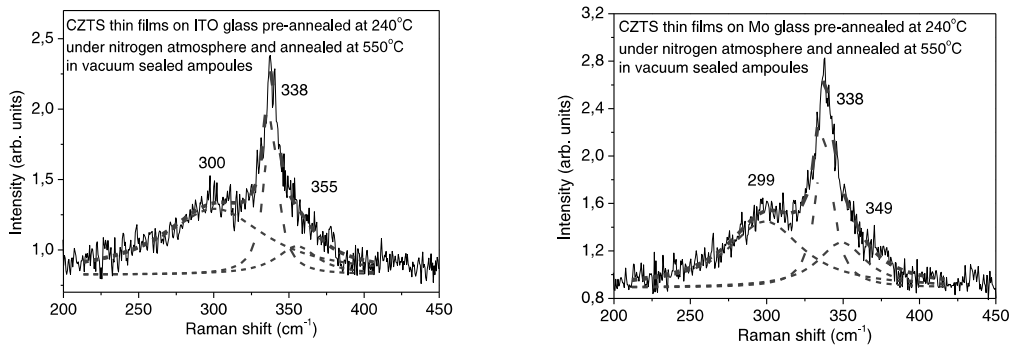
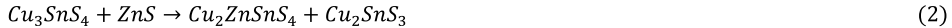
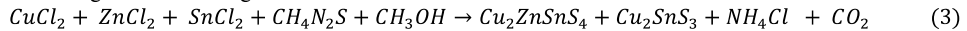


Figure 6. Raman spectra of pre-annealed in nitrogen atmosphere CZTS thin films on ITO (left) and on Mo glass substrates (right) and annealed at 550°C in vacuum sealed ampoules

The probable chemical reaction in thin films during the annealing at 550°C is the conversion of ternary Cu_3SnS_4 and binary ZnS phase into quaternary Cu_2ZnSnS_4 and ternary Cu_2SnS_3 phases (Eq. 2).



The overall formation of Cu_2ZnSnS_4 thin films in nitrogen atmosphere on Mo and/or ITO glass can be proposed as going on according to the following scheme:

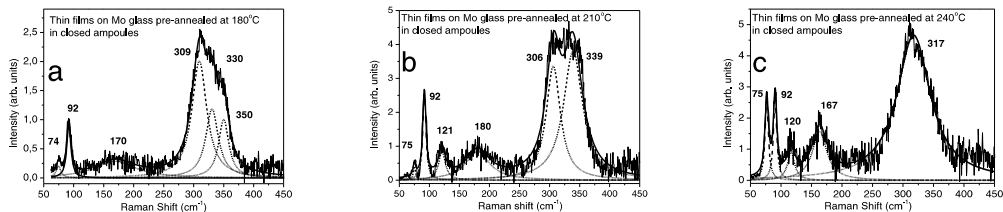


3.2. Vacuum-annealed thin films

The as-deposited thin films were dried and pre-annealed at various temperatures: 180°C, 210°C, 240°C, 270°C and 300°C in vacuum sealed ampoules and then the second step annealing was performed at 550°C in the same closed ampoules. Thin films on Mo glass substrates pre-annealed and post-annealed in vacuum sealed ampoules show lot of cracks on the surface (Figure 8) while thin films prepared in nitrogen atmosphere show very few cracks and uniform morphology (Figure 3 and 4).

3.2.1. Raman studies of thin films pre-annealed in vacuum ampoules

Raman spectra of thin films pre-annealed at different temperatures are presented in figure 9. Raman peak positions observed in CZTS thin films on Mo, pre-annealed at 180°C and 210°C in vacuum sealed ampoules are at 306-309 cm^{-1} and 330 and 339 cm^{-1} which could correspond to binary and ternary sulphides of copper and tin [11,13]. Raman peak positions observed in CZTS thin films on Mo, pre-annealed at 240°C and 270°C in vacuum sealed ampoules are at 317 cm^{-1} and 321 cm^{-1} which could correspond to ternary sulphide of copper and tin [1,11,13].



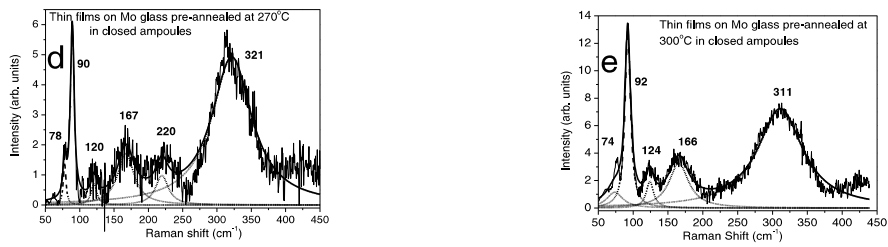
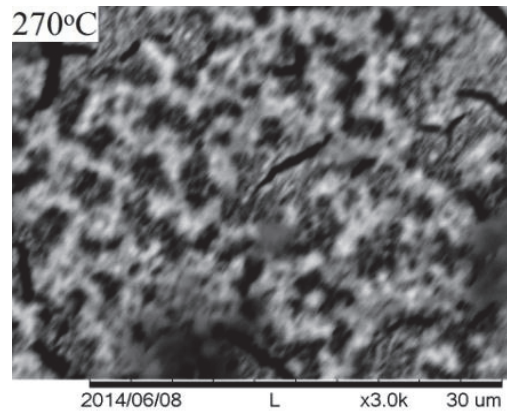
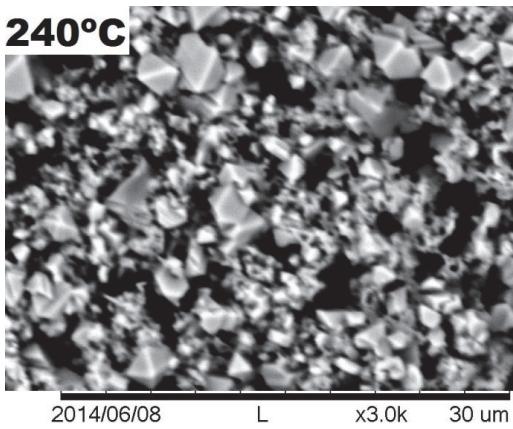
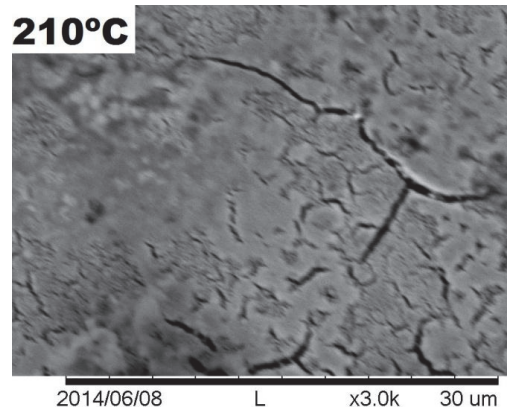
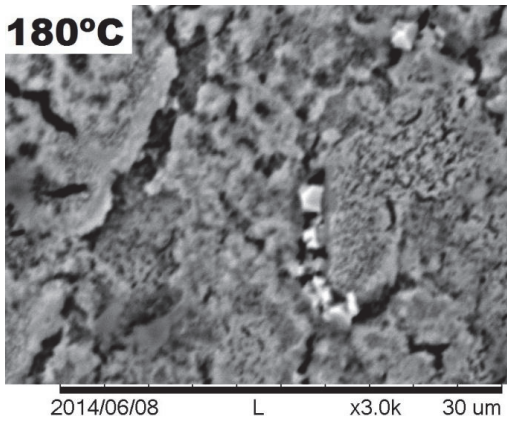


Figure 7 Raman spectra of thin films on Mo glass substrates pre-annealed at 180°C (a), 210°C (b), 240°C (c), 270°C (d) and 300°C (e) in closed ampoules.



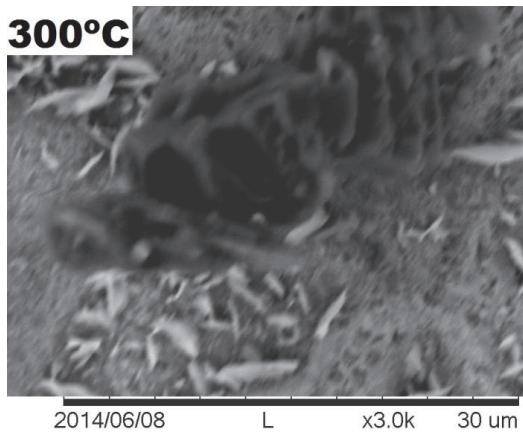


Figure 8 SEM images CZTS thin films on Mo glass pre-annealed at 180°C, 210°C, 240°C, 270°C and 300°C and post-annealed at 550°C in closed vacuum ampoules.

Raman peak positions observed in CZTS thin films pre-annealed at 180°C and 210°C on Mo glass and post-annealed at 550°C in vacuum sealed ampoules are at 307-310 cm^{-1} and 299-300 cm^{-1} which could correspond to Sn_2S_3 and Cu_2SnS_3 phases respectively (Figure 9) [5,11,12,13]. CZTS thin films pre-annealed at 240°C and 270°C and post annealed at 550°C in vacuum sealed ampoules show Raman peak positions at 304-309 cm^{-1} and 336-339 cm^{-1} which could correspond to Cu_2SnS_3 and $\text{Cu}_2\text{ZnSnS}_4$ phases, respectively (Figure 9) [5,11,12]. The thin films on Mo glass pre-annealed in vacuum sealed ampoules above 240°C i.e. 240°C, 270°C and 300°C, show quaternary CZTS phase along with ternary CTS phase.

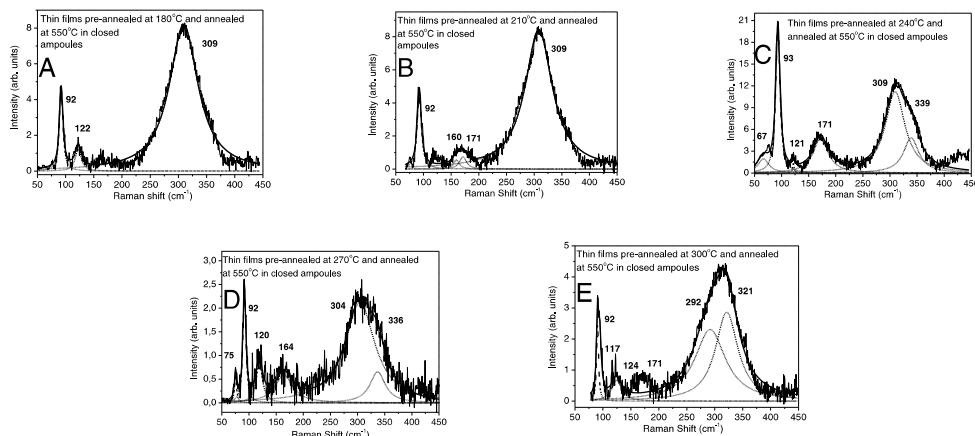


Figure 9 Raman spectra of thin films on Mo glass substrates pre-annealed at 180°C (A), 210°C (B), 240°C (C), 270°C (D) and 300°C (E) in closed ampoules and post-annealed at 550°C in the same vacuum sealed ampoules.

The thin films on Mo glass pre-annealed in vacuum sealed ampoules pre-annealed below 240°C show binary sulphides and ternary Cu_xSnS_y phase. The thin films on Mo glass in vacuum sealed ampoules pre-annealed above 240°C show quaternary CZTS phase and ternary CTS phase. Analysis of different phases present in thin films shows that at pre-annealing stages binary and ternary phase form and at post-annealing stages they are converted to quaternary CZTS and ternary CTS phases.

4. Summary

The formation of CZTS thin films from solution of metal salt precursors in methanol with initial composition of Cu:Zn:Sn:S = 2:1:1:4 was studied. CZTS films were dip coated onto different substrates i.e. Mo, ITO and soda lime glass. The EDS results show that the composition of thin films on different substrates (ITO, Mo and soda lime glass) is different probably due to more effective adhesion of metal thiourea complex gel with Mo and ITO substrates. It was found that the applied pre-annealing in nitrogen atmosphere resulted in crack free films with uniform morphology while the pre-annealing in vacuum sealed ampoules gave lot of cracks on the surface. The thickness of as-deposited thin films could be increased by repeated dip coating. Elemental composition of thin films deposited on Mo and ITO glasses and pre-annealed at 240°C in nitrogen atmosphere are close to the stoichiometric composition of $\text{Cu}_2\text{ZnSnS}_4$ in comparison to the films deposited onto glass substrate. The development of phase composition in CZTS thin films on Mo or ITO substrates was studied and compared. Thin films pre-annealed at 240°C under nitrogen atmosphere showed the ternary Cu_3SnS_4 phase and binary ZnS phase that was converted to quaternary $\text{Cu}_2\text{ZnSnS}_4$ and ternary Cu_2SnS_3 phases during annealing at 550°C in vacuum sealed ampoules. Probably the using of copper-poor initial composition could lead to the formation of single phase $\text{Cu}_2\text{ZnSnS}_4$ compound.

Acknowledgment

This work was supported by the Estonian Science Foundation grant ETF9369, ETF9425, by the institutional research funding IUT 19–28 of the Estonian Ministry of Education and Research, and by the European Union through the European Regional Development Fund, Project TK141, Advanced materials and high-technology devices for energy recuperation systems.

References

- [1] Fernandes P A, Salome P M P, Cunha A F. $\text{Cu}_x\text{SnS}_{x+1}$ ($x=2, 3$) thin films grown by sulphurization of metallic precursors deposited by dc magnetron sputtering, *Phys Status Solidi, C7* (3-4) (2010) 901.
- [2] Katagiri H, Nishimura M, Onozawa T, Maruyama S, Fujita M, Segata T, Watanabe T. PCC-Nagaoka'97, IEEE, 1997, p. 1003.
- [3] Madarasz J, Bombicz P, Okuya M, Kaneb S. Thermal decomposition of thiourea complexes of Cu(I), Zn(II) and Sn(II) chlorides as precursors for the spray pyrolysis deposition of sulphide thin films, *Solid State Ionics* (2001) 439-141.
- [4] Yeh M Y, Lee C, Wu D S. Influence of synthesizing temperatures on the properties of $\text{Cu}_2\text{ZnSnS}_4$ prepared by sol gel spin coated deposition, *Journal sol gel Sci Technol* (2009) 52-65.
- [5] Jiang M, Li Y, Dhakal R, Thapaliya P, Mastro M, Caldwell J D, Kub F, Yan X. $\text{Cu}_2\text{ZnSnS}_4$ polycrystalline thin films with large densely packed grains prepared by sol-gel method, *Journal of Photonics for Energy* 1, (2011) (019501-1–6).
- [6] Cao L, Ma S, Sui J, Bai J, Dong H, Zhang Q, Dong L. Kesterite $\text{Cu}_2\text{ZnSn}(\text{S}_{1-x}\text{Se}_x)_4$ film synthesis through ethanol-thermal route with sulphurization/selenization treatments. *Materials Letters* 139 (2015) 101–103.
- [7] Chaudhuri T, Tiwari D. Earth-abundant non-toxic $\text{Cu}_2\text{ZnSnS}_4$ thin films by direct liquid coating from metal–thiourea, *Solar Energy Materials and Solar Cells* 101 (2012) 46–50.
- [8] Fernandes P A, Salome P M P, Cunha A F. Study of polycrystalline $\text{Cu}_2\text{ZnSnS}_4$ films by Raman scattering, *Journal of Alloys and Compounds* 509 (2011) 7600-7606.
- [9] Tanaka K, Fukui Y, Moritake N, Uchikih H. Chemical composition dependence of morphological and optical properties of $\text{Cu}_2\text{ZnSnS}_4$ thin films deposited by sol-gel sulphurization and $\text{Cu}_2\text{ZnSnS}_4$ thin film solar cell efficiency, *sol energy matter sol cells* (2011) 95-838.
- [10] Moriya K, Tanaka K, Uchiki H. $\text{Cu}_2\text{ZnSnS}_4$ thin films annealed in H_2S atmosphere for solar cell absorber prepared by pulsed laser deposition, *Japan Journal App. Phys* (2008) 47-602.
- [11] Tanaka T, Kawasaki D, Nishio N, Guo Q, Ogawa H. Fabrication of $\text{Cu}_2\text{ZnSnS}_4$ thin films by co-evaporation, *Phys status solidi* (2006) 3-2844.
- [12] Katagiri H, Sasaguchi N, Hando S, Hishinos, J. Ohashi, Yokota T. *Journal sol energy matter sol cells* (1996) 49-745.
- [13] Altosaar M, Varema T, Mellikov E. Surface Degreasing and Activation as important Factor for Cu Electroplating on ITO Substrates.
- [14] Chalapathi U, Kumar Y B K, Uthanna S, Raja V S. Investigations of Cu_3SnS_4 thin films prepared by spray pyrolysis, *Thin Solid Films* 556 (2014) 61-67.
- [15] Kim J H, Rho H, Kim J, Choi Y J, Park J G. Raman spectroscopy of ZnS nanostructures, *Wiley Online Library* March (2012).
- [16] Price L S, Parkin P I, Hardy M E A, Clark J H, Hibbert T G, Molloy K C. Atmospheric pressure chemical vapour deposition of tin sulphides (SnS , Sn_2S_3 and SnS_2) on glass, *Glass. Chem. Mater.* 1999, 11, 1792-1799.
- [17] Wiberg, E, Wiberg, N. Inorganic Chemistry, 2001, Academic Press, p, 614, ISBN 0-12-352651-5.

Curriculum Vitae

1. Personal data

Name: Suresh Kumar
Date of birth: 05.10.1983
Place of birth: Bhiwani, Haryana, India
Citizenship: Indian
E-mail: sureshkumarnara@gmail.com

2. Education

Educational institution	Graduation year	Education (field of study/degree)
Tallinn University of Technology	2018	Chemical and Materials Technology
University of Madras	2010	M. Sc. Physics
Maharajas College Ernakulam, Mahatma Gandhi University	2005	B. Sc. Physics, <i>Gold Medallist</i>
Kendriya Vidyalaya No. 1, Ambala Cantt, Haryana	2001	Higher Secondary Education
Kendriya Vidyalaya, Karanja, Maharashtra	1999	Secondary Education

3. Language competence

Language	Level
Hindi	Native
English	Fluent

4. Special Course/Conferences/Scientific Work

Period	Educational or other organisation
01.08.2001–31.01.2002	Diploma of Computer Application (DCA), LBS institute of Science and Technology, Alwaye, Kerala, <i>Gold Medallist</i>
01.09.2002–30.04.2005	NCC "C" certificate Army Wing, 21 KER NCC BN, Ernakulam
01.08.1999–31.03.2001	Celebration Captain, Student Council Member, KV No. 1, Ambala Cantt, Haryana
13.11.2014–14.11.2014	5 th European Kesterite Workshop, Tallinn, Estonia
20.04.2015–24.04.2015	NextGen 2015, Minorca, Spain
02.05.2016–06.05.2016	E-MRS Spring Meeting, Lille, France
07.03.2017–08.03.2017	FMTDK Scientific Conference 2018, Tartu, Estonia
22.05.2017–26.05.2017	E-MRS Spring Meeting, Strasbourg, France
09.10.2017–13.10.2017	Conference and Advanced Concepts in Photovoltaic Research, DTU - RISØ Campus, Denmark

07.03.2018–08.03.2018	FMTDK Scientific Conference 2018, Tallinn, Estonia
-----------------------	---

5. Professional employment

Period	Organisation	Position
01.06.2011–31.05.2012	SIPL, Delhi, India	Assistant Manager
21.06.2012–10.08.2013	Ganga Technical Campus	Assistant Professor
20.08.2013–31.12.2016	Tallinn University of Technology	Junior Researcher
01.03.2017–31.08.2018	Tallinn University of Technology	Engineer

6. Research Activity

Projects

01.01.2011–31.12.2014	ETF8964 "Synthesis and tailoring the properties of $\text{Cu}_2\text{ZnSn}(\text{Se},\text{S})_4$ -type powders as solar cell absorber materials and formation of p-n junction on their bases"
01.01.2012–31.12.2015	ETF9425 "Processes and factors limiting the yield of $\text{Cu}_2\text{ZnSn}(\text{S},\text{Se})_4$ monograin powders in synthesis of solar cell absorber materials in molten salts"
01.01.2012–31.01.2017	ETF9369 "Optical studies of kesterite type absorber materials"
01.01.2014–31.12.2019	IUT19-28 "New materials and technologies for solar energetics"
01.01.2016–01.03.2023	TK141 "Advanced materials and high-technology devices for sustainable energetics, sensorics and nanoelectronics"

Supervision

01.09.2013–30.06.2014	Bharath Kasubosula, "Synthesis of $\text{Cu}_2\text{ZnSnS}_4$ solar cell absorber materials by solution based process", defended 2014 (Erasmus Exchange Master Student), Tallinn University of Technology
01.09.2015–30.06.2016	Vikash Kumar, "Synthesis of $\text{Cu}_2\text{ZnSnS}_4$ nano-powders by nano-powder ink technology", Defended 2016 (Erasmus Exchange Master Student), Tallinn University of Technology

Elulookirjeldus

1. Isikuandmed

Nimi: Suresh Kumar
Sünniaeg: 05.10.1983
Sünnikoht: Bhiwani, Haryana, India
Kodakondsus: India
E-post: sureshkumarnara@gmail.com

2. Hariduskäik

Õppeasutus	Lõpetamise aeg	Haridus (eriala/kraad)
Tallinna Tehnikaülikool	2018	Keemia- ja materjali-tehnoloogia
Madrased Ülikool	2010	M. Sc. Füüsika
Maharaja kõrgkool Ernakulam, Mahatma Gandhi Ülikool	2005	B. Sc. Füüsika, kuldmedalist
Kendriya Vidyalaya No. 1, Ambala Cantt, Haryana	2001	keskharidus
Kendriya Vidyalaya, Karanja, Maharashtra	1999	põhiharidus

3. Keelteoskus

Keel	Tase
Hindi	emakeel
Inglise keel	kõrgtase

4. Erikursus / konverentsid / teadustöö

Õppimise aeg	Täiendusõppe korraldaja, nimetus
01.08.2001–31.01.2002	Diploma of Computer Application (DCA), LBS institute of Science and Technology, Alwaye, Kerala, <i>kuldmedal</i>
01.09.2002–30.04.2005	NCC "C" certificate Army Wing, 21 KER NCC BN, Ernakulam
01.08.1999–31.03.2001	Celebration Captain, Student Council Member, KV No. 1, Ambala Cantt, Haryana
13.11.2014–14.11.2014	5th European Kesterite Workshop, Tallinn, Eesti
20.04.2015–24.04.2015	NextGen 2015, Minorca, Hispaania
02.05.2016–06.05.2016	E-MRS kevadkonverents 2016, Lille, Prantsusmaa
07.03.2017–08.03.2017	FMTDK Teaduskonverents 2017, Tartu, Eesti
22.05.2017–26.05.2017	E-MRS kevadkonverents, 2017, Strasbourg, Prantsusmaa

09.10.2017–13.10.2017	Conference and Advanced concepts in Photovoltaic Research, Taani Tehnikaülikool - RISØ Campus, Taani
07.03.2018–08.03.2018	FMTDK Teaduskonverents 2018, Tallinn, Eesti

5. Teenistuskäik

Töötamise aeg	Tööandja nimetus	Ametikoht
01.06.2011–31.05.2012	SIPL, Delhi, India	juhiabi
21.06.2012–10.08.2013	Ganga Tehnikakeskus	professori abi
20.08.2013–31.12.2016	Tallinna Tehnikaülikool	nooremteadur
01.03.2017–31.08.2018	Tallinna Tehnikaülikool	insener

6. Teadustegevus

Osalemine projektides

01.01.2011–31.12.2014	ETF8964 "Päikesepatarei $\text{Cu}_2\text{ZnSn}(\text{Se},\text{S})_4$ -tüüpi absorbermaterjalide süntees, omaduste kujundamine ja p-n siirde formeerimine"
01.01.2012–31.12.2015	ETF9425 "Protsesside ja mehhanismide uurimine, mis limiteerivad $\text{Cu}_2\text{ZnSn}(\text{S},\text{Se})_4$ kui päikesepatarei absorbermaterjali saagist sünteesil sulade soolade keskkonnas"
01.01.2012–31.01.2017	ETF9369 "Kesteriitsete absorbermaterjalide optilised uuringud"
01.01.2014–31.12.2019	IUT19-28 "Uued materjalid ja tehnoloogiad päikeseenergeetikale"
01.01.2016–01.03.2023	TK141 "Uudsed materjalid ja kõrgtehnoloogilised seadmed energia salvestamise ja muundamise süsteemidele"

Juhendamine

01.09.2013–30.06.2014	Bharath Kasubosula, "Päikesepatarei absorbermaterjali $\text{Cu}_2\text{ZnSnS}_4$ süntees vedeliksadestuse meetodil", kaitstud 2014 (Erasmus'e vahetusüliõpilane, magistrant), Tallinna Tehnikaülikool
01.09.2015–30.06.2016	Vikash Kumar, " $\text{Cu}_2\text{ZnSnS}_4$ nano-pulbrite süntees kasutades nanopulber-suspensioon tehnoloogiat", kaitstud 2016 (Erasmus'e vahetusüliõpilane, magistrant), Tallinna Tehnikaülikool

